NASA TECHNICAL NOTE

NASA TN D-3463

NASA TN D-3463

REVISED THREE DEGREE OF FREEDOM PARTICLE TRAJECTORY PROGRAM CO3E FOR THE IBM 7094 COMPUTER

by Wilber R. Boykin

Manned Spacecraft Center
Houston, Texas

NATIONAL AERONAUTICS AND SPACE ADMINISTRATION • WASHINGTON, D. C. • OCTOBER 1966

REVISED THREE DEGREE OF FREEDOM PARTICLE TRAJECTORY PROGRAM CO3E FOR THE IBM 7094 COMPUTER

By Wilber R. Boykin

Manned Spacecraft Center
Houston, Texas

NATIONAL AERONAUTICS AND SPACE ADMINISTRATION

For sale by the Clearinghouse for Federal Scientific and Technical Information
Springfield, Virginia 22151 – Price $3.75

ABSTRACT

This IBM 7094 computer program simulates the motion of a spacecraft by the numerical integration of its spherical polar equations of motion; the spacecraft is represented as a point mass subjected to aerodynamic and thrust forces near an oblate, rotating earth. The program is written primarily in absolute FAP, but also it contains some relocatable FAP and FORTRAN II subroutines. It can be run either under or independently of the FORTRAN II monitor system.

CONTENTS

FIGURES

ACKNOWLEDGEMENT

This program was developed from the particle trajectory program CO3E originally written by Mr. John N. Shoosmith of the NASA-Space Task Group for the IBM 704 computer in 1960-61. The features of the original program were retained and to these were added a number of outputs and special options requested by users. The program was actually rewritten in order to obtain an accurate program listing and source cards, and to update and extend it where necessary. Listings and source programs were similarly obtained for all the library and supporting routines required. This procedure was essential, since a large number of additions to the program were to be made subsequently.

Mr. Shoosmith had also completed a document for an early version of the program which was oriented primarily toward the user. The present document is intended to explain the theory and develop the mathematics employed as well as give instructions on program usage.

REVISED THREE DEGREE OF FREEDOM PARTICLE TRAJECTORY PROGRAM CO3E FOR THE IBM 7094 COMPUTER

By Wilber R. Boykin
Manned Spacecraft Center

SUMMARY

The use of spherical polar equations of motions for an orbiting spacecraft has the advantage that they normally vary smoothly with time and are therefore well suited to numerical integration techniques. The inherent disadvantage is that the differential equation in $\ddot{\lambda}$ contains the factor secant L and therefore the program cannot be used to compute a polar orbit when $L = \frac{\pi}{2}$.

Since both absolute and relocatable routines are permitted in the program, lengthy or complex equations can be written in FORTRAN. The completely self-contained set of library routines permits a fast-loading procedure which is a distinct asset in real-time computing applications.

1.0 INTRODUCTION

This program has been developed over a period of time and has been tailored to meet user demands. The underlying philosophy of the program is that it should be as automatic and easy to use as possible and should still retain reasonable program flexibility to allow for future modifications.

The program has been in use for over 5 years, including considerable real-time (trajectory determination while a mission is in progress) computing applications during the Project Mercury and the Gemini Program. Retrorocket firing times were accurately predicted in these missions, and consequently, the program has enjoyed a high degree of confidence.

This writeup is in two major divisions: the first explains program usage and available features; while the second, section 15.0 and the appendixes, gives the mathematical equations employed in the program. This latter section also gives information of interest to a programer concerned with program functions or modifications. Appendix K contains the symbols and the constants.

The major portion of the program is written in absolute FAP, and there are several subsections of "subroutines" which perform specific functions as subsequently outlined. The numerical integration routine QUIKE is the most important of these since it controls program operation as well as the integration of the equations of motion.

2.0 PROGRAM USAGE: ORGANIZATION OF DATA INPUT

Before beginning a description of the various operations performed by the program during computation of a trajectory, certain preliminary remarks are in order. A single trajectory is termed a case. Each case may consist of one or more sections; data input changes are allowed from case to case and from section to section to obtain the desired trajectory simulation. Several cases may be stacked to form a single computer run.

The program is normally stored in the computer or on tape as a part of the monitor system. Figure 2.0-1 gives a drawing of a typical deck setup to run two cases of several sections each. A distinction must be made between case data and section data, since each is used at a different time during the computation of the trajectory; the two cannot be mixed.

Case data consist of (1) the case identification, (2) the input coordinate system definition, (3) initial time, (4) initial position and velocity, and (5) initial weight. Special options may be included in case data if desired. It should be noted that the initial conditions, namely time, position, and velocity, can be input only once per case. Case data are terminated by a TRA 3,4 card, and at this point the program performs the appropriate input conversion and initializes the case conditions.

The first section data follow next, beginning with section identification. Also required will be the initial integration step size, print frequency, the coordinate system in which the termination conditions are specified if computations are to be halted on position or velocity, and outputs to be activated or deactivated. Special options to be activated or deactivated may also be included as section data. Attitude control, range option, and the range reference point should be included as section data. Table control cards are

normally section data, although their associated tables may be either section or case data. If Special Options 7 or 23 are used, heating rate constants are required, and, in addition, a table of K^{-1} values for Special Option 23. The aerodynamic reference area, weight decrement, I_{sp}, thrust information, density multiplier, the tolerance for radar stations to pick up the satellite, and constants for Special Option 15, are section data. Section data must include at least one termination condition. A TRA 3, 4 card terminates the section data, and at this point computations begin on the first section of the trajectory.

Data for the second section are then given. It will be similar to that of the first, but generally will not be as extensive since outputs, special options, attitude control, computing interval, tables, thrust parameters, and constants carry over from case to case and section to section. A new termination condition must be specified for each section, and the data for each section are terminated by a TRA 3, 4 card.

In like manner, the data for all subsequent sections are prepared. A TRA 2, 4 card signals the end of the case, whereupon the program expects data for the next case. If more cases are to follow, the case data for each will be organized similar to that of the first. Initial position and velocity, along with many other items, carry over unless updated in the new case, thus less input is generally required in later cases.

Section data for succeeding cases are organized in the same manner as that of the first case. Again a TRA 2, 4 card signifies the end of the case, and a second TRA 2, 4 terminates the computer run.

Monitor control cards are necessary with each data deck. These must conform to changing monitor requirements, and therefore will not be discussed here.

The following discussion elaborates on the block diagram of the program given in figures 2.0-2 through 2.0-4. The purpose, at the present, is to give both a discussion and graphical description of the program features and coordinate systems employed to better enable the reader to understand program use and operation. The actual derivation and listing of mathematical equations will be largely reserved for the appendixes. It is advisable that one become thoroughly familiar with the symbols listed in appendix K representing the variables of the program before proceeding to other sections of this document. All the symbols used are defined in the symbols list, and no description of these symbols will be given elsewhere.

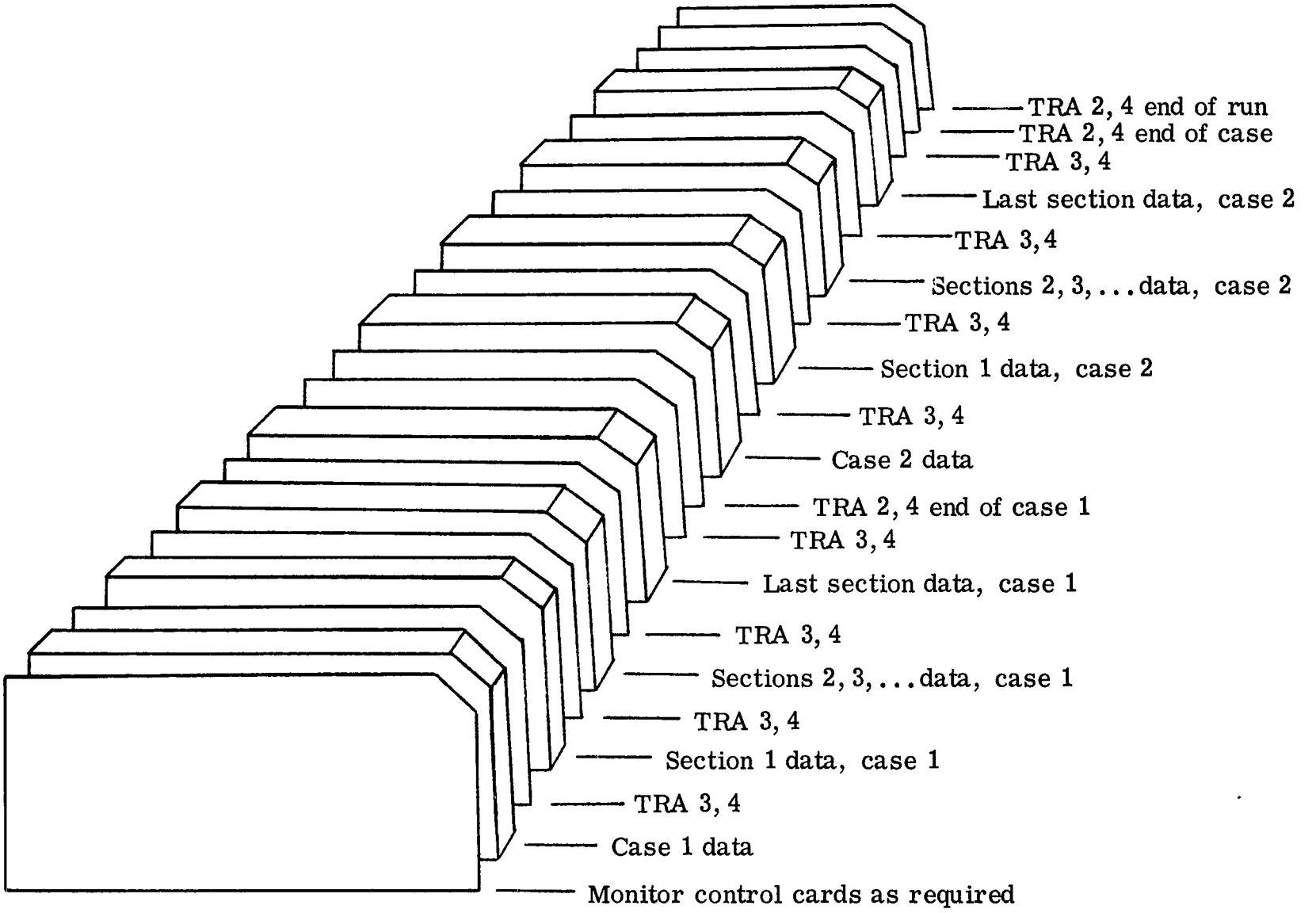

Figure 2.0-1. - Typical CO3E data deck setup consisting of a regular run of two cases containing several sections each.

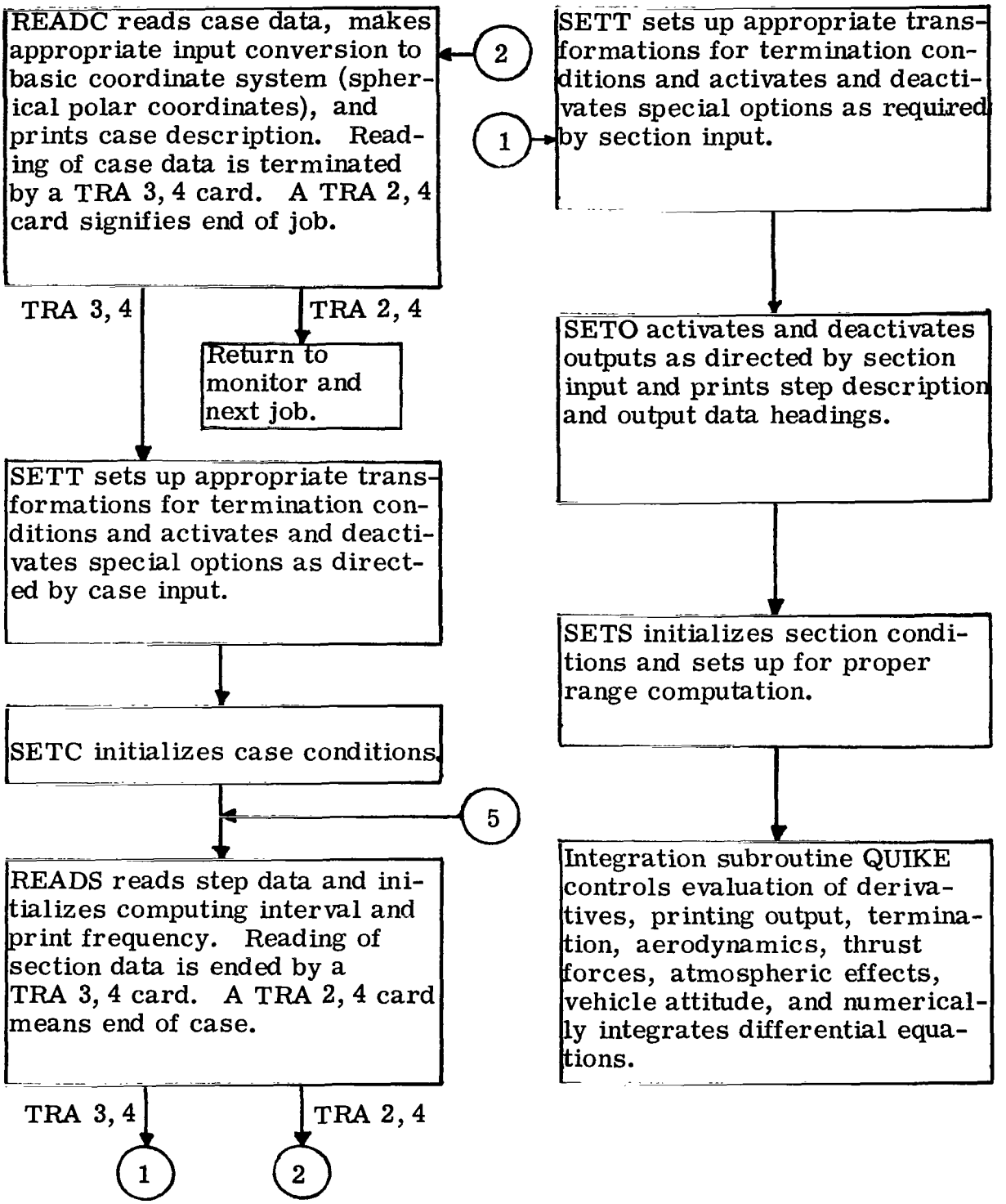

Figure 2.0-2. - Simplified flow chart by subroutines of particle trajectory program CO3E.

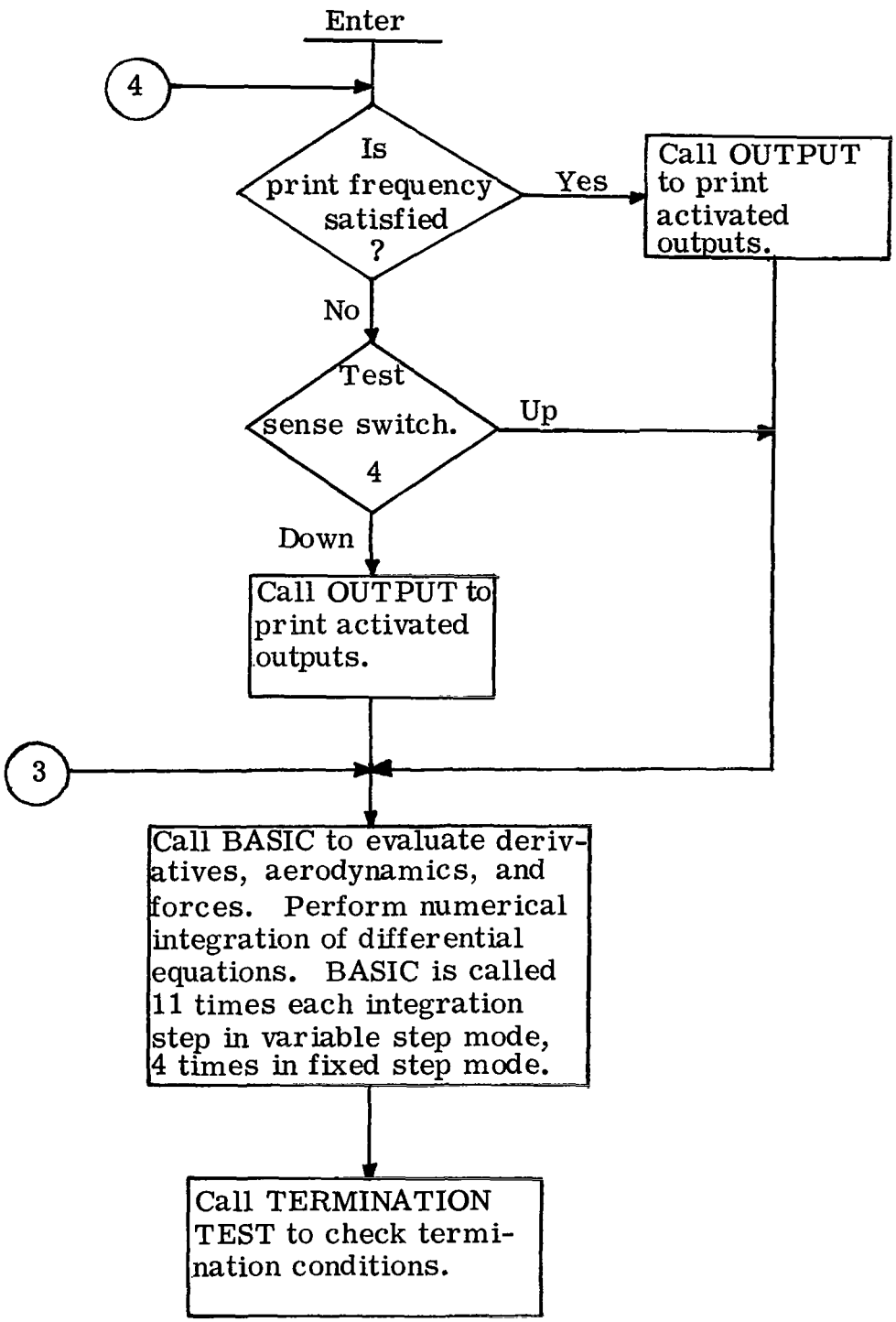

Figure 2.0-3. - Simplified flow chart of integration subroutine QUIKE.

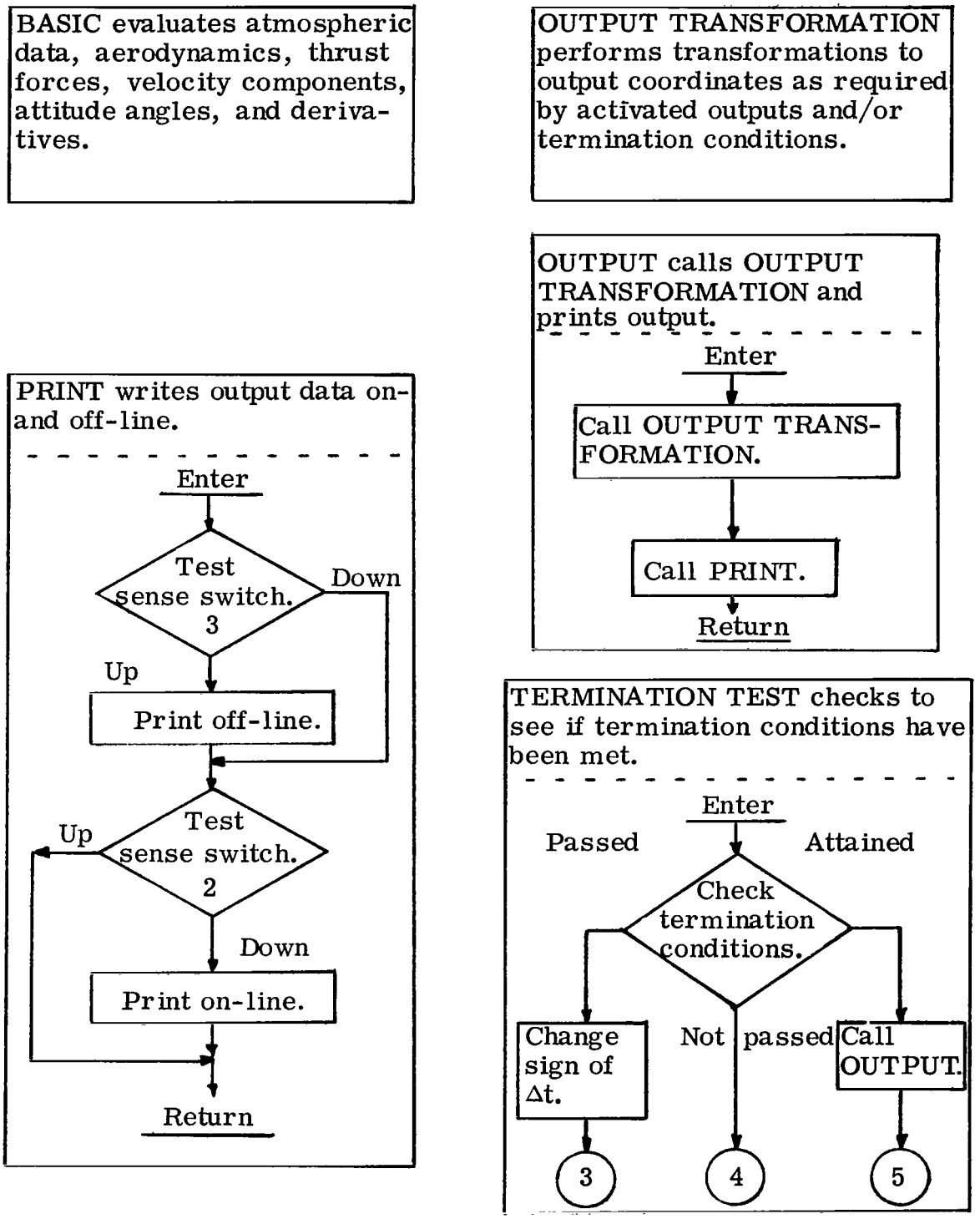

Figure 2.0-4. - Fundamental CO3E subroutines controlled by QUIKE.

Figures 2.0-2 through 2.0-4 give diagrams of the main segments of the program and their chief functions. These three diagrams should be considered as a unit, since the transfer points (circled numerals) are not confined to a single page. Figure 2.0-2 gives the complete program flow chart in simplified form, while figure 2.0-3 is a more detailed diagram of the numerical integration routine. Figure 2.0-4 gives the flow charts of several other supporting routines.

3.0 EQUATIONS OF MOTION

The primary coordinate system is an earth-fixed, right-hand Cartesian set of axes with the Z-axis positive through the North Pole, and the X-Y plane coinciding with the earth equatorial plane. The X-axis is through the Greenwich meridian. The position, velocity, and acceleration of the vehicle in this system are given by the spherical polar coordinates of east longitude λ, north geocentric latitude L, and radius from the center of the earth r, and their time derivatives. The earth rotational velocity is ω_e; F_λ, F_L, F_r are external forces, and g_L and g_r are gravitational forces.

The spherical polar equations of motion (ref. 1) for a particle near an oblate, rotating earth are given by equations (1) through (6), and are derived in appendix A. Expressed as first-order equations, these are:

$$\frac{d\dot{\lambda}}{dt} = \ddot{\lambda} = \frac{1}{r \cos L}\left[\frac{F_\lambda}{m} - 2\dot{r}\left(\dot{\lambda} + \omega_e\right)\cos L + 2r\dot{L}\left(\dot{\lambda} + \omega_e\right)\sin L\right] \tag{1}$$

$$\frac{d\dot{L}}{dt} = \ddot{L} = \frac{1}{r}\left[\frac{F_L}{m} + g_L - 2\dot{r}\dot{L} - r\left(\dot{\lambda} + \omega_e\right)^2 \sin L \cos L\right] \tag{2}$$

$$\frac{d\dot{r}}{dt} = \ddot{r} = \left[\frac{F_r}{m} + g_r + r\dot{L}^2 + r\left(\dot{\lambda} + \omega_e\right)^2 \cos^2 L\right] \tag{3}$$

$$\frac{d\lambda}{dt} = \dot{\lambda} \tag{4}$$

$$\frac{dL}{dt} = \dot{L} \tag{5}$$

$$\frac{dr}{dt} = \dot{r} \tag{6}$$

In order to avoid round-off error, it is convenient to employ increments of position in the equations of motion. If L_o, λ_o, H_o are the geocentric latitude, longitude, and altitude coordinates respectively, on a geocentric sphere of radius equal to the equatorial radius of the earth at an initial time t_o, and L, λ, H are these quantities at some other time t, then equations (4) through (6) may be rewritten in the following manner, where $\Delta L = L - L_o$, $\Delta\lambda = \lambda - \lambda_o$, $H = r - r_e$:

$$\frac{d\ \Delta\lambda}{dt} = \dot{\lambda} \tag{7}$$

$$\frac{d\ \Delta L}{dt} = \dot{L} \tag{8}$$

$$\frac{dH}{dt} = \dot{r} \tag{9}$$

Normally the dominating terms in equations (1) through (3) will be the external forces F_λ, F_L, F_r. These represent thrust and aerodynamic forces acting on the vehicle. It is appropriate at this point to show how these forces are computed.

3.1 Aerodynamic and Thrust Forces

It is shown in the discussion of the numerical integration technique that the derivatives are evaluated 11 times in the variable step-size mode, and 4 times in the fixed step-size mode. At each evaluation, the thrust and aerodynamic forces, as well as gravitational forces, must be computed. There are two basic body-attitude control options, and the thrust and aerodynamic forces are computed differently, depending on the 644 card. These will be

discussed separately. Figures 3.1-1 and 3.1-2 show the aerodynamic forces acting on the body. Under both attitude control options, aerodynamic and thrust forces are computed in the body coordinates, and then transformed to spherical polar coordinates for inclusion in the equations of motion.

If 644 DEC 1 is used, all aerodynamic and thrust forces are aligned with the aerodynamic velocity vector, and hence no thrust misalignment and lift are permitted: $F_{a_y} = F_{a_z} = 0$ in figures 3.1-1 and 3.1-2, and

$$F_{a_x} = -C_a \bar{q} S \tag{10}$$

Thrust along the body x-axis is obtained as a linear function of time from a table. The quantity I_{sp} must be specified for weight decrementing, or a weight versus time table used instead. Note that in this case, $\tau = \sigma = 0$ and $T_x = T$ in figure 3.1-4.

$$T_x = T(t) \tag{11}$$

The total force acting on the body, then, has only one component which is transformed from the body coordinates to the local geodetic system whose axes are labeled east E, north N, and up U.

$$F_x = F_{a_x} + T_x \tag{12}$$

$$F_E = F_x \left(\frac{V_{a_E}}{V_a} \right) \tag{13}$$

$$F_N = F_x \left(\frac{V_{a_N}}{V_a} \right) \tag{14}$$

$$F_U = F_x \left(\frac{V_{a_U}}{V_a} \right) \tag{15}$$

Equation (30) then completes the transformation from the local geodetic frame to the spherical polar coordinates.

If 644 DEC 2, N, M is the attitude control used, then in addition to axial thrust and atmospheric drag, off-axial thrusts and aerodynamic lift forces are permitted. The body aerodynamic forces are given by equations (18) through (20) and shown in figure 3.1-1, except when the roll angle φ_r is specified by Special Option 10 or 32 (fig. 3.1-2). Then for the aerodynamic forces expressed in the body centered coordinates one has

$$F_n = C_n \bar{q} S \tag{16}$$

$$\theta_a = \tan^{-1} \left(\frac{w_a}{v_a} \right) \tag{17}$$

$$F_{a_x} = -C_a \bar{q} S \tag{18}$$

$$F_{a_y} = -F_n \cos \theta_a \tag{19}$$

$$F_{a_z} = -F_n \sin \theta_a \tag{20}$$

If Special Option 10 or 32 is activated, the orientation of the normal force vector F_n in the y_b-z_b plane is specified by the roll angle φ_r, as in figure 3.1-2. The y and z components of F_n are then

$$F_{a_y} = F_n \sin \varphi_r \tag{21}$$

$$F_{a_z} = -F_n \cos \varphi_r \tag{22}$$

There are two ways of computing thrust forces in the body coordinates under attitude control 644 DEC 2, N, M. Equation (11) may be used, in which the thrust has only an x component. If, however, the thrust values are constant, the "retro" thrust mode may be employed which permits off-axial or misaligned thrusts. Up to three such thrusts are used, along with their associated cant angles τ, rotation angles σ, start times t_i and stop times t_f, and nozzle exhaust area A. The cant angle τ is the angle between the body x-axis, and the thrust vector T, and σ, the rotation angle, is the angle between z_b axis and the projection of the thrust vector onto the body y-z plane. The rotation angle σ is measured counterclockwise. Figure 3.1-4 shows both τ and σ. The required input for this type of thrust is shown below. The value of I_{sp} must be the same for all rockets.

718 DEC	I_{sp}	specific impulse, sec
721 DEC	A_1, A_2, A_3	exhaust area, ft^2
724 DEC	τ_1, τ_2, τ_3	inclination angles, deg
727 DEC	$\sigma_1, \sigma_2, \sigma_3$	rotation angles, deg
730 DEC	T_1, T_2, T_3	thrusts, lb
733 DEC	$t_{i\,1}, t_{i\,2}, t_{i\,3}$	start times from start of section, sec
736 DEC	t_{f1}, t_{f2}, t_{f3}	stop times from start of section, sec

Special Option 21 permits up to 10 such retrothrusts to be used, but the data locations are different. A complete description of the use of this option is given in section 7. 0. Sea level thrust in both the "retro" mode and that given by equation (11) is corrected for atmospheric density changes due to altitude by the equation $T'_i = T_i + A_i \left(P_o - P\right)$ for each rocket i.

By referring to figures 3. 1-3 through 3. 1-6, it can be seen that the body thrust forces are given by:

$$T_x = \sum_i T_i \cos \tau_i \tag{23}$$

$$T_y = -\sum_i T_i \sin \tau_i \sin \sigma_i \tag{24}$$

$$T_z = \sum_i T_i \sin \tau_i \cos \sigma_i \tag{25}$$

Equations (26) through (28) give the total body forces

$$F_x = F_{a_x} + T_x \tag{26}$$

$$F_y = F_{a_y} + T_y \tag{27}$$

$$F_z = F_{a_z} + T_z \tag{28}$$

Equation (29) then is used to transform the forces from the body system to the local geodetic coordinates. Appendix B gives the derivation of these transformation matrices. The angles of the matrix T_{B2G} are shown in figures 3. 1-7 through 3. 1-9 and the forces in the local geodetic coordinates are

$$\begin{bmatrix} F_E \\ F_N \\ F_U \end{bmatrix} = T_{B2G} \begin{bmatrix} F_x \\ F_y \\ F_z \end{bmatrix} \tag{29}$$

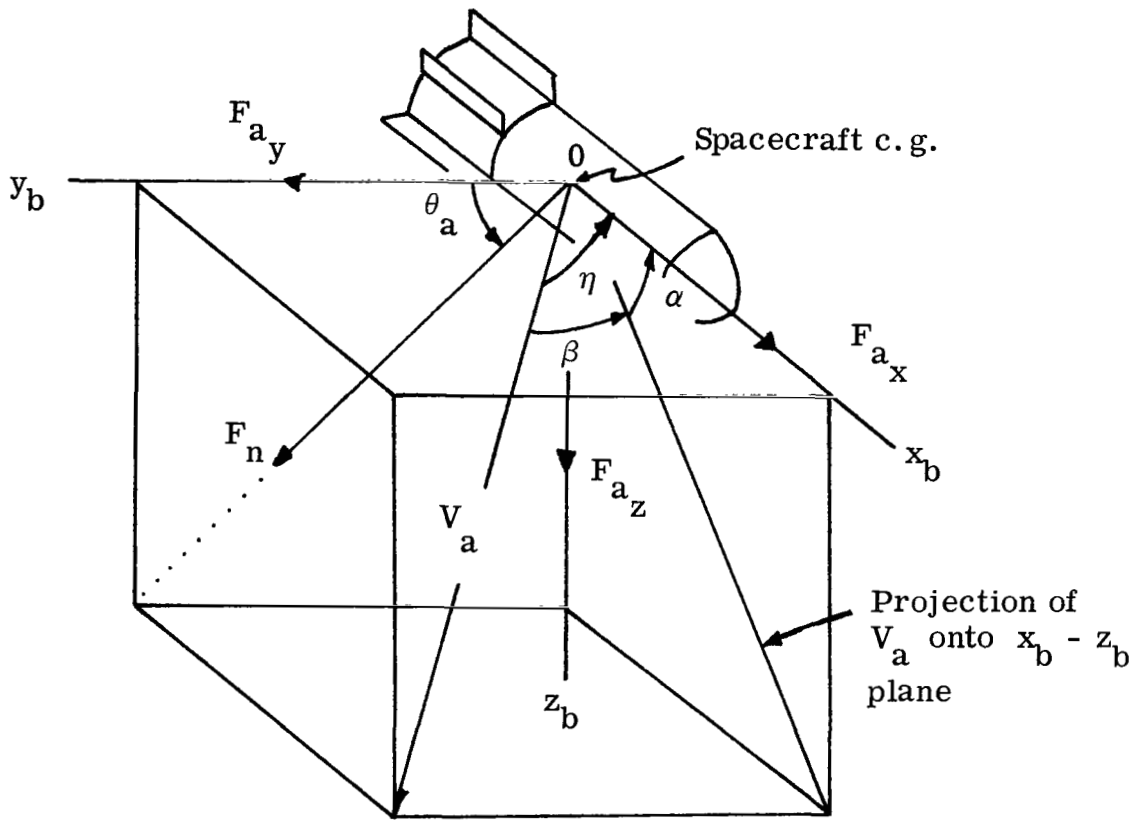

Figure 3.1-1. - Aerodynamic forces F_{a_x}, F_{a_y}, and F_{a_z} in the body coordinate system. The force F_n is perpendicular to x_b and lies in the y_b-z_b plane; it also lies in the plane defined by x_b-0-V_a, and F_n is computed from C_n, and the angle θ_a is used to resolve F_n into the two components F_{a_y} and F_{a_z}. The axis z_b is positive toward the earth.

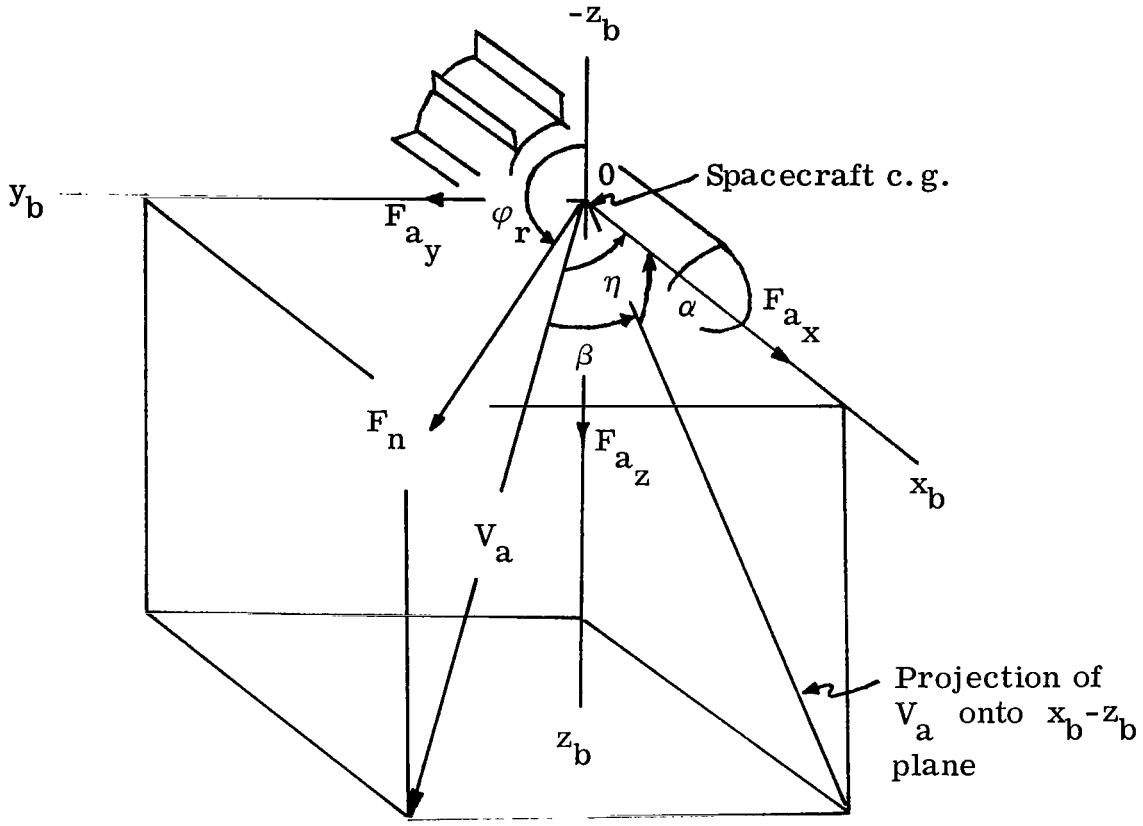

Figure 3.1-2. - Aerodynamic forces F_{a_x}, F_{a_y}, and F_{a_z} in the body coordinate system and roll angle φ_r, where F_n is perpendicular to x_b and lies in the y_b-z_b plane, but not in the x_b-0-V_a plane as in figure 3.1-1. The force F_n is computed from C_n as in figure 3.1-1, but in this case the roll angle φ_r is used to resolve F_n into y and z components. Note that z_b is positive toward the earth and that φ_r is measured counterclockwise from the negative z_b axis.

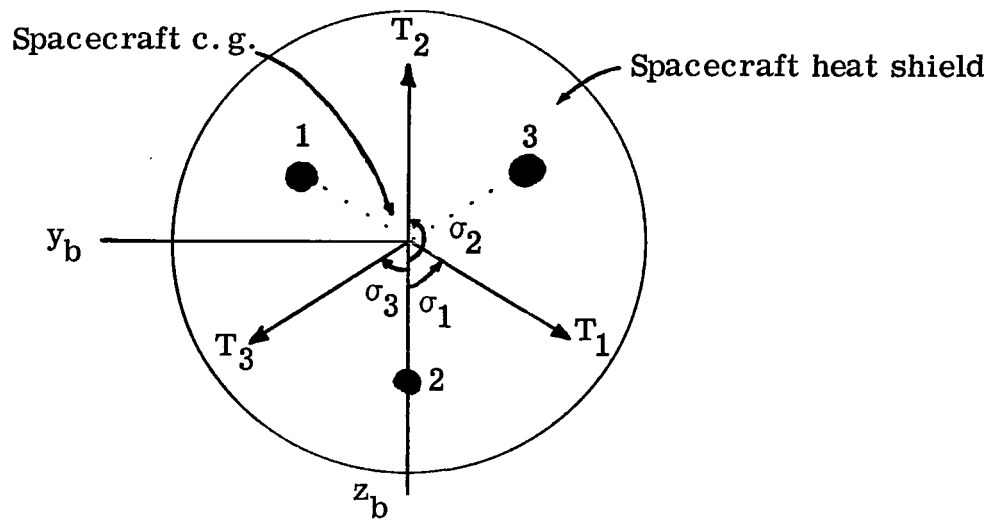

Figure 3.1-3. - Heat-shield view of spacecraft in the y_b-z_b plane illustrating thrust vectors for each retrorocket projected onto the y_b-z_b plane. The thrust vectors T_1, T_2, and T_3 are actually directed into the plane of the page through the spacecraft center of gravity (c.g.). The rotation angles σ_1, σ_2, and σ_3 are measured in the y_b-z_b plane as shown. The x_b axis is perpendicular to and positive out of the plane of the page.

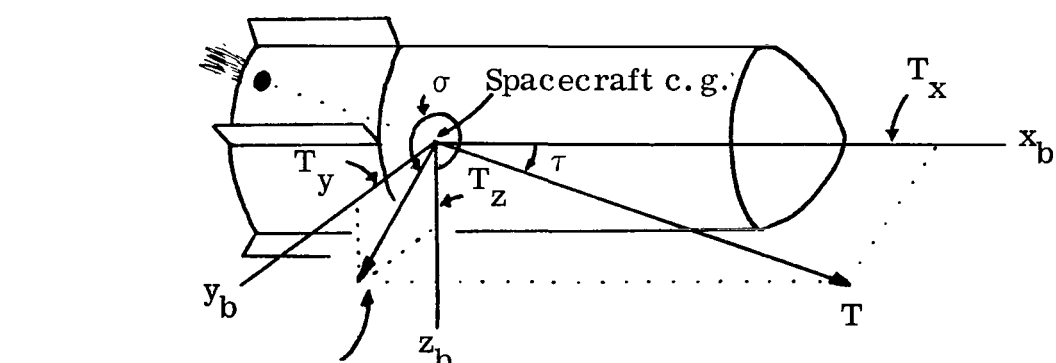

Figure 3.1-4. - Illustration of a general thrust vector T, its three components along the body coordinates, its cant angle τ, and rotation angle σ. The angle τ is between T and x_b, and σ is measured in the y_b-z_b plane.

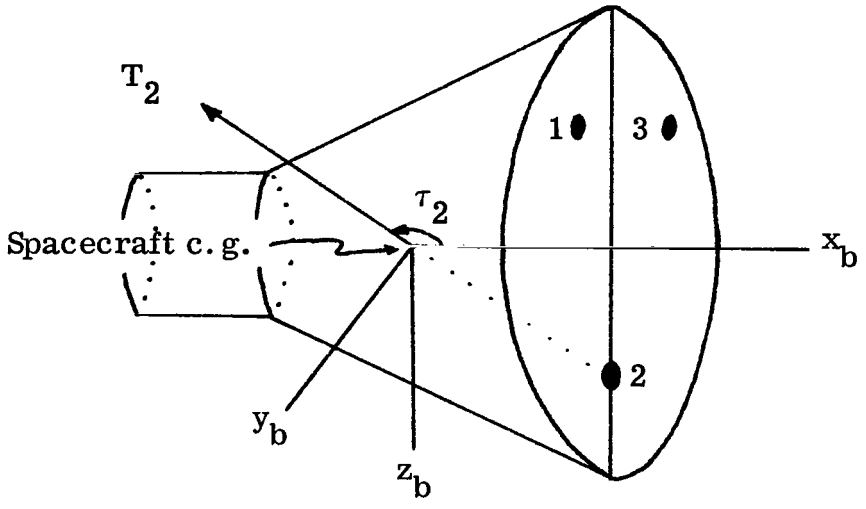

Figure 3.1-5. - Spacecraft showing three retrorockets, the thrust vector T_2 associated with rocket 2, and the thrust vector cant angle τ_2. Note that rocket 2 and T_2 both lie in the x_b-z_b plane, and hence τ_2 is measured in this plane.

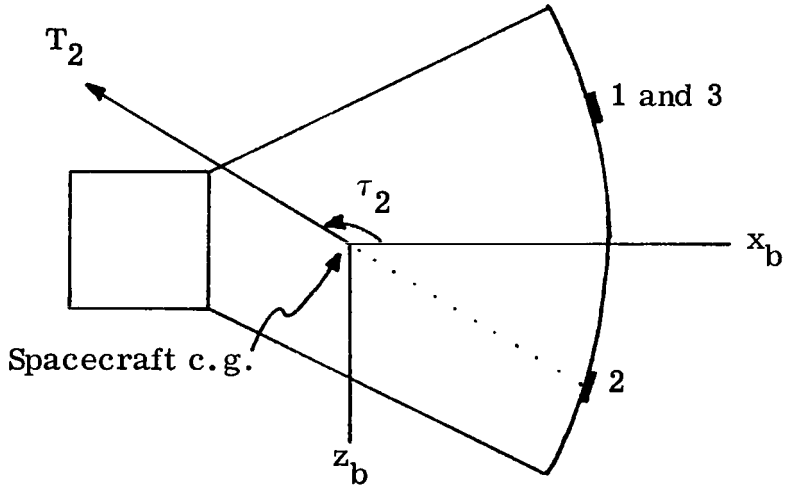

Figure 3.1-6. - Side view of spacecraft in the x_b-z_b plane showing rocket 2, T_2, and τ_2. The y_b axis is perpendicular to and positive out of the plane of the page.

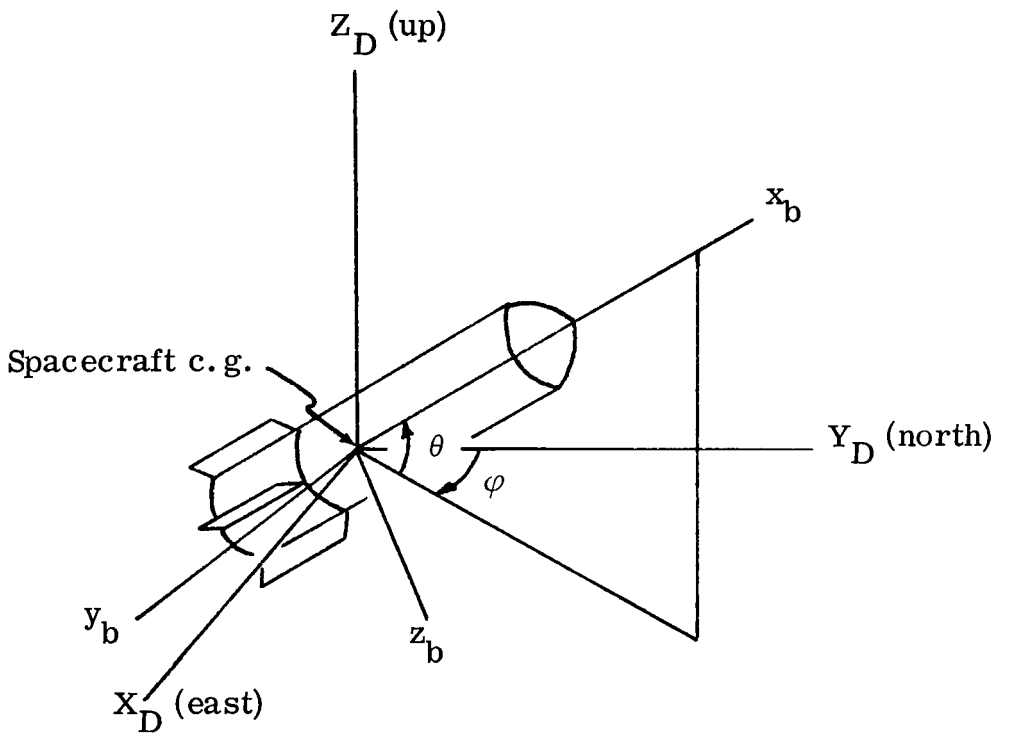

Figure 3.1-7. - Pitch θ and yaw φ of the body coordinate system measured with respect to the local geodetic coordinate frame. The angles θ and φ may be specified directly or with respect to one of the three velocity vectors (fig. 3.1-8).

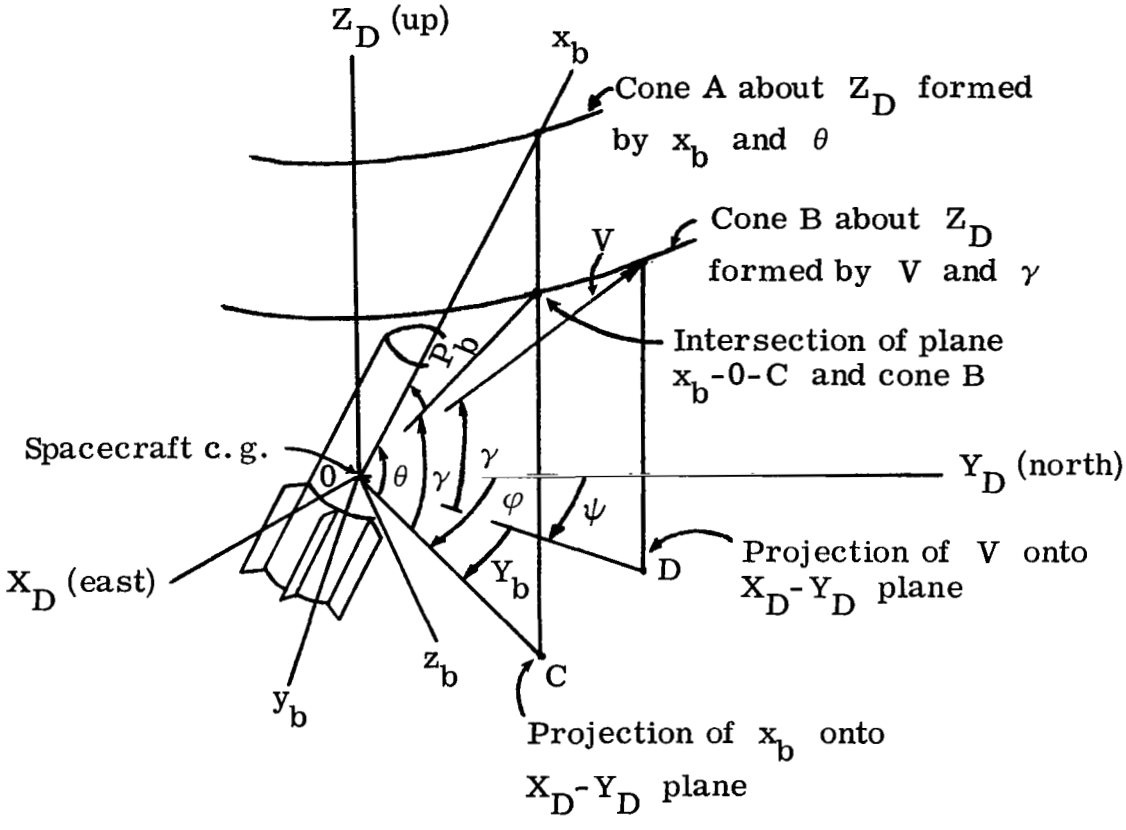

Figure 3.1-8. - Tabular inputs body pitch P_b and body yaw Y_b with respect to the velocity vector V. Note that the yaw from north is given by $\varphi = \psi + Y_b$, and the pitch from the local geodetic plane is $\theta = \gamma + P_b$ (fig. 3.1-7) where Y_b is the angle between the planes V-0-D and x_b-0-C; P_b is the angle between cones A and B.

Cones A and B are concentric about Z_D at angles $\frac{\pi}{2} - \theta$ and $\frac{\pi}{2} - \gamma$, respectively. Attitude controls 644 DEC 2, N, M (N = 0, 1, 2, M = 0, 1, 2) are depicted by this illustration.

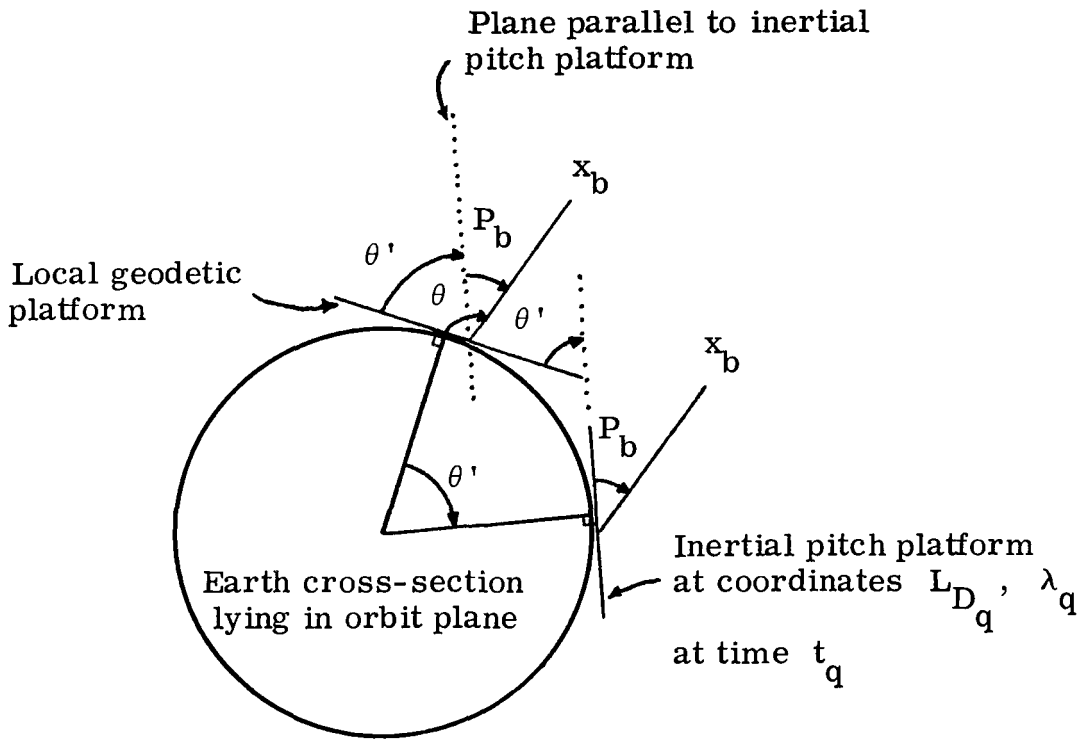

Figure 3.1-9.- Orientation of the body x-axis with respect to an inertial pitch platform. The plane of the page is that of the orbit. The axis x_b is inclined at the angle P_b with respect to the inertial platform, and θ' is the angle between the inertial platform and the local geodetic platform, that is, the angle between the normals to these two planes. Then, x_b makes the angle $\theta = \theta' + P_b$ with respect to the local geodetic platform, and θ' is given by the law of cosines for spherical triangles as shown by equation (113). Attitude controls 644 DEC 2, 3, M are illustrated by this diagram.

Under both attitude controls, equation (30) then transforms the forces from the local geodetic system to the spherical polar coordinates for inclusion in the equations of motion, equations (1) through (3). This final transformation of forces gives

$$\begin{bmatrix} F_\lambda \\ F_L \\ F_r \end{bmatrix} = T_{G2C} \begin{bmatrix} F_E \\ F_N \\ F_U \end{bmatrix} \tag{30}$$

3.2 Gravitational Forces

The earth model used is an oblate spheroid, flattened at the poles, with a circular cross section at the equator. The gravitational force (ref. 2) then has both radial and latitudinal components, and these are obtained by differentiation of the potential function U with respect to r and L. Figure 3.2-1 illustrates the vectors $\vec{g}_L$ and $\vec{g}_r$. No gravitational effects from the sun or from other planets are included. It is assumed that these forces are negligible compared to the earth's gravitational field. The gravitational forces are obtained as follows

$$U = \frac{\mu}{r}\left[1 + \frac{J_1'}{3}\left(\frac{r_e}{r}\right)^2\left(1 - 3\sin^2 L\right)\right.$$

$$+ \frac{H_1'}{5}\left(\frac{r_e}{r}\right)^3\left(3\sin L - 5\sin^3 L\right)$$

$$\left. + \frac{K_1'}{30}\left(\frac{r_e}{r}\right)^4\left(3 - 30\sin^2 L + 35\sin^4 L\right) + \ldots\right] \tag{31}$$

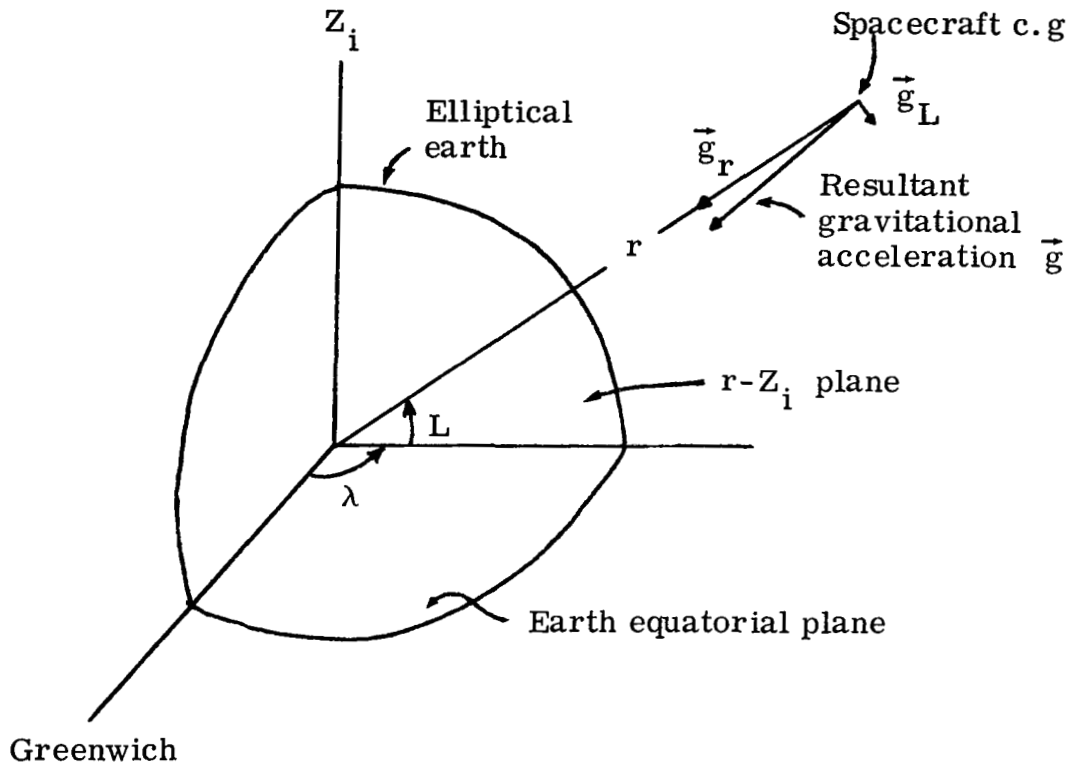

Figure 3.2-1. - Radial $\vec{g}_r$ and perpendicular $\vec{g}_L$ components of earth's gravitational acceleration vector $\vec{g}$. The plane of the page is that formed by the radius vector r and the Z_i axis. The perpendicular component $\vec{g}_L$ is always directed toward the equator.

$$\vec{g}_r = \hat{r}\frac{\partial U}{\partial r} = \frac{-\mu}{r^2}\left[1 + J_1'\left(\frac{r_e}{r}\right)^2\left(1 - 3\sin^2 L\right)\right.$$

$$+ \frac{4}{5} H_1'\left(\frac{r_e}{r}\right)^3\left(3\sin L - 5\sin^3 L\right)$$

$$\left. + \frac{K_1'}{6}\left(\frac{r_e}{r}\right)^4\left(3 - 30\sin^2 L + 35\sin^4 L\right)\right]\hat{r} \qquad (32)$$

$$\vec{g}_L = \frac{\hat{L}}{r}\frac{\partial U}{\partial L} = \frac{-\mu}{r^2}\left[2J_1'\left(\frac{r_e}{r}\right)^2 \sin L \cos L\right.$$

$$+ \frac{3}{5} H_1'\left(\frac{r_e}{r}\right)^3\left(5\sin^2 L - 1\right)\cos L$$

$$\left. + 2K_1'\left(\frac{r_e}{r}\right)^4\left(\sin L - \frac{7}{3}\sin^3 L\right)\cos L\right]\hat{L} \qquad (33)$$

3.3 Other Formulas Used

In addition to the differential equations of motion, four other derivatives are evaluated and integrated.

Equation (34) gives the differential equation for weight except when weight is obtained from a table

$$\frac{dW}{dt} = -\frac{T}{I_{sp}} \qquad (34)$$

in which case

$$\frac{dW}{dt} = 0 \qquad (35)$$

Convective heat rate is taken as the smaller of equations (36) or (37), and the radiative heat rate is given by equation (38). The constants C_1 and C_2 are functions of velocity. Thus,

$$\frac{dH_c}{dt} = F'_c \frac{17600}{\sqrt{R_n}} \left(\frac{\rho}{\rho_o}\right)^{\frac{1}{2}} \left(\frac{V_a}{26000}\right)^{3.15} \tag{36}$$

$$\frac{dH_c}{dt} = F'_c \frac{\rho V_a^{\,3}}{1556} \tag{37}$$

$$\frac{dH_r}{dt} = F'_r C_1 R_n \left(\frac{\rho}{\rho_o}\right)^{1.78} \left(\frac{V_a}{10000}\right)^{C_2} \tag{38}$$

Ground track is given by

$$\frac{d\chi}{dt} = \frac{r_D V_{e\,hor}}{r} \tag{39}$$

The earth model is described by equatorial and polar radii, or by the equatorial radius and the reciprocal of the flattening,

$$\frac{1}{f} = \frac{r_e}{r_e - r_p} \tag{40}$$

The radius of the earth at a geocentric latitude L is

$$r_D = r_e \left[1 - \frac{1}{2} C \sin^2 L + \frac{3}{8} C^2 \sin^4 L\right] \tag{41}$$

where

$$C = \left(\frac{r_e}{r_p}\right)^2 - 1 \tag{42}$$

The altitude h above the oblate spheroid is related to the height H above the equatorial sphere by

$$h = H + r_e\left[\frac{1}{2}C\sin^2 L - \frac{3}{8}C^2\sin^4 L\right] \tag{43}$$

Figure 3.3-1 shows the relation between geodetic and geocentric latitudes, as expressed by

$$\tan L_D = \left(\frac{r_e}{r_p}\right)^2 \tan L \tag{44}$$

It is necessary to have available the components of the velocity vector in order to compute the flight path and heading angles. The subscripts L, λ, r refer to components of the velocity vector expressed in a right-handed, geocentric, Cartesian coordinate system designated by geocentric latitude L, longitude λ, and radius vector r; likewise, the subscripts E, N, U refer to a geodetic coordinate system having east-, north-, and up-axes. The subscript e denotes earth referenced, or relative velocity, and i signifies inertial. Figure 3.3-2 shows the following relations

$$V_\lambda = r\left(\dot{\lambda} + \omega_e\right)\cos L \tag{45}$$

$$V_{e_\lambda} = r\dot{\lambda}\cos L \tag{46}$$

$$V_L = V_{e_L} = r\dot{L} \tag{47}$$

$$V_r = V_{e_r} = \dot{H} = \dot{r} \tag{48}$$

Figure 3.3-3 illustrates V_{e_E}, V_{e_N}, V_{e_U}, and the transformation equation (48):

$$\begin{bmatrix} V_{e_E} \\ V_{e_N} \\ V_{e_U} \end{bmatrix} = T_{C2G} \begin{bmatrix} V_{e_\lambda} \\ V_{e_L} \\ V_{e_r} \end{bmatrix} \tag{49, 50, 51}$$

The transformation of the inertial velocity vector components is similar to that depicted in figure 3.3-3 for V_e

$$\begin{bmatrix} V_{i_E} \\ V_{i_N} \\ V_{i_U} \end{bmatrix} = T_{C2G} \begin{bmatrix} V_\lambda \\ V_L \\ V_r \end{bmatrix} \tag{52, 53, 54}$$

Addition of the east W_E and north W_N wind velocity components to the relative velocity vector gives the aerodynamic velocity vector components, denoted by the subscript a (fig. 3.3-3). Thus,

$$V_{a_E} = V_{e_E} + W_E \tag{55}$$

$$V_{a_N} = V_{e_N} + W_N \tag{56}$$

$$V_{a_U} = V_{e_U} \tag{57}$$

The magnitudes of the relative, aerodynamic, and inertial velocity vectors are given by equations (58) through (60)

$$V_e = \sqrt{V_{e_E}^2 + V_{e_N}^2 + V_{e_U}^2} \tag{58}$$

$$V_a = \sqrt{V_{a_E}^2 + V_{a_N}^2 + V_{a_U}^2} \tag{59}$$

$$V_i = \sqrt{V_{i_E}^2 + V_{i_N}^2 + V_{i_U}^2} \tag{60}$$

It is convenient to be able to express the aerodynamic velocity vector in body-centered coordinates, u, v, w (fig. 3.3-4). This transformation is

$$\begin{bmatrix} u_a \\ v_a \\ w_a \end{bmatrix} = T_{G2B} \begin{bmatrix} V_{a_E} \\ V_{a_N} \\ V_{a_U} \end{bmatrix} \tag{61, 62, 63}$$

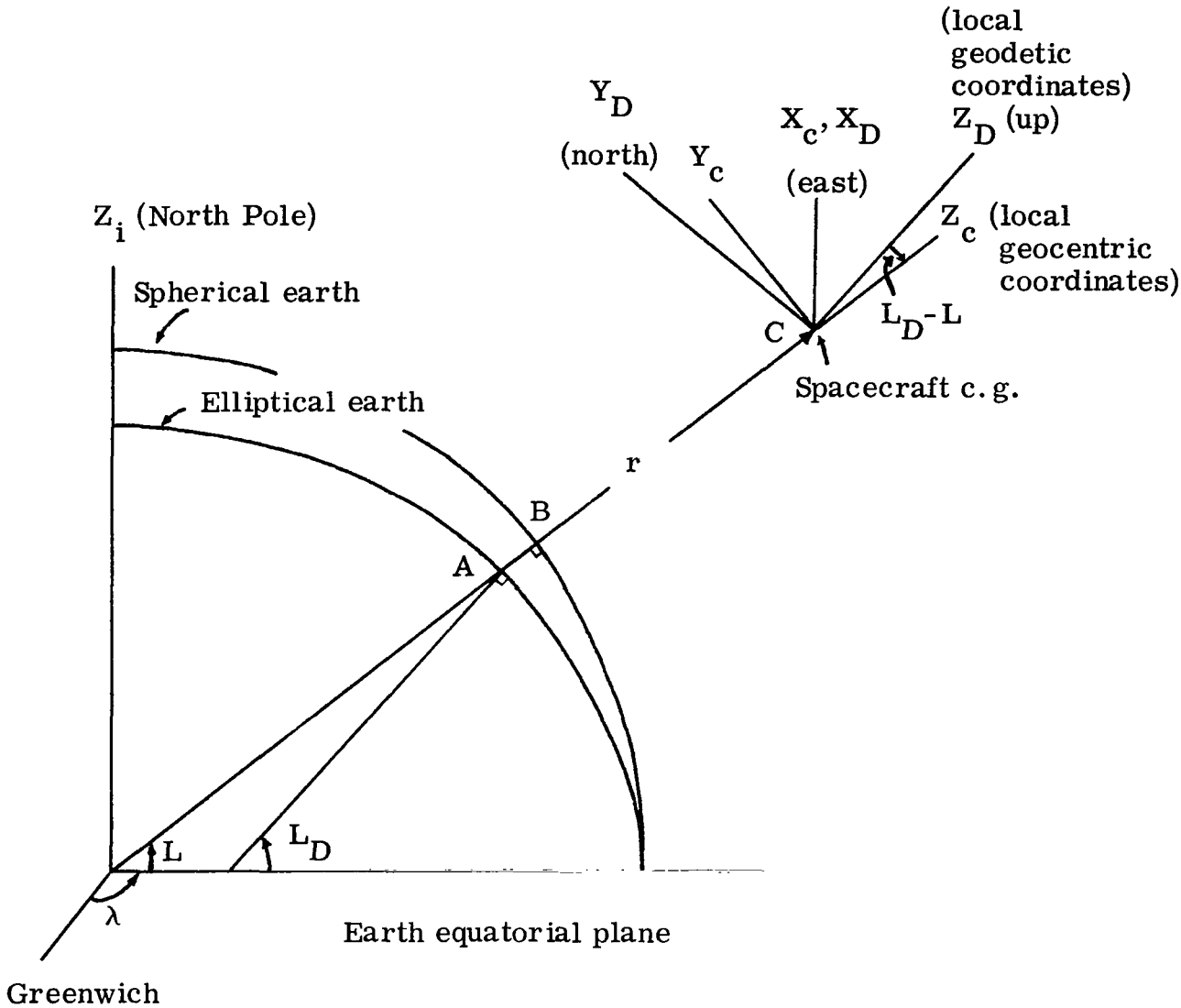

Figure 3.3-1. - Relation between local geocentric and local geodetic coordinates. The plane of the page is that defined by the Z_i axis and the meridian of longitude at λ° east of Greenwich, where AC is the altitude h above the elliptical earth, and BC is the height above the equatorial sphere.

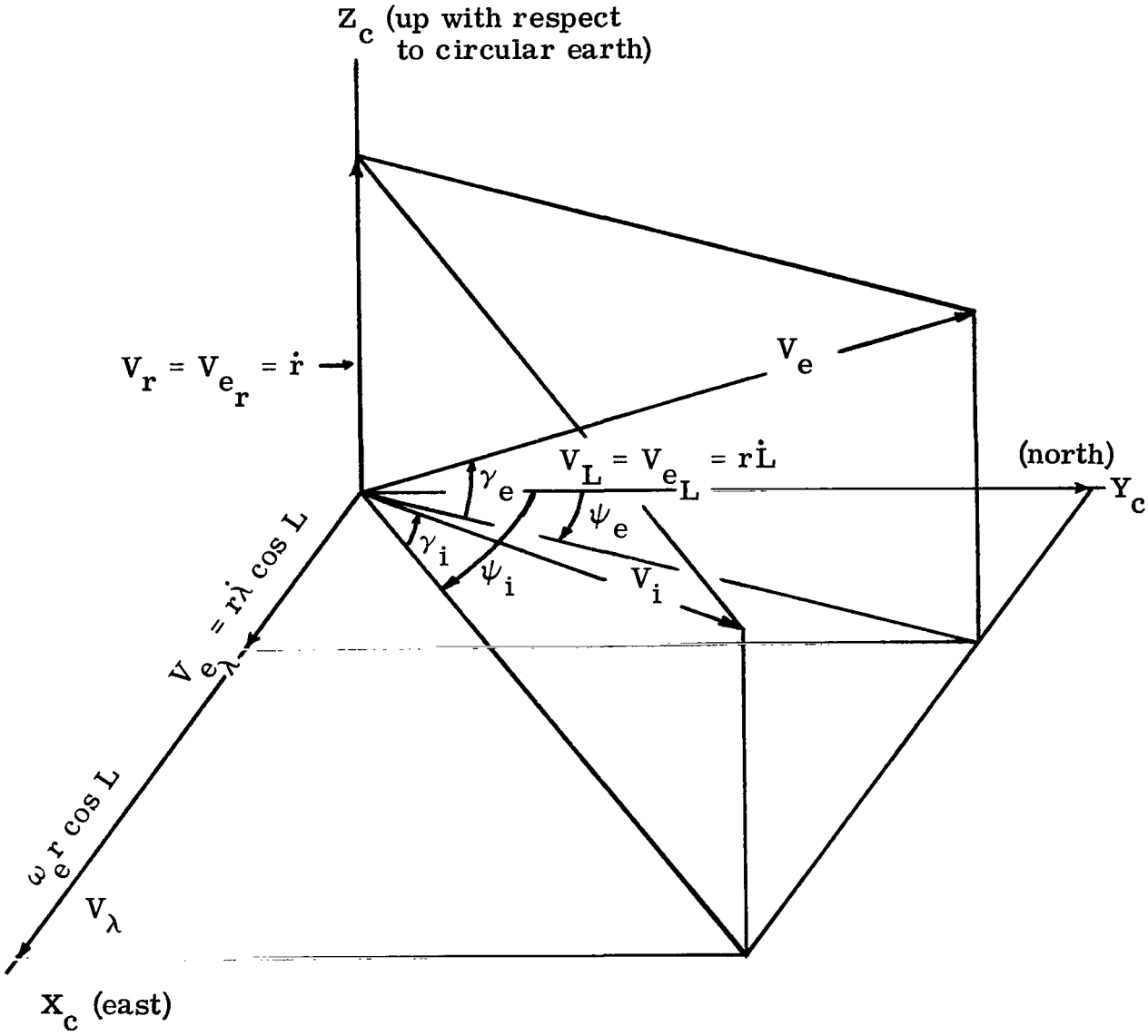

Figure 3.3-2. - Components of relative (earth referenced, V_e) and inertial velocity (V_i) vectors and their associated azimuths and flight path angles.

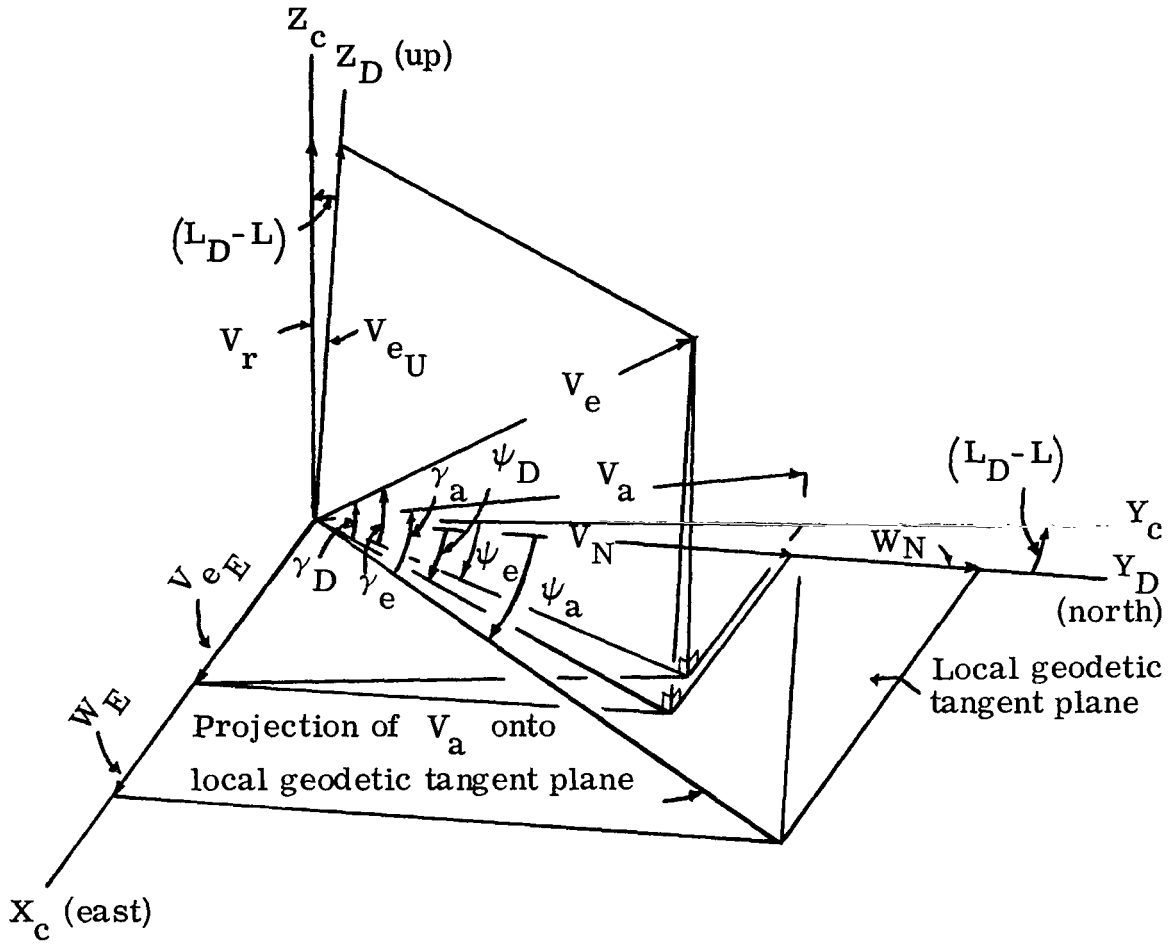

Figure 3.3-3. - Transformation of relative velocity V_e to local geodetic coordinates and addition of east and north winds to give aerodynamic velocity V_a. The transformation of inertial velocity V_i to local geodetic coordinates is similar to that of V_e, and γ_D and ψ_D are the angles that V_e makes with respect to the local geodetic horizontal and north, respectively. The angles γ_a and ψ_a are the angles that V_a makes with respect to the local geodetic horizontal and north, respectively.

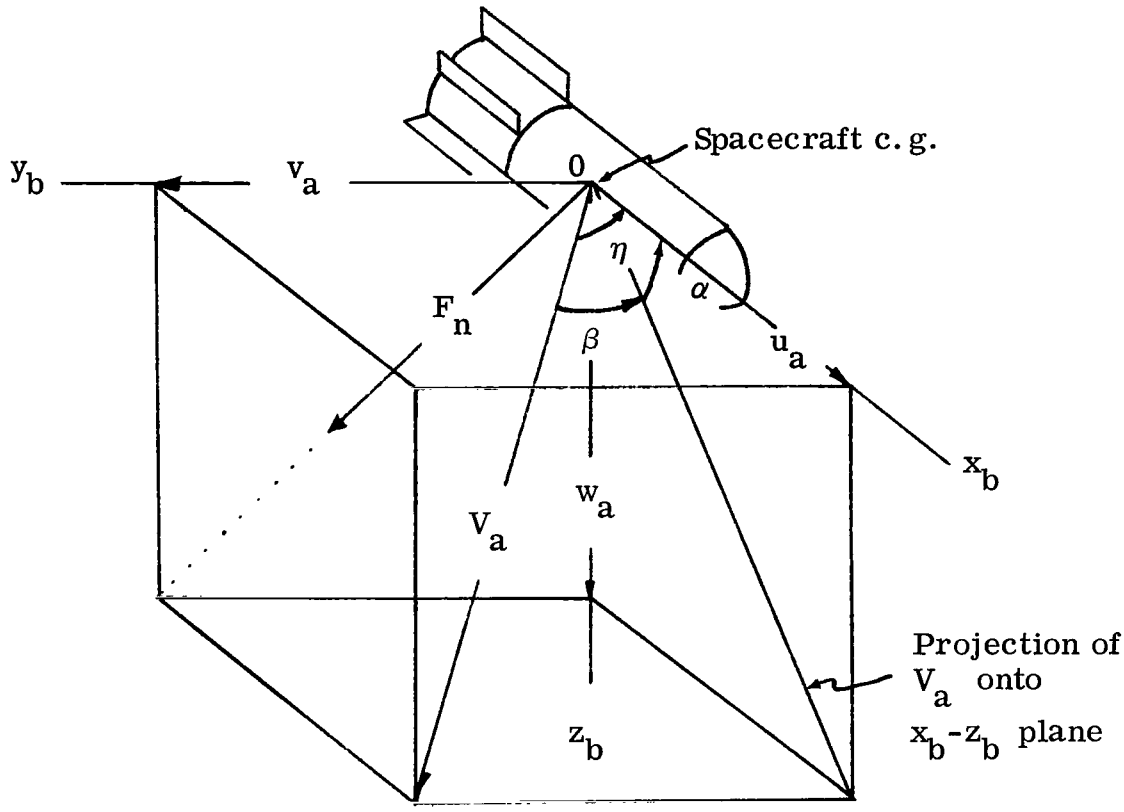

Figure 3.3-4. - Body coordinate system illustrating total angle of attack η, pitch angle of attack α, angle of sideslip β, and the components of the aerodynamic velocity vector V_a in the body system, u_a, v_a, and w_a. The longitudinal axis of the vehicle corresponds to x_b, and z_b is positive toward the earth. Figure 3.3-5 illustrates the body aerodynamic forces resolved into normal force F_n and drag F_{a_x} components.

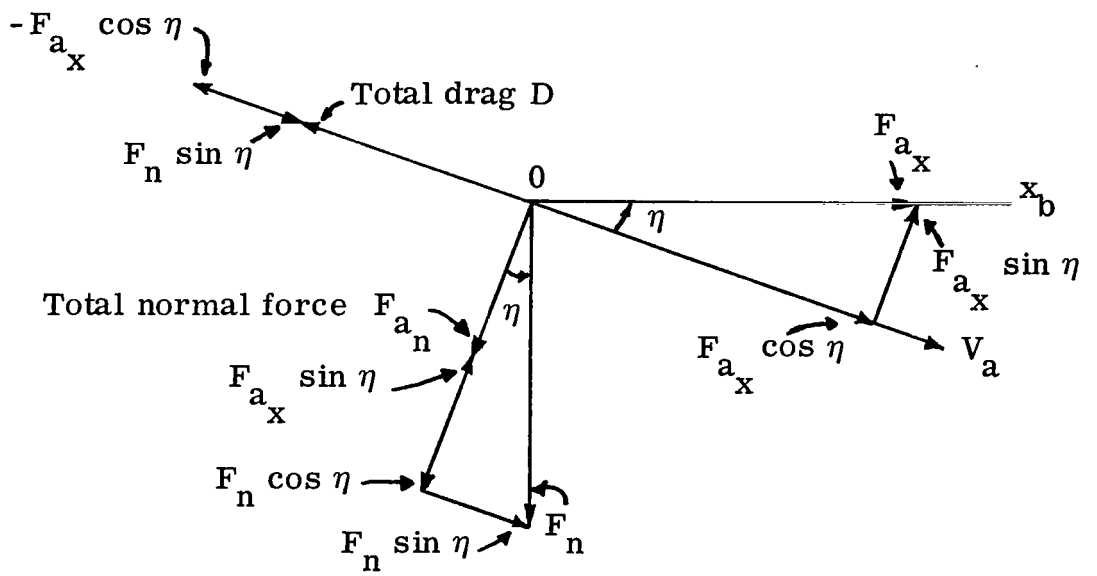

Figure 3.3-5. - Normal force vector F_n normal to x_b, drag F_{a_x} along x_b, lift vector F_{a_n} normal to V_a, and total drag D along V_a. The plane of the page is that defined by x_b-V_a-F_n in figure 3.3-4.

4.0 DESCRIPTION OF INPUT AND INPUT COORDINATE SYSTEMS

The initial position and velocity of the body may be specified in any one of several coordinate systems. The appropriate transformation is made from this system to rotating spherical, polar coordinates in which integration of the equations of motion is performed. The six coordinates (three position and three velocity) are each premultiplied by a constant (cards 801 through 806) before the input transformation is made. Normally this constant is unity, but the constant may be changed as a part of case data. The allowed input coordinates and the corresponding code to be used on the 588 DEC N card are now defined. All coordinate systems are right-handed, and input codes carry over from case to case. Appendix C gives the equations used in these input transformations.

Input 1

Position is given in geodetic coordinates and velocity in polar, body-centered coordinates. Figure 3.3-1 illustrates the position coordinates of this input, and figure 3.3-2 shows the velocity coordinates.

841 DEC	L_D	geodetic latitude, deg
842 DEC	λ	longitude relative to Greenwich, deg
843 DEC	h	altitude above reference spheroid, ft
844 DEC	V_i	magnitude of inertial velocity, ft/sec
845 DEC	γ_i	inertial flight path angle, deg
846 DEC	ψ_i	inertial azimuth angle, deg

Geocentric latitude in degrees instead of geodetic latitude may be input on the 841 card by including the card 583 DEC 1 with the case data. Since the 583 card carries over, the initial latitude on all subsequent cases will be assumed to be geocentric until a 583 DEC 0 is included with case data.

Latitude, either geodetic or geocentric as indicated on the 583 card, may be input in degrees, minutes, and seconds by substituting the 832 card for the

841 card above. Likewise, the 842 card, containing longitude in degrees, may be replaced by the 836 card which allows longitude input in degrees, minutes, and seconds.

832 DEC degrees, minutes, seconds. Geodetic or geocentric latitude

836 DEC degrees, minutes, seconds. Longitude relative to Greenwich

Input 2

Position is given in geodetic coordinates the same as Input 1, but velocity is relative to the rotating earth in polar, body-centered coordinates (figs. 3.3-1 and 3.3-2).

844 DEC V_e magnitude of relative (earth referenced) velocity, ft/sec

845 DEC γ_e relative flight path angle, deg

846 DEC ψ_e relative azimuth angle, deg

Input 3

Position and velocity are specified in inertial, geocentric, rectangular coordinates. The X_i axis is fixed by a longitude λ_x and a time t_x. The Z_i axis is positive through the North Pole, and the X_i-Y_i plane coincides with the earth equatorial plane. See figure 4.0-1 for a graphical description of this coordinate system.

650 DEC λ_x longitude of X_i axis relative to Greenwich at time t_x, deg

651 DEC t_x sec

841-843 DEC X_i, Y_i, Z_i ft

844-846 DEC $\dot{X}_i, \dot{Y}_i, \dot{Z}_i$ ft/sec

Input 4

There are quasi-inertial, geocentric, rectangular coordinates. The coordinate axes rotate with the earth, but the velocity is inertial. Through the North Pole Z_q is positive, and the X_q-Y_q plane and the earth equatorial plane are coincident. The X_q axis is positioned by the longitude on the 650 card. Figures 4.0-1 and 4.0-2 demonstrate this system.

650 DEC	λ_x	longitude of X_q axis relative to Greenwich, deg
841-843 DEC	X_q, Y_q, Z_q	ft
844-846 DEC	$\dot{X}_q, \dot{Y}_q, \dot{Z}_q$	ft/sec

Input 5

This coordinate system is a rotational, geocentric, rectangular one. It is the same coordinate system as that of Input 4 except both position and velocity are measured with respect to the rotating coordinates. The X_e axis is positioned in exactly the same manner as the X_q axis. Figure 4.0-2 shows this coordinate system.

650 DEC	λ_x	longitude of X_e axis relative to Greenwich, deg
841-843 DEC	X_e, Y_e, Z_e	ft
844-846 DEC	$\dot{X}_e, \dot{Y}_e, \dot{Z}_e$	ft/sec

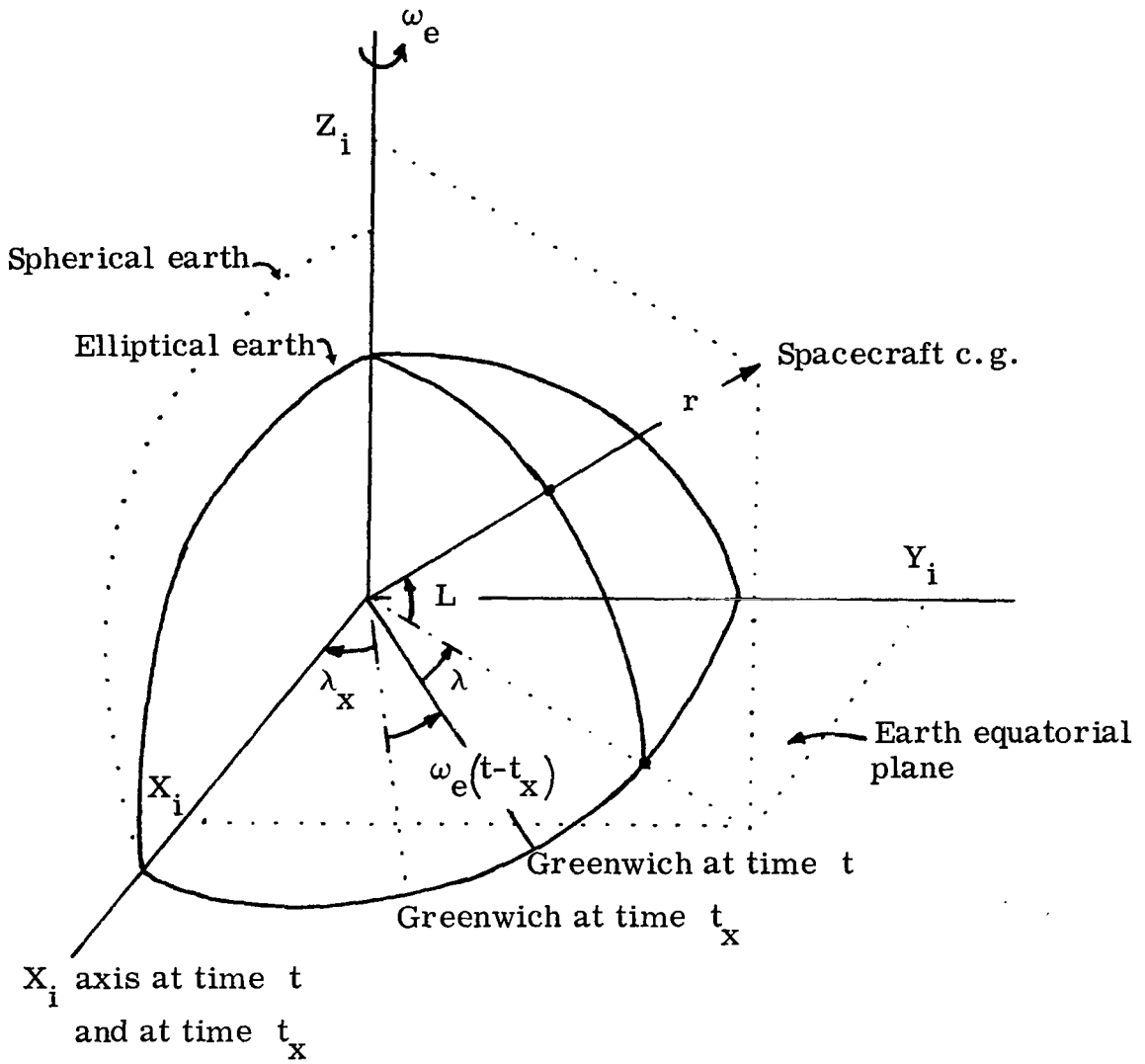

Figure 4.0-1. - Inertial, earth-centered, rectangular coordinate system X_i, Y_i, Z_i. The position and velocity components of Input-Output 3 and the velocity components of Input-Output 4 are measured with respect to this system.

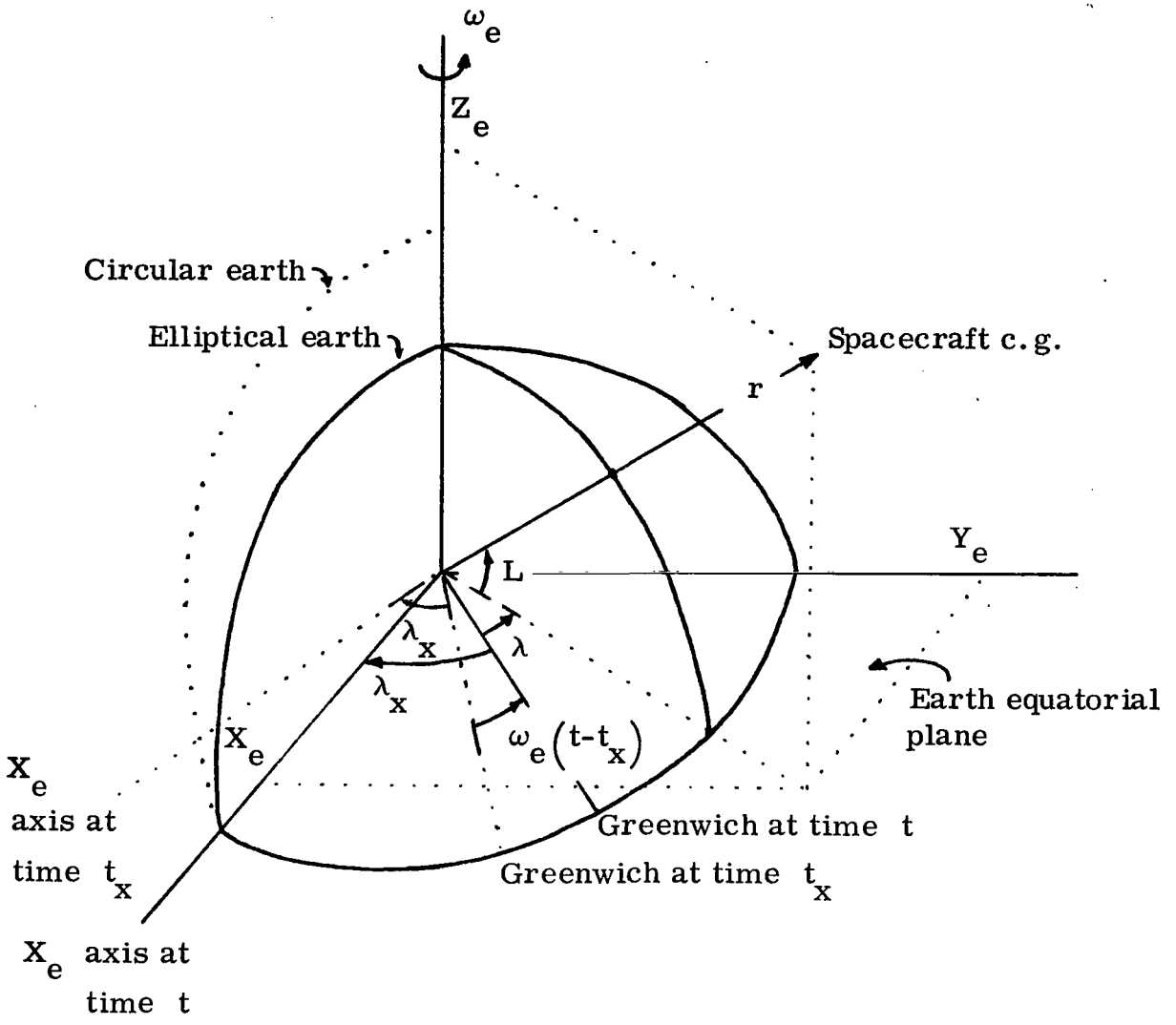

Figure 4.0-2. - Rotating, earth-fixed, and earth-centered, rectangular, coordinate system X_e, Y_e, Z_e. The position components of Input-Output 4 and both the position and velocity components of Input-Output 5 are referenced to this system.

Input 6

This is an inertial, topocentric, rectangular coordinate system whose origin is fixed in space by a longitude λ_q relative to Greenwich, the time t_q at which the origin was at longitude λ_q, geodetic latitude L_{D_q}, and altitude h_q of the origin above the reference spheroid. The x-axis is oriented at an azimuth angle A_q from north. The x-y plane is parallel to the spheroid surface at coordinates L_{D_q}, λ_q, h_q at time t_q, and the z-axis is positive away from the spheroid center. Both position and velocity are inertial. Figure 4.0-3 shows this coordinate system.

653 DEC	L_{D_q}	geodetic latitude of origin, deg
654 DEC	λ_q	longitude of origin relative to Greenwich at time t_q, deg
655 DEC	h_q	altitude of origin above reference spheroid, ft
656 DEC	A_q	azimuth of x-axis east of north, deg
657 DEC	t_q	time at which origin was at longitude λ_q, sec
841-843 DEC	x, y, z	ft
844-846 DEC	$\dot{x}, \dot{y}, \dot{z}$	ft/sec

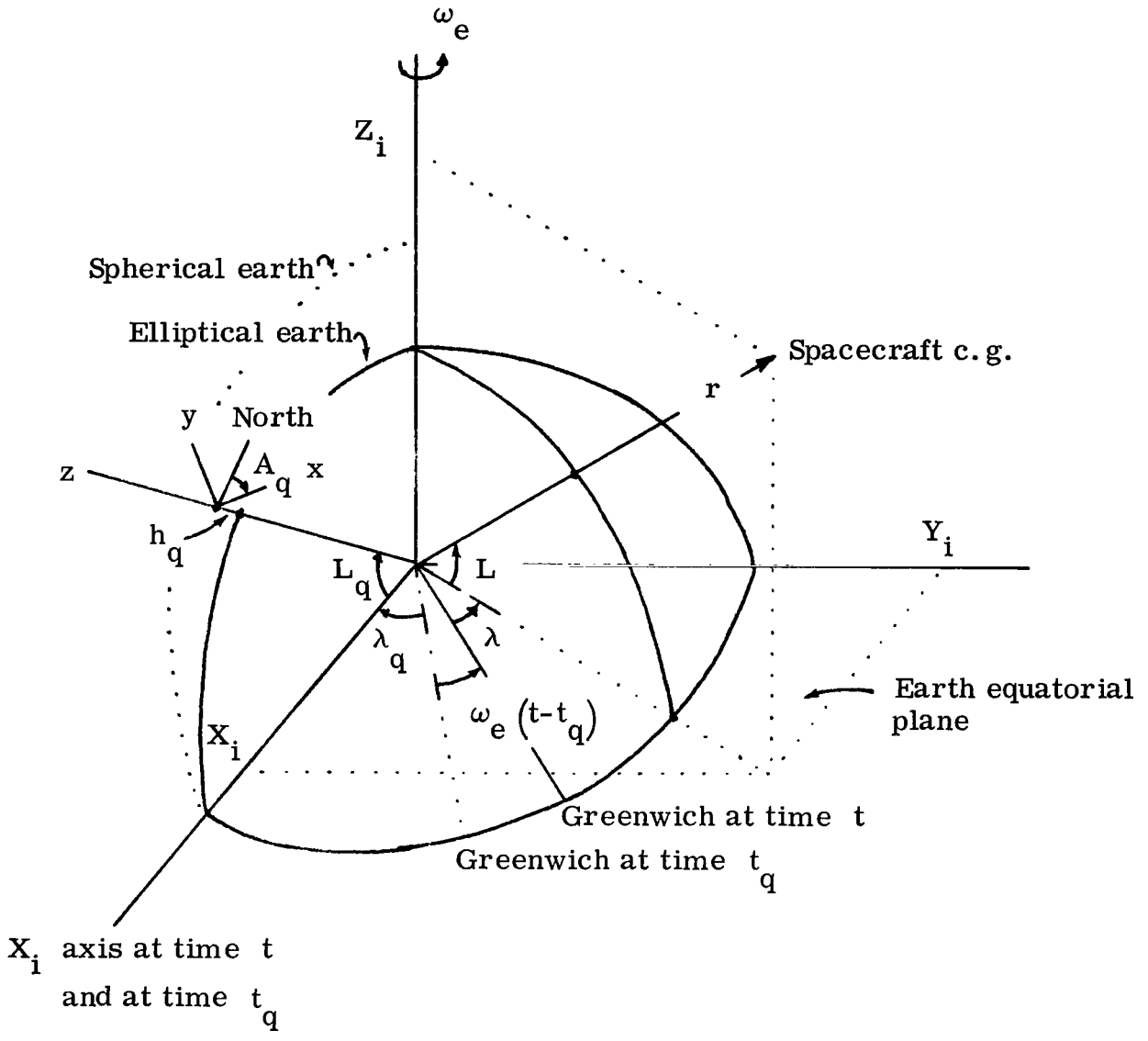

Figure 4.0-3. - Inertial, topocentric, rectangular coordinates x, y, z. The position and velocity components of Input-Output 6 and the velocity components of Input-Output 7 are measured in this system. The origin of the x, y, z system lies in the X_i-Z_i plane and hence remains fixed in space.

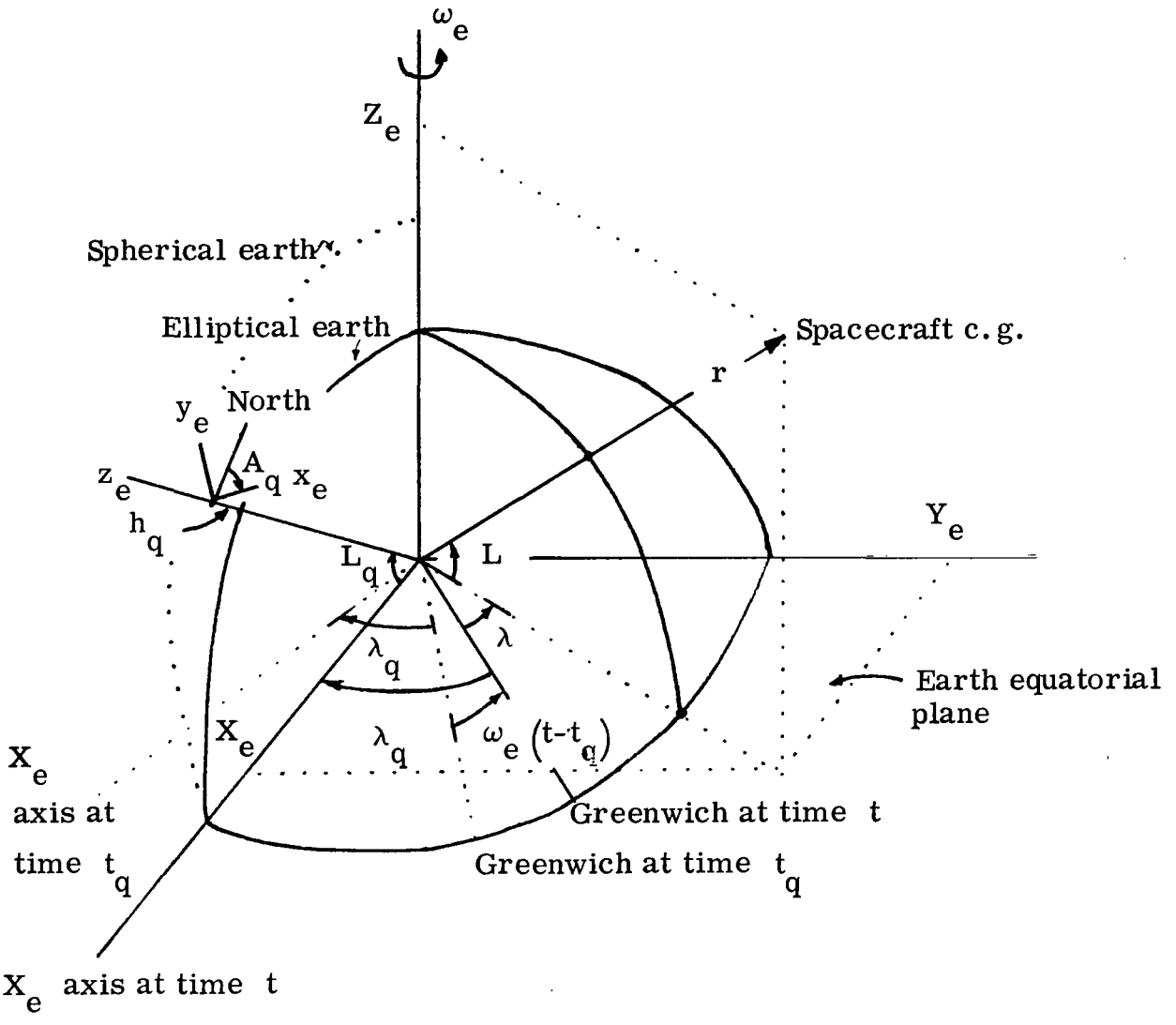

Figure 4.0-4. - Rotating, topocentric, rectangular coordinates x_e, y_e, z_e. The position components of Input-Output 7 and both the position and velocity components of Input-Output 8 are referenced to these coordinates. The radar station data of Output 9 are also measured with respect to a system of this type whose origin is at the radar station antenna and whose x_e axis always points north. The x_e, y_e, z_e system origin remains in the X_e-Z_e plane and thus rotates with the earth.

Input 7

These coordinates are quasi-inertial, topocentric, rectangular. The origin of the system rotates with the earth, hence the time t_q on card 657 is not required, but cards 653 through 656 are still necessary. The coordinate origin has coordinates L_{D_q}, λ_q, h_q on the rotating earth; the x_q-y_q plane is parallel to the spheroid surface at the aforementioned coordinates, and the x_q axis is inclined at an aximuth A_q east of north. The z_q axis is positive up as in Input 6. Position is measured with respect to the rotating coordinates, but velocity is inertial. Figures 4.0-3 and 4.0-4 give a graphical representation of this system.

653 DEC	L_{D_q}	geodetic latitude of origin, deg
654 DEC	λ_q	longitude of origin relative to Greenwich, deg
655 DEC	h_q	altitude of origin above reference spheroid, ft
656 DEC	A_q	azimuth of x_q axis east of north, deg
841-843 DEC	x_q, y_q, z_q	ft
844-846 DEC	$\dot{x}_q, \dot{y}_q, \dot{z}_q$	ft/sec

Input 8

The coordinates in this system are rotational, topocentric, and rectangular. This coordinate system is the same as that of Input 7 except both

position and velocity are measured with respect to the rotating coordinates. Cards 653 through 656 are required. See figure 4.0-4 for a diagram of this system.

653 DEC	L_{D_q}	geodetic latitude of origin, deg
654 DEC	λ_q	longitude of origin relative to Greenwich, deg
655 DEC	h_q	altitude of origin above reference spheroid, ft
656 DEC	A_q	azimuth of x_e axis east of north, deg
841-843 DEC	x_e, y_e, z_e	ft
844-846 DEC	$\dot{x}_e, \dot{y}_e, \dot{z}_e$	ft/sec

5.0 NUMERICAL INTEGRATION OF DIFFERENTIAL EQUATIONS

QUIKE, a variable step-size numerical integration routine, written by Mr. Frederick Nau of NASA-MSC, is used to integrate the differential equations of motion and to control the program operation. Integration with a constant step-size is also available. A fourth-order Runge-Kutta (ref. 3) technique is employed which approximates a fifth-order method by the addition of an error term to each of the dependent variables. The beginning time and the initial value of each of the dependent variables are input in single precision; thereafter, all variables are incremented in double precision to minimize truncation error.

Numerical integration of a differential equation is in reality a summing of small increments of the dependent variable over the range of integration. A general discussion of the manner in which the Runge-Kutta scheme operates, when applied to a first-order differential equation, will give a better idea of how a trajectory can be computed as a function of time.

In this program 10 differential equations or dependent variables are integrated as a function of one independent variable, time. The discussion here will be restricted to one dependent variable as a function of one independent variable, but it is easy to generalize to m dependent variables.

Let the independent variable be x, and the dependent variable be $y = y(x)$, with the increment or integration step size Δx in the independent variable. At the initial point n of the integration, the values of x and y, say x_n and y_n, will be known, and from this information we can evaluate the derivative of y with respect to x. We are now in a position to compute approximations for the increment Δy in the dependent variable and to evaluate y at the end of an interval Δx.

In order to simplify the discussion it will be necessary first to establish a convention of superscripts and subscripts. The ith evaluation of the derivative $\dot{y} = \frac{dy}{dx}$ at the point $x = x_n + j\,\Delta x$ be denoted by $\dot{y}^i_{n+j}$. Thus at $x = x_n + \frac{1}{2}\Delta x$, the third evaluation of $\dot{y}$ would be $\dot{y}^3_{n+\frac{1}{2}}$. The ith approximation for the increment Δy as determined from the ith evaluation of the derivative $\dot{y}^i_{n+j}$ at $x = x_n + j\,\Delta x$ taken over an interval $k\,\Delta x$ will be represented by Δy^i_{n+k}. For example, the third approximation of Δy using the interval Δx and the third evaluation of the derivative at $x = x_n + \frac{1}{2}\Delta x$ is written $\Delta y^3_{n+1} = \Delta x \dot{y}^3_{n+\frac{1}{2}}$.

In a similar manner the ith approximation of the value of y at the end of an increment $k\,\Delta x$ will be defined as $y^i_{n+k} = y_n + \Delta y^i_{n+k}$. Continuing the foregoing example gives for the third approximation to y at the point $x = x_n + \Delta x$, $y^3_{n+1} = y_n + \Delta y^3_{n+1}$.

Returning to the discussion of the Runge-Kutta technique, evaluate the derivative $\dot{y}$ at the point x_n, y_n and from it obtain a first approximation to Δy. Thus,

$$\dot{y}_n{}^1 = \frac{dy_n{}^1}{dx_n} \tag{64}$$

$$\Delta y^1_{n+1} = \Delta x \dot{y}_n{}^1 \tag{65}$$

Sufficient information is now available to evaluate the derivative again, this time at the midpoint of the interval at $x = x_n + \frac{1}{2}\Delta x = x_{n+\frac{1}{2}}$, $y = y_n + \frac{1}{2}\Delta y^1_{n+1} = y^2_{n+\frac{1}{2}}$, and to obtain a second approximation to Δy over the interval Δx

$$\dot{y}^2_{n+\frac{1}{2}} = \frac{dy^2_{n+\frac{1}{2}}}{dx_{n+\frac{1}{2}}} \tag{66}$$

$$\Delta y^2_{n+1} = \Delta x \dot{y}^2_{n+\frac{1}{2}} \tag{67}$$

Again the derivative is computed at the midpoint of the interval with $x = x_n + \frac{1}{2}\Delta x = x_{n+\frac{1}{2}}$, $y = y_n + \frac{1}{2}\Delta y^2_{n+1} = y^3_{n+\frac{1}{2}}$, and a third approximation to Δy is determined over the whole interval Δx

$$\dot{y}^3_{n+\frac{1}{2}} = \frac{dy^3_{n+\frac{1}{2}}}{dx_{n+\frac{1}{2}}} \tag{68}$$

$$\Delta y^3_{n+1} = \Delta x \dot{y}^3_{n+\frac{1}{2}} \tag{69}$$

With this third approximation, the derivative is evaluated at the end of a whole interval where $x = x_n + \Delta x = x_{n+1}$, $y = y_n + \Delta y^3_{n+1} = y^4_{n+1}$, and a new Δy determined

$$\dot{y}^4_{n+1} = \frac{dy^4_{n+1}}{dx_{n+1}} \tag{70}$$

$$\Delta y^4_{n+1} = \Delta x \dot{y}^4_{n+1} \tag{71}$$

Both variables are now incremented in double precision to obtain their values at the end of the interval Δx; the "integration" of one interval has been completed: $\Delta y = \int_{x_n}^{x_n+\Delta x} \dot{y}\, dx$. Thus,

$$x_{n+1} = x_n + \Delta x \tag{72}$$

$$\Delta y_{n+1} = \frac{1}{6}\left(\Delta y^1_{n+1} + 2\,\Delta y^2_{n+1} + 2\,\Delta y^3_{n+1} + \Delta y^4_{n+1}\right) \tag{73}$$

$$y_{n+1} = y_n + \Delta y_{n+1} \tag{74}$$

It should be noted that the increment in the dependent variable is a weighted average of the sum of the four increment approximations. The increment values obtained from evaluation of the derivative at the interval midpoint have twice the influence of those determined from the derivatives computed at the interval end points.

When a constant interval is used (Special Option 16), QUIKE now proceeds to the next integration step and repeats the foregoing process. Four evaluations of the derivative were required.

In the variable step mode, QUIKE next evaluates the dependent variable over the interval Δx as the sum of the evaluations over the two half-intervals $x + \frac{1}{2}\Delta x$ and $\left(x + \frac{1}{2}\Delta x\right) + \frac{1}{2}\Delta x$ and compares this result with the evaluation over the whole interval which was previously described. The step size is halved and the current integration step repeated, or it is doubled, or remains constant for the next integration step, depending on the results of this comparison.

The derivative was retained at $x = x_n$, $y = y_n$, thus eliminating a redundant evaluation. From equation (64) given these values for the fifth evaluation, the derivative, which will be denoted by the superscript 1a, is evaluated at $x = x_n$, $y = y_n$. A first approximation to Δy over the first half-interval can now be formed

$$\dot{y}_n^{1a} = \dot{y}_n^{1} = \frac{dy_n}{dx_n} \tag{75}$$

$$\Delta y_{n+\frac{1}{2}}^{1a} = \frac{1}{2}\Delta x \dot{y}_n^{1a} \tag{76}$$

As a parallel to the example over the whole interval, the derivative is next evaluated at $x = x_n + \frac{1}{4}\Delta x = x_{n+\frac{1}{4}}$, $y = y_n + \frac{1}{2}\Delta y_{n+\frac{1}{2}}^{1a} = y_{n+\frac{1}{4}}^{5}$, and from it, a second approximation to Δy over the half-interval $\frac{1}{2}\Delta x$

$$\dot{y}_{n+\frac{1}{4}}^{5} = \frac{dy_{n+\frac{1}{4}}^{5}}{dx_{n+\frac{1}{4}}} \tag{77}$$

$$\Delta y_{n+\frac{1}{2}}^{5} = \frac{1}{2}\Delta x \dot{y}_{n+\frac{1}{4}}^{5}$$

Again the derivative is evaluated at the quarter-interval $x = x_n + \frac{1}{4}\Delta x = x_{n+\frac{1}{4}}$, $y = y_n + \frac{1}{2}\Delta y^5_{n+\frac{1}{2}} = y^6_{n+\frac{1}{4}}$, and from it a third approximation for Δy

$$\dot{y}^6_{n+\frac{1}{4}} = \frac{dy^6_{n+\frac{1}{4}}}{dx_{n+\frac{1}{4}}} \tag{78}$$

$$\Delta y^6_{n+\frac{1}{2}} = \frac{1}{2}\Delta x \dot{y}^6_{n+\frac{1}{4}} \tag{79}$$

The process is repeated at

$$x = x_n + \frac{1}{2}\Delta x = x_{n+\frac{1}{2}}, \quad y = y_n + \Delta y^6_{n+\frac{1}{2}} = y^7_{n+\frac{1}{2}}$$

Note that this is at the end of the first half-interval. This gives

$$\dot{y}^7_{n+\frac{1}{2}} = \frac{dy^7_{n+\frac{1}{2}}}{dx_{n+\frac{1}{2}}} \tag{80}$$

$$\Delta y^7_{n+\frac{1}{2}} = \frac{1}{2}\Delta x \dot{y}^7_{n+\frac{1}{2}} \tag{81}$$

Both variables are now incremented in double precision so that they reflect the values at the midpoint of the interval, that is, at $\frac{1}{2}\Delta x$

$$x_{n+\frac{1}{2}} = x_n + \frac{1}{2}\Delta x \tag{82}$$

$$\Delta y_{n+\frac{1}{2}} = \frac{1}{6}\left(\Delta y^{1a}_{n+\frac{1}{2}} + 2\,\Delta y^{5}_{n+\frac{1}{2}} + 2\,\Delta y^{6}_{n+\frac{1}{2}} + \Delta y^{7}_{n+\frac{1}{2}}\right) \tag{83}$$

$$y_{n+\frac{1}{2}} = y_n + \Delta y_{n+\frac{1}{2}} \tag{84}$$

It should be noted that the derivatives were evaluated only three times over the first half of the interval Δx.

This same procedure is repeated for the second half of the interval, namely evaluating the derivative at each end point and twice in the middle of the half interval $\left(\text{at } x = x_n + \frac{1}{2}\Delta x,\ x = x_n + \frac{3}{4}\Delta x,\ x = x + \Delta x\right)$, and from these derivatives is computed an increment Δy. By using the same symbolism as before, the values for the second half-interval are determined as shown, where $y^{8}_{n+\frac{1}{2}} = y_{n+\frac{1}{2}}$ from equation (84). Thus,

$$\dot{y}^{8}_{n+\frac{1}{2}} = \frac{dy^{8}_{n+\frac{1}{2}}}{dx_{n+\frac{1}{2}}} \tag{85}$$

$$\Delta y^{8}_{n+\frac{1}{2}+\frac{1}{2}} = \frac{1}{2}\,\Delta x \dot{y}^{8}_{n+\frac{1}{2}} \tag{86}$$

$$\dot{y}^{9}_{n+\frac{1}{2}+\frac{1}{4}} = \frac{dy^{9}_{n+\frac{1}{2}+\frac{1}{4}}}{dx_{n+\frac{1}{2}+\frac{1}{4}}} = \frac{d\left(y^{8}_{n+\frac{1}{2}} + \frac{1}{2}\,\Delta y^{8}_{n+\frac{1}{2}+\frac{1}{2}}\right)}{d\left(x_{n+\frac{1}{2}} + \frac{1}{4}\,\Delta x\right)} \tag{87}$$

$$\Delta y^{9}_{n+\frac{1}{2}+\frac{1}{2}} = \frac{1}{2}\,\Delta x \dot{y}^{9}_{n+\frac{1}{2}+\frac{1}{4}} \tag{88}$$

$$\dot{y}^{10}_{n+\frac{1}{2}+\frac{1}{4}} = \frac{dy^{10}_{n+\frac{1}{2}+\frac{1}{4}}}{dx_{n+\frac{1}{2}+\frac{1}{4}}} = \frac{d\left(y^{8}_{n+\frac{1}{2}} + \frac{1}{2}\,\Delta y^{9}_{n+\frac{1}{2}+\frac{1}{2}}\right)}{d\left(x_{n+\frac{1}{2}} + \frac{1}{4}\,\Delta x\right)} \tag{89}$$

$$\Delta y^{10}_{n+\frac{1}{2}+\frac{1}{2}} = \frac{1}{2}\,\Delta x \dot{y}^{10}_{n+\frac{1}{2}+\frac{1}{4}} \tag{90}$$

$$\dot{y}^{11}_{n+\frac{1}{2}+\frac{1}{2}} = \frac{dy^{11}_{n+\frac{1}{2}+\frac{1}{2}}}{dx_{n+\frac{1}{2}+\frac{1}{2}}} = \frac{d\left(y^{8}_{n+\frac{1}{2}} + \Delta y^{10}_{n+\frac{1}{2}+\frac{1}{2}}\right)}{d\left(x_{n+\frac{1}{2}} + \frac{1}{2}\,\Delta x\right)} \tag{91}$$

$$\Delta y^{11}_{n+\frac{1}{2}+\frac{1}{2}} = \frac{1}{2}\,\Delta x \dot{y}^{11}_{n+\frac{1}{2}+\frac{1}{2}} \tag{92}$$

Incrementing of both variables over the interval Δx can now be done as the sum of the evaluations over two half-intervals $\frac{1}{2}\,\Delta x$. Double precision addition is used. The equations for this are

$$x_{n+\frac{1}{2}+\frac{1}{2}} = x_{n+\frac{1}{2}} + \frac{1}{2}\,\Delta x \tag{93}$$

$$\Delta y_{n+\frac{1}{2}+\frac{1}{2}} = \frac{1}{6}\left(\Delta y^{8}_{n+\frac{1}{2}+\frac{1}{2}} + 2\,\Delta y^{9}_{n+\frac{1}{2}+\frac{1}{2}} + 2\,\Delta y^{10}_{n+\frac{1}{2}+\frac{1}{2}} + \Delta y^{11}_{n+\frac{1}{2}+\frac{1}{2}}\right) \quad (94)$$

$$y_{n+\frac{1}{2}+\frac{1}{2}} = y_{n+\frac{1}{2}} + \Delta y_{n+\frac{1}{2}+\frac{1}{2}} = y_n + \Delta y_{n+\frac{1}{2}} + \Delta y_{n+\frac{1}{2}+\frac{1}{2}} \quad (95)$$

For the second half of the interval, four evaluations of derivatives were required. Over the two half-intervals the derivatives were computed a total of seven times making a total of eleven times for the whole interval.

The foregoing integration over the whole interval Δx and then over the two successive half-intervals $\frac{1}{2}\,\Delta x$ is carried out for each of the 10 dependent variables y_i. Here the subscript i denotes the ith dependent variable. The absolute error E_i between the whole and half-step integrations is determined from equations (73), (83), and (94).

$$E_i = \left(\Delta y_{n+\frac{1}{2}} + \Delta y_{n+\frac{1}{2}+\frac{1}{2}}\right)_i - \left(\Delta y_{n+1}\right)_i \quad (96)$$

An error term $\frac{E_i}{15}$ is then added to each of the y_i to approximate the accuracy attained by a fifth-order Runge-Kutta method. This term gives

$$y_i^{\,e} = \left(y_{n+\frac{1}{2}+\frac{1}{2}}\right)_i + \frac{E_i}{15} \quad (97)$$

The relative error is

$$R_i = \frac{\frac{E_i}{15}}{y_i^{\,e}} \quad (98)$$

and this value determines whether the interval Δx is to be halved, doubled, or is to remain constant.

If for any y_i,

$$|R_i| > \epsilon_i \tag{99}$$

and, if for the same y_i,

$$|y_i^e| > \delta_i \tag{100}$$

the current interval Δx is halved and the procedure beginning with equation (64) repeated. If $|y_i^e| \leq \delta_i$, then no halving occurs, where ϵ_i and δ_i are accuracy and small value criteria, respectively, for the ith dependent variable y_i.

The next integration interval Δx is doubled, and the current integration is accepted as valid if for all y_i,

$$|R_i| \leq \frac{\epsilon_i}{100} \tag{101}$$

The current integration is accepted, and the next interval remains unchanged if

$$\frac{\epsilon_i}{100} \leq |R_i| < \epsilon_i \tag{102}$$

for any y_i and the halving condition equation (99) is not met for any y_i.

If for any y_i, $\left|y_i^e\right| \leq \delta_i$, then this variable is not allowed to cause halving of the current interval size and will not prohibit doubling of the interval in the next step. The integration interval is never halved more than 20 times in any one step, in which case an error message "No convergence" is printed, and the case is terminated. Note that during a successful integration in the variable step-size mode, 11 evaluations of the derivatives were required: 4 over the whole interval Δx, 3 in the first half-interval $\frac{1}{2}\Delta x$, and 4 in the second half-interval.

The foregoing discussion of the Runge-Kutta method covered first-order differential equations. Equations of motion generally involve second derivatives, $\ddot{y} = \frac{d^2y}{dx^2}$. A second-order differential equation is treated as a first order by writing it $\ddot{y} = \frac{d\dot{y}}{dx}$, and numerically integrating it in the previously described manner.

The small value and accuracy criteria are normally set equal to 10^{-5} in the program, but including the following two cards with the trajectory case or section data will allow these values to be set by the user

520 DEC $\epsilon_1, \epsilon_2, \ldots, \epsilon_{10}$ accuracy criteria

550 DEC $\delta_1, \delta_2, \ldots, \delta_{10}$ small-value criteria

QUIKE performs another function, that of program control. It calls a section of the program which computes the derivatives at the appropriate time and tests at the end of each successful integration step to ascertain whether the termination condition has been met or passed. If the termination condition has not been achieved, the print frequency is checked, and if it is satisfied, the current data are printed in accordance with the activated outputs; if not, QUIKE then proceeds to integrate over the next interval. If the termination condition has been met, the results of the last integration step are printed, and the program then reads and prepares to execute the next step of the trajectory. When any integration step passes the termination condition, the computing interval is reduced so as to attain the desired stop conditions.

Figures 2.0-3 and 2.0-4 illustrate the control function of QUIKE.

6.0 ATTITUDE CONTROL

Body attitude may be specified in one of two ways. If 644 DEC 1 is used, all thrust and aerodynamic forces and the x_b axis are aligned with the aerodynamic velocity vector; the y_b and z_b axes are undefined. Thus $\alpha = \beta = \eta = 0$.

If 644 DEC 2, N, M is used, the positive z_b axis is defined to lie in the half-plane containing the downward geodetic vertical and the x_b axis, that is, z_b, is positive toward the earth. The x_b axis is defined in one of four ways given below, and the y_b axis completes a right-handed Cartesian coordinate system.

In the computation of pitch and yaw angles involving the arctangent function, it is possible that the arguments can be of such relative magnitudes that the angles are ill defined. When this is the case, the angles are set to zero.

The table control for attitude input is locations 710 through 712, and is a double table consisting of pitch and yaw as functions of section time or total elapsed time, depending on the special option used. The use of tables is explained in section 10.0.

The reader is referred to figures 3.1-7 and 3.1-8 for a graphical description of the angles used in the following description of control 644 DEC 2, N, M, where P_b is the pitch of the x_b axis measured positive up from the velocity vector, and Y_b is measured positive right from the velocity vector; both P_b and Y_b are obtained from a table. Note that θ and φ are the angles relating the body coordinates to the local geodetic coordinate system as shown in figures 3.1-7 and 3.1-8. The available attitude controls and their descriptions are now given.

644 DEC 2, 0, M (103)

The x_b axis is aligned with respect to one of the velocity vectors V_a, V_e, or V_i, as M = 0, 1, 2, respectively.

644 DEC 2, 0, 0 (104)

The x_b axis is aligned with respect to the aerodynamic velocity vector, and the body attitude angles are

$$\theta = \gamma_a + P_b$$

$$\varphi = \psi_a + Y_b$$

It is recommended that attitude control, 644 DEC 2, 0, 0, be used during a lifting or rolling reentry (Special Options 10 and 32).

644 DEC 2, 0, 1 (105)

The x_b axis is aligned with respect to the relative velocity vector. For the body attitude angles one has

$$\theta = \gamma_e + P_b$$

$$\varphi = \psi_e + Y_b$$

644 DEC 2, 0, 2 (106)

The x_b axis is aligned with respect to the inertial velocity vector, and the body attitude angles are

$$\theta = \gamma_i + P_b$$

$$\varphi = \psi_i + Y_b$$

644 DEC 2, 1 (107)

Under this attitude control, the x_b axis pitch is measured from the local geodetic platform and x_b axis azimuth from north. This attitude control should be used for vertical launches from the surface of the earth. In this case the body attitude angles are

$$\theta = P_b$$

$$\varphi = Y_b$$

644 DEC 2, 2, M (108)

This attitude control permits the x_b axis to be pitched with respect to the local geodetic platform and yawed with respect to one of the velocity vectors V_a, V_e, V_i as M = 0, 1, 2, respectively. For all values of M in this case, the body pitch with respect to the local geodetic platform is

$$\theta = P_b$$

644 DEC 2, 2, 0 (109)

Yaw the x_b axis with respect to the aerodynamic velocity vector, with φ given by

$$\varphi = \psi_a + Y_b$$

644 DEC 2, 2, 1 (110)

Yaw the x_b axis with respect to the relative velocity vector, thus φ is

$$\varphi = \psi_e + Y_b$$

644 DEC 2,2,2 (111)

Yaw the x_b axis with respect to the inertial velocity vector, and φ is thus

$$\varphi = \psi_i + Y_b$$

644 DEC 2, 3, M (112)

Pitch the x_b axis with respect to an inertial geodetic platform, and yaw the x_b axis from the aerodynamic, relative, or inertial velocity vector as M = 0, 1, 2, respectively. Figures 3.1-7 and 3.1-9 illustrate this attitude control.

The inertial geodetic platform is fixed in space, and is parallel to the earth's surface at coordinates L_{D_q}, λ_q, at time t_q. The platform is specified by the following information, which, for convenience, is taken to be the same as that required to define the coordinate system for Input-Output 6

653 DEC L_{D_q} geodetic latitude of inertial platform, deg

654 DEC λ_q longitude of inertial platform relative to Greenwich, deg

657 DEC t_q time at which the platform was at longitude λ_q, sec

where L_q is the geocentric equivalent of L_{D_q} as determined from equation (44). Even though the vehicle pitch is referenced to the inertial geodetic platform, the pitch θ relative to the local geodetic platform must be obtained to relate the body and local geodetic coordinate systems. For all values of M in this case θ is given by the law of cosines for spherical triangles:

$$\theta = \cos^{-1}\left(\cos \Delta L - 2 \cos L \cos L_q \sin^2 \frac{\Delta\lambda}{2}\right) + P_b \qquad (113)$$

where

$$\Delta L = L - L_q$$

$$\Delta\lambda = \lambda - \lambda_q + \omega_e \left(t - t_q\right)$$

644 DEC 2, 3, 0 (114)

Yaw of the x_b axis is measured from the aerodynamic velocity vector, hence φ is

$$\varphi = \psi_a + Y_b$$

644 DEC 2, 3, 1 (115)

Yaw of the x_b axis is measured from the relative velocity vector, and for φ we have

$$\varphi = \psi_e + Y_b$$

644 DEC 2, 3, 2 (116)

Yaw of the x_b axis is measured from the inertial velocity vector, so φ is given by

$$\varphi = \psi_i + Y_b$$

7.0 SPECIAL OPTIONS

Special options are additional computational features which allow more flexibility in the program. These can be called in or out at will. As an example, card 610 DEC K, L, -M will activate Special Options K and L and deactivate Special Option M. The 610 card can be used in both case data and section data. Special options are activated at the start of each case and at the start of each section and, with the exception of Special Options 13 and 33, carry over from section to section and from case to case.

Some special options result in internal changes in program logic, namely Special Option 1, while others generate output such as Special Option 7. Tables are required by some of the options, resulting in a table control card being necessary. The section on tabular data gives these details. Generally, when a special option is activated, the program performs additional computations not normally done.

A block of 30 locations, 610 through 639, is reserved for activation and/or deactivation of special options. There are more than 30 such options, but it is not likely that even 30 will be called in or out simultaneously.

Special Option 1

Look up body weight as a function of section time. The table control card locations are 705 through 707.

Special Option 2

Look up body weight as a function of elapsed time. The table control locations are 705 through 707.

Special Option 3

Look up aerodynamic coefficients C_a (altitude control 644 DEC 1) or C_a and C_n (attitude control 644 DEC 2, N, M) as functions of section time instead of functions of Mach number. The table control locations are 691 through 693 for C_a and 694 through 697 for C_n.

Special Option 4

Look up aerodynamic coefficients C_a and C_n as functions of elasped time instead of functions of Mach number. Table control locations are the same as those for Special Option 3.

Special Option 5

Look up thrust as a function of elasped time instead of a function of section time. Table control locations are 715 through 717.

Special Option 6

Look up body attitude $\left(\text{body pitch } P_b \text{ and body yaw } Y_b\right)$ as functions of elapsed time instead of functions of section time. Attitude control 644 DEC 2, N, M is required. Table control locations are 710 through 712.

Special Option 7

Compute the radiative and convective heat rates and integrate these to obtain total heat content. See Output 13 for a description of the two lines of data generated by this option. Equations (36), (37), and (38) are used in these calculations. The following information is required for Special Option 7 and may be considered as either case or section data

685 DEC R_n	spacecraft nose radius, ft
686 DEC d	characteristic length required for Reynolds number calculation, ft

687 DEC F'_c convective heating-rate multiplier

688 DEC F'_m free molecular heating-rate multiplier

689 DEC F'_r radiative heating-rate multiplier

Special Option 8

Look up atmospheric density as a function of altitude. Atmospheric pressure, molecular air temperature, and sound speed are computed in the usual manner. Table control locations are 751 through 753.

Special Option 9

Terminate this case after the next altitude stop.

Special Option 10

Look up the direction (roll angle φ_r) of the aerodynamic normal force vector F_n as a function of Mach number, where φ_r is positive counterclockwise from the negative z-body axis; the positive z_b axis points toward the earth (fig. 3.1-2). Table control locations are 700 through 702. See Special Option 32 for details on a roll rate capability. It is recommended that attitude control 644 DEC 2, 0, 0 be used with Special Option 10.

Special Option 11

Use the plumb bob horizon instead of the geodetic. The elements of the geodetic to geocentric transformation matrix (eq. (B5)), derived in appendix B, are computed by equations (117) through (120):

$$a_1 = g_r + r\omega_e^2 \cos^2 L \tag{117}$$

$$a_2 = g_L - r\omega_e^2 \sin L \cos L \tag{118}$$

$$\cos\left(L_D - L\right) = \frac{-a_1}{\sqrt{a_1^2 + a_2^2}} \tag{119}$$

$$\sin\left(L_D - L\right) = \frac{-a_2}{\sqrt{a_1^2 + a_2^2}} \tag{120}$$

Special Option 12

Use the geocentric horizon instead of the geodetic, that is, the geodetic to geocentric transformation matrix T_{G2C}, equation (B5), becomes a unit matrix.

Special Option 13

When Special Option 16 is used in two consecutive sections, the last integration interval in section n-1, Δt_{n-1}, and the first integration interval in section n, Δt_n, will obey the relation

$$\Delta t = \Delta t_{n-1} + \Delta t_n \tag{121}$$

where Δt is the integration interval specified on the 580 card. It is easy to see that if the value on the 580 card is changed in going from step n-1 to step n the first integration interval in step n will have an unexpected value, as given by equation (121). Special Option 13 prevents this occurrence, and should be activated when the integration interval on the 580 card is changed in going from one section to the next and when Special Option 16 is used in both sections. All integration steps including the first in the second section will then have the value on the 580 card. This option deactivates itself after being used once, hence the negative code has no meaning.

Special Option 14

Write a binary tape for use by other programs. The case and step descriptions (locations 500 through 519 and 640 through 643, respectively) are written at the start of each section. Tape B7 is used unless the card 115 BCD 1XN is included in the section or case data where Special Option 14 is activated; X denotes the channel A or B, and N denotes the tape numbers 1 through 10, inclusive. If an illegal channel or tape designation is given, an appropriate error message is printed on- and off-line and the case is terminated. Appendix E explains the tape format and lists the quantities written. One end of file mark is written on the tape if Special Option 14 was left activated through the end of the case.

Special Option 15

Calculate V_i/V_{i_r}, the ratio of inertial velocity to the minimun required orbital inertial velocity. Two constants K_6 and K_7 are required in locations 787 and 788, respectively; V_i/V_{i_r} is printed by Output 14, and is given by equation (D130).

Special Option 16

Use fixed integration interval. The step size specified on the 580 card will be used until subsequently changed by another 580 card. No halving or doubling of the step-size will occur. Termination of a section can be made on any termination quantity using fixed interval integration. If Special Option 16 was activated in a preceding section and the last interval in the last section, Δt_{n-1} was not a whole interval (as given on the 580 card), the first interval in the next section, Δt_n will obey equation (121) which is given under Special Option 13. This allows the user to print trajectory data at any desired time points as an aid to plotting or other uses. See Special Option 13 for further discussion.

Special Option 17

This Special Option controls Output 12, a general output, that can be varied as demands require. At present it is set to write the current values of elapsed time in seconds; altitude in feet; and aerodynamic velocity in

feet/second in format 3E19.8 on tape B1 whenever altitude is less than 400 000 ft and/or convective heat rate $\dot{H}_c$ is greater than 0.25 Btu/ft^2-sec. Any tape can be substituted for B1 by using the card 115 DEC N at the time this option is activated; N is the tape logical number.

Special Option 18

Suppress data heading printout and page restoring at the start of all succeeding sections.

Special Option 19

Print on-line the output data corresponding to the first time-point of the current section. This option deactivates itself after being used once, thus the negative code has no meaning. Only those outputs which are activated are printed on-line.

Special Option 20

Write on microfilm any output that is currently activated and printed on tape A3. Outputs that do not appear on A3 cannot be put on microfilm, for example the binary tape of Special Option 14.

Special Option 21

This Special Option allows up to 10 retrorockets to be used. The same quantities are required as for the three-retro mode, but different storage locations are employed.

340 DEC $A_1, A_2, \ldots, A_{10}$	exhaust-nozzle area, ft^2
350 DEC $\tau_1, \tau_2, \ldots, \tau_{10}$	thrust vector cant angles, deg
360 DEC $\sigma_1, \sigma_2, \ldots, \sigma_{10}$	thrust vector rotation angles, deg
370 DEC $T_1, T_2, \ldots, T_{10}$	thrust values, lb

380 DEC	$t_{i1}, t_{i2}, \ldots, t_{i10}$	thrust start times, sec
390 DEC	$t_{f1}, t_{f2}, \ldots, t_{f10}$	thrust stop times, sec
440 DEC	N	number of rockets

The thrust vector orientation angles are displayed graphically in figures 3.1-3 and 3.1-4. The thrust start- and stop-times are referenced to the start of the current section. If the number of retrorockets is omitted, or if Special Option 21 is activated prior to the section in which it is to be used, an error comment is printed on- and off-line, and the case is discontinued.

Special Option 22

This option is activated and used internally by the program in connection with Output 10 and Special Options 20 and 27. Certain data must be transferred into specific locations for these outputs and options to function properly, and this transfer is effected by Special Option 22.

Special Option 23

Calculate and integrate the convective, free molecular and radiative heating rates for Gemini or Apollo reentries. The convective heating rate $\dot{H}_c$ is the same as that in Special Option 7, however, radiative and free molecular heating rates are given by the formulas in appendix D. Free molecular heating-rate is not computed below 400 000 ft, and radiative heating rate is calculated only when the altitude is less than 300 000 ft. Data cards 685 through 689 are required the same as in Special Option 7. A table control card (739) and a table of K^{-1} values is required.

Special Option 24

Use equation (D131) to calculate the incremental change in the x component of velocity in the body-centered coordinates since the start of the current section.

Special Option 25

Look up aerodynamic coefficients C_a and C_n as functions of Mach number and pitch angle of attack α instead of functions of Mach number only. This option is not effective with attitude control 644 DEC 1.

Special Option 26

Use the 1962 U. S. Standard Atmosphere model to calculate atmospheric density, pressure, molecular scale temperature, speed of sound, and coefficient of viscosity.

Special Option 27

This Special Option uses Output 19 to write a plotter tape suitable for use on the Pace X-Y plotter; the plotter tape is written in 200 BPI density on A7. Card 581 controls the frequency at which data points are written.

In order to use this option, several things about the data must be known. Any regular output quantity that is printed on tape A3 as a floating point number can be plotted. Each output item has a unique index, and 15 such indexes must be specified during a plotting run. Appendix F gives these indexes. A scale factor U' (degrees per centimeter, feet per $\frac{1}{2}$ in., and so forth) is required for each of the 15 quantities plotted. Each scale factor U' must satisfy the relation

$$-10000 < \frac{200\left(x_{max.} - C'\right)}{U'} < 10000 \qquad (122)$$

where $x_{max.}$ is the maximum value (positive or negative, whichever magnitude is larger) that the quantity x will attain; C' is a constant subtracted from x to allow better resolution of the plot. For example, if it is desired to plot velocity V which has the range V = 25 500 ± 300 ft/sec, C' could be set to 25 000 in this case. Thus V - 25 000 would be plotted, resulting in a smaller scale factor being used and more detail in the plot. If at any time, the scale factor is such that equation (122) is violated, the last good data point is plotted until such time as the violation ceases to exist. When a violation first occurs, an on- and off-line message stating that the scale factor

for the Jth variable in the array of 15 is too small. This message is repeated off-line until the violation no longer exists, at which time another on- and off-line message states that plotting is resumed for the Jth variable. Note that equation (122) merely defines the minimum value the scale factor may have.

The Mercator projection of geodetic latitude versus longitude is available by putting a "1" in location 32076. A "1" in location 32077 will give symbol plotting as opposed to line or point plotting, and for this case, 15 symbol codes must be supplied. The available symbols and their respective codes are also given in appendix F. An example of the most general plot run is given.

32016 DEC $C'_{15}, C'_{14}, \ldots, C'_1$	constants used to expand plot
32031 DEC $S_{15}, S_{14}, \ldots, S_1$	symbol codes
32046 DEC $U'_{15}, U'_{14}, \ldots, U'_1$	scale factors
32061 DEC $I_{15}, I_{14}, \ldots, I_1$	indexes of quantities to be plotted
32076 DEC 1	for Mercator plotting of latitude
0	for no Mercator plotting of latitude
32077 DEC 1	for symbol plotting
0	for no symbol plotting

Special Option 28

Activation of this option deletes all off-line output on tape A3 and is of use when only microfilm, X-Y plotter, or binary tape output is desired.

Special Option 29

This Special Option allows the value on the 581 card to control the print frequency during the retroprediction mode. If this option is not activated, only the initial and final data points in each section are printed. This option should be activated in case-data for the retroprediction run.

Special Option 30

This Special Option deletes all on-line output.

Special Option 31

This Special Option prints the last data point of the current section on-line and then deactivates itself.

Special Option 32

Use a roll rate to determine the direction of the aerodynamic normal force vector F_n instead of the table lookup of roll angle φ_r in Special Option 10. The roll rate $\dot{\varphi}_r$ is specified on card 700 and should be zeroed out by the user when Special Option 32 is deactivated. Note that Special Options 10 and 32 cannot be used simultaneously, and that deactivation of Special Option 10 in effect deactivates 32. The use of altitude control 644 DEC 2, 0, 0 is recommended with Special Option 32.

Special Option 33

The ability to update position and velocity at the start of a section is provided by this option. Only Inputs 1 and 2 are permitted and must be specified on the 588 card. Any one or all the six position and velocity coordinates may be updated, and for any coordinate not updated, the program uses the current computed value for this coordinate. A zero should be used for any coordinate which is not updated. To update a coordinate to the value zero, use some small value, say 10^{-10}, which is not explicitly zero. Geocentric latitude cannot be used to update position; only geodetic latitude is permitted. This option automatically deactivates itself after each use, and consequently the negative code (-33) has no meaning. The updating information is input on the following cards

588 DEC N	N = 1 for Input 1 (inertial)
	N = 2 for Input 2 (relative)
91 DEC L_D	geodetic latitude, deg
92 DEC λ	longitude relative to Greenwich, deg

93 DEC h altitude above reference spheroid, ft

94 DEC V velocity, ft/sec

95 DEC γ flight path angle, deg

96 DEC ψ azimuth, deg

8.0 ATMOSPHERE MODELS

Three atmosphere models are available, plus the capability to look up atmospheric density as a function of altitude provided by Special Option 8. The three models are (1) the 1959 ARDC Atmosphere (ref. 4), (2) the MSC Composite Atmosphere, and (3) the 1962 U. S. Standard Atmosphere (ref. 5). In all three models the atmosphere is considered to be divided into several layers, and algebraic relations are used to determine the atmosphere in each layer.

The 1959 ARDC Atmosphere model is used unless otherwise specified. To obtain the MSC Composite Atmosphere, constants defining the model must be included with the trajectory data. These are given below. Activating Special Option 26 gives the 1962 U. S. Standard Atmosphere.

The MSC Composite Atmosphere model was formulated by Mr. Jack B. Hartung of the NASA-MSC in 1961. The following data cards are required to obtain the MSC Composite Atmosphere

2550 DEC 0, 49212.598, 101706.04, 154199.48, 173884.51, 252624.67
DEC 295275.59, 344488.19, 508530.18, 557742.73, 1377952.8
DEC 2296587.9

2562 DEC -6.0793687, -7.7515454, -10.424206, -12.757610, -13.482824
DEC -16.656321, -19.199217, -22.016699, -26.547104, -27.073640
DEC -32.408995, -36.180719

2574 DEC 300.06, 201.06, 231.46, 282.66, 282.66, 174.66, 174.66, 234.66
DEC 1184.66, 1334.66, 2334.66, 3314.66

2586 DEC -.00201168, .00057912, .00097536, 0, -.0013716, 0, .0012192
DEC .0057912, .003048, .0012192, .0010668

2544 DEC 870.92027

9.0 RANGE

Range over a spherical earth is computed in one of two ways from a reference point R_o. If location 680 contains a zero, it is assumed that R_o is given in east x_o and north y_o coordinates in feet from the initial point L_o, λ_o of the trajectory projected onto the surface of the earth. The range R is computed as the square root of the sum of the squares of the east and north components up to a maximum range of 300 000 ft, beyond which a spherical trigonometric formula is used.

680 DEC 0 — range option

681 DEC x_o, y_o — east and north coordinates of reference point R_o with respect to the initial point of the trajectory projected onto the surface of the earth, ft

If location 680 contains a "1", then the geodetic latitude and longitude of the reference point R_o are given in locations 681 and 682, respectively. The spherical trigonometric formula is then employed to compute the range.

680 DEC 1 — range option

681 DEC L_{D_r}, λ_r — geodetic latitude and longitude of range reference point, respectively, deg

Appendix G gives the formulas used in computing range using both of the foregoing options.

10.0 TABULAR INPUT

In addition to the initial input conditions, certain quantities dependent on the current trajectory conditions may be obtained from tabular data, for example, weight or thrust. The program provides the independent variables, determines the location, type, and size of the table from the appropriate table control locations, and then performs a linear interpolation to obtain the required information. The control locations are fixed, but the location of the

tables themselves is not. Locations 6000_{10} to 6400_{10} inclusive can be used and for very large tables locations 24576_{10} to 28672_{10} are available.

There are three types of tables:

(1) Univarient: one independent and one dependent variable,

$$y = f(x)$$

(2) Bivarient: two independent variables and one dependent variable,

$$z = f(x, y)$$

(3) Double: one independent variable and two dependent variables,

$$y_1 = f_1(x), y_2 = f_2(x)$$

An example of each table will illustrate its use. First, consider the univarient table. It is desired to interpolate thrust T from a table of five entries of thrust versus time t. The table control card provides the information about the table in locations 715 through 717; the zero in location 717 indicates that the table is univarient. The table itself begins in location 6000_{10}.

715 DEC 6000, 5, 0

6000 DEC $t_1, t_2, \ldots, t_5$

6005 DEC $T_1, T_2, \ldots, T_5$

For the bivarient table, consider the interpolation of the axial drag coefficient C_a as a function of four values of Mach number M and three

values of pitch angle of attack α. The table control locations are 691 through 693, and the table begins in location 6010_{10}.

691 DEC 6010, 4, 3

6010 DEC M_1, M_2, M_3, M_4

6014 DEC $\alpha_1, \alpha_2, \alpha_3$

6017 DEC $C_{a11}, C_{a12}, C_{a13}, C_{a14}$

6021 DEC $C_{a21}, C_{a22}, C_{a23}, C_{a24}$

6025 DEC $C_{a31}, C_{a32}, C_{a33}, C_{a34}$

Interpolation of body pitch P_b and body yaw Y_b as functions of time demonstrate the use of the double table. There are three values each of time t, P_b, and Y_b. Locations 710 through 712 provide the table control information, and the table begins in location 6030_{10}. The "2" in location 712 and the 6033 DEC 1,2 card denote a double table. Note that P_b precedes Y_b in the table.

710 DEC 6030, 3, 2

6030 DEC t_1, t_2, t_3

6033 DEC 1, 2

6035 DEC P_{b1}, P_{b2}, P_{b3}

6038 DEC Y_{b1}, Y_{b2}, Y_{b3}

In each of the tables it is possible to set the dependent variable or variables to constant values. For the univarient table, let the thrust have the constant value 1000; the table then reduces to the single card

715 DEC 0, 1000., 0

A constant C_a of 0.5 would be represented in the bivarient table as

691 DEC 0, .5, 0

In the double table, the constant values $P_b = 60°$ and $Y_b = 75°$ would be written

710 DEC 0, 60., 75.

All tables require three items of control information. A list of the available table controls is given.

691 DEC 0, 0, 0	axial drag coefficient C_a
694 DEC 0, 0, 0	aerodynamic normal force coefficient, C_n
697 DEC 0, 0, 0	wind table, north wind W_N followed by east wind W_E
700 DEC 0	roll rate (Special Option 32)
700 DEC 0, 0, 0	roll angle (Special Option 10)
705 DEC 0, 0, 0	weight (Special Options 1 or 2)
710 DEC 0, 0, 0	body attitude angles pitch P_b followed by yaw Y_b

715 DEC 0,0,0 thrust T

739 DEC 0,0,0 aerodynamic constant K^{-1} for Gemini-Apollo heating equations (Special Option 23)

751 DEC 0,0,0 atmospheric density ρ (Special Option 8)

11.0 INPUT DATA FORMAT

CO3E uses an input routine which will recognize three types of data: decimal DEC, octal OCT, and alphanumeric BCD. Each card should have a decimal number in columns 1 through 6 giving the memory location into which the data on the card are to be stored. If columns 1 through 6 are blank, the data on the card are stored beginning in location n+1 where location n was the last location used in storing data on the preceding card. Columns 8 through 10 denote the type of data, DEC, OCT, or BCD; the data will begin in column 12 for DEC and OCT and in column 13 for BCD. BCD data will often have a one-digit number in column 12 denoting the number of six-character words on the card. If column 12 is blank on a BCD card, then 10 words are assumed (60 characters, including blanks). Words in excess of the number specified in column 12 are ignored.

Normally a blank occurring in column 12 or thereafter on DEC or OCT cards will result in no more data being read from that card. The one exception is on the DEC card: a single blank immediately following an E, denoting a power of 10 by which the number is to be multiplied, will be ignored. Thus output cards generated by a FORTRAN program can be used as CO3E input. It is possible to have several numbers on the same DEC or OCT card, separated by commas. In this case the number beginning in column 12 goes into location n specified in columns 1 through 6, the second number on the card into location n+1, and so forth. A number cannot be divided between two cards, and no comma follows the last number on a card.

Decimal data will consist of one or more numerals without spaces, and may or may not contain a decimal point, as required by the input quantity. Decimal numbers are of two types, integers without decimals, and floating point with a decimal. If the E is used, the decimal point may be omitted under certain circumstances. The constant π illustrates this:

π =3.14159 =.314159E+1 = .314159E 1 =314.159E-02 =314159E-5

Octal data consist of 1 to 12 of the digits 0 through 7 and must be right justified. This type of data is used primarily to make program corrections at execution time.

12.0 TERMINATION CONDITIONS

Computation in any section can be terminated on any one of a number of quantities. If several termination conditions are specified, the first one to be met results in cessation of computation for that section.

When termination is to be made on position or velocity, the appropriate coordinate system must be specified on the 589 card. Termination coordinate systems 1 through 8 and 10 are permitted and are the same as the corresponding output coordinate systems which have been explained.

The available termination parameters are tabulated below.

Location	Quantity
900 DEC t	total elapsed time, sec
901 DEC x 902 DEC y 903 DEC z	three position coordinates as determined by the 589 card
904 DEC $\dot{x}$ 905 DEC $\dot{y}$ 906 DEC $\dot{z}$	three velocity coordinates indicated by the 589 card
907 DEC W	weight, lb
908 DEC R	range, ft or n. mi., depending on the range option, card 680
909 DEC χ	track, n. mi.
911 DEC t_c	time from beginning of case, sec

Location	Quantity
912 DEC t_s	time from beginning of section, sec
913 DEC H_c	convective heating content, Btu/ft^2
914 DEC H_r	radiative heating content, Btu/ft^2
915 DEC $\bar{q}$	dynamic pressure, lb/ft^2
916 DEC g	total g load, g units
918 DEC θ_c	central angle, deg
919 DEC ΔV	delta V, ft/sec, if Special Option 24 is activated
450 DEC H, M, S.	total elapsed time, hr, min, sec
453 DEC H, M, S.	section time, hr, min, sec
456 DEC N, λ	revoluation number, longitude in deg
456 DEC N, , $\lambda_d, \lambda_m, \lambda_s$	revolution number, longitude in deg min, sec
461 DEC N, v	revolution number, true anomaly in deg
754 DEC D, H, M, S.	GMT, days, hr, min, sec

In the retroprediction mode only, the card

790 DEC N, λ_i	revolution number, impact longitude in revolution N, deg

is required to signify the desired impact longitude. This must always be included with the termination conditions. Note that a termination condition in this usage is only a first estimate to the time or point to fire the

retrorockets, and that the program then adjusts the retrofire time to hit the desired target.

If 790 DEC 0 is used, no iteration will occur, but instead the retrorockets will be fired at the specified termination condition, and the spacecraft will simply reenter.

13.0 DESCRIPTION OF OUTPUT AND OUTPUT COORDINATE SYSTEMS

The information computed has been grouped into blocks which can be printed conveniently as a related unit; for example, position and velocity in a particular coordinate system. Output M is activated by using the card 590 DEC M, and Output N is deactivated by putting a -N on the same card. At the start of each section, outputs are activated and/or deactivated as directed by the 590 card and remain so throughout that section. Outputs carry over from section to section and from case to case until a subsequent change by another 590 card. The 590 card is designated as section data and should not be used as case input. Headings are printed for all activated outputs at the start of each section.

With the exception of Outputs 12 and 19, each output consists of one or more lines of data; these exceptions are explained under the appropriate output. In order to make the program more efficient, the output transformations from the L, λ, r coordinate system, in which integration occurs, is not effected unless an activated output or a termination condition requires such transformation.

All output coordinate systems are right-hand, and are exactly the same as the corresponding input coordinate system. For this reason, the description of the output coordinate systems will be brief; a complete discussion of each coordinate system is included in section 4.0.

It should be noted that the activated outputs are always printed in the order in which they are listed below, irrespective of the order of the codes on the 590 card.

Output 0

This output consists of three lines which are always printed regardless of the information on the 590 card. See figures 3.1-2, 3.3-1, and 3.3-3.

First Line

t	elapsed time, sec
t	elapsed time, hr, min, sec
t_s	section time, sec
t_c	case time, sec
GMT	Greenwich mean time, days, hr, min, sec
L_D	geodetic latitude, deg, min, sec
N	current revolution number
λ	earth referenced longitude, deg, min, sec

Second Line

L	geocentric latitude, deg
L_D	geodetic altitude, deg
λ	Greenwich referenced longitude, deg
h	altitude above reference spheroid, ft
R	range, ft or n. mi., depending on the range option
V_a	aerodynamic velocity, ft/sec
γ_a	aerodynamic flight path angle, deg
ψ_a	aerodynamic azimuth, deg

Third Line

g_x load factor along the x_b axis, g units

g_y load factor along the y_b axis, g units

g_z load factor along the z_b axis, g units

r orbit radius, ft

T total thrust, lb

W vehicle weight, lb

M Mach number

$\bar{q}$ dynamic pressure, lb/ft^2

Output 1

See figures 3.3-2 and 3.3.3 for diagrams of some output 1 quantities.

V_i inertial velocity, ft/sec

γ_i inertial flight path angle, deg

ψ_i inertial azimuth, deg

V_e relative velocity, ft/sec

γ_e relative flight path angle, deg

ψ_e relative azimuth, deg

γ_D geodetic flight path angle, deg

ψ_D geodetic azimuth, deg

Output 2

Figures 3.1-7, 3.3-4, and 3.3-5 show some Output 2 items.

η total angle of attack, deg

α pitch angle of attack, deg

β side slip angle, deg

D drag force along the wind axis, lb

F_{a_n} aerodynamic normal force perpendicular to the wind axis, lb

φ_n angle between F_{a_n} and the vertical plane defined by V_a and Z_D

θ body pitch angle measured from local geodetic plane, deg

φ body azimuth angle measured in local geodetic plane, deg

Outputs 3 through 8 are the same coordinate systems as the corresponding inputs, with the coordinates being specified in exactly the same fashion. For a more complete description, refer to the appropriate Input, section 4.0.

Output 3

Output 3 is an inertial, geocentric, rectangular coordinate system with the X_i axis specified by a longitude λ_x and a time t_x as in Input 3. Both position and velocity are inertial. See Input 3 and figure 4.0-1 for more information.

X_i, Y_i, Z_i ft

$\dot{X}_i, \dot{Y}_i, \dot{Z}_i$ ft/sec

Output 4

This is a quasi-inertial, geocentric, rectangular coordinate system with the X_q axis defined by a longitude λ_x, the same as Input 4. The position is with respect to the rotating earth but velocity is inertial. Input 4 and figures 4.0-1, 4.0-2 give more detail.

X_q, Y_q, Z_q ft

$\dot{X}_q, \dot{Y}_q, \dot{Z}_q$ ft/sec

Output 5

These coordinates form a geocentric, rectangular, rotating system with both position and velocity measured in the rotating frame. The X_e axis is specified by a longitude λ_x in the same manner as Input 5. More description can be found under Input 5 and in figure 4. 0-2.

X_e, Y_e, Z_e ft

$\dot{X}_e, \dot{Y}_e, \dot{Z}_e$ ft/sec

Output 6

Output 6 is an inertial topocentric, rectangular coordinate frame. The origin is positioned in space by a geodetic latitude L_{D_q}, a longitude λ_q, an altitude h_q, and a time t_q. The axis is yawed east of north by an azimuth A_q like Input 6. Position and velocity are inertial. Input 6 gives a more complete description; see also figure 4.0-3.

x, y, z ft

$\dot{x}, \dot{y}, \dot{z}$ ft/sec

Output 7

This coordinate system is a quasi-inertial, topocentric, rectangular one with the origin being specified by a geodetic latitude L_{D_q}, a longitude λ_q, and an altitude h_q as in Input 7. The x_q axis is yawed east of north by an angle A_q. Position is measured with respect to the rotating coordinate system, but the velocity is inertial. For a more detailed description, see Input 7 and figures 4.0-3 and 4.0-4.

x_q, y_q, z_q ft

$\dot{x}_q, \dot{y}_q, \dot{z}_q$ ft/sec

Output 8

This is a rotating, topocentric, rectangular coordinate system whose origin is defined by a geodetic latitude L_{D_q}, a longitude λ_q, and an altitude h_q in the same way as Input 8. The x_e axis is yawed from north by an azimuth A_q. Position and velocity are measured relative to the rotating coordinates. See Input 8 and figure 4.0-4 for more details.

x_e, y_e, z_e ft

$\dot{x}_e, \dot{y}_e, \dot{z}_e$ ft/sec

Output 9

The position and velocity of the spacecraft expressed in radar station centered polar coordinates is printed for any one of 30 radar stations whenever the vehicle is within a prescribed range of the station. See appendix H for the format of the radar station input data, a description of the radar

station coordinate system, and the vehicle pickup tolerances. Figure 13.0-1 illustrates some of Output 9 quantities.

Station Name

R_r slant range from radar station to vehicle, n. mi.

E_r elevation angle from the local geodetic horizontal at the radar station, deg

A_r azimuth from north, deg

$\dot{R}_r$ $\frac{dR_r}{dt}$ ft/sec

$\dot{E}_r$ $\frac{dE_r}{dt}$ deg/sec

$\dot{A}_r$ $\frac{dA_r}{dt}$ deg/sec

h_s altitude of the line of sight, ft

Output 10

This output gives orbital parameters (refs. 6, 7, 8) for a particle mass in a near earth orbit. The inertial X_i, Y_i, Z_i coordinates and velocities of Output 3 are required as input for this portion of the program; consequently, any time Output 10 is activated, the program automatically activates Output 3. When Output 10 is deactivated, Output 3 is not deactivated by the program.

One should be cautious in the use of Output 10. When the orbit about the earth has been perturbed or altered, as on a reentry, the altitudes of apogee and perigee may become negative. This means that the particular orbit resulting in negative or other unusual altitudes is one whose apogee or perigee actually lies inside the earth spheroid, which is not mathematically meaningless as the earth is treated as if all its mass were concentrated at its center.

See figures 13.0-2 and 13.0-3 for a graphical description of this output.

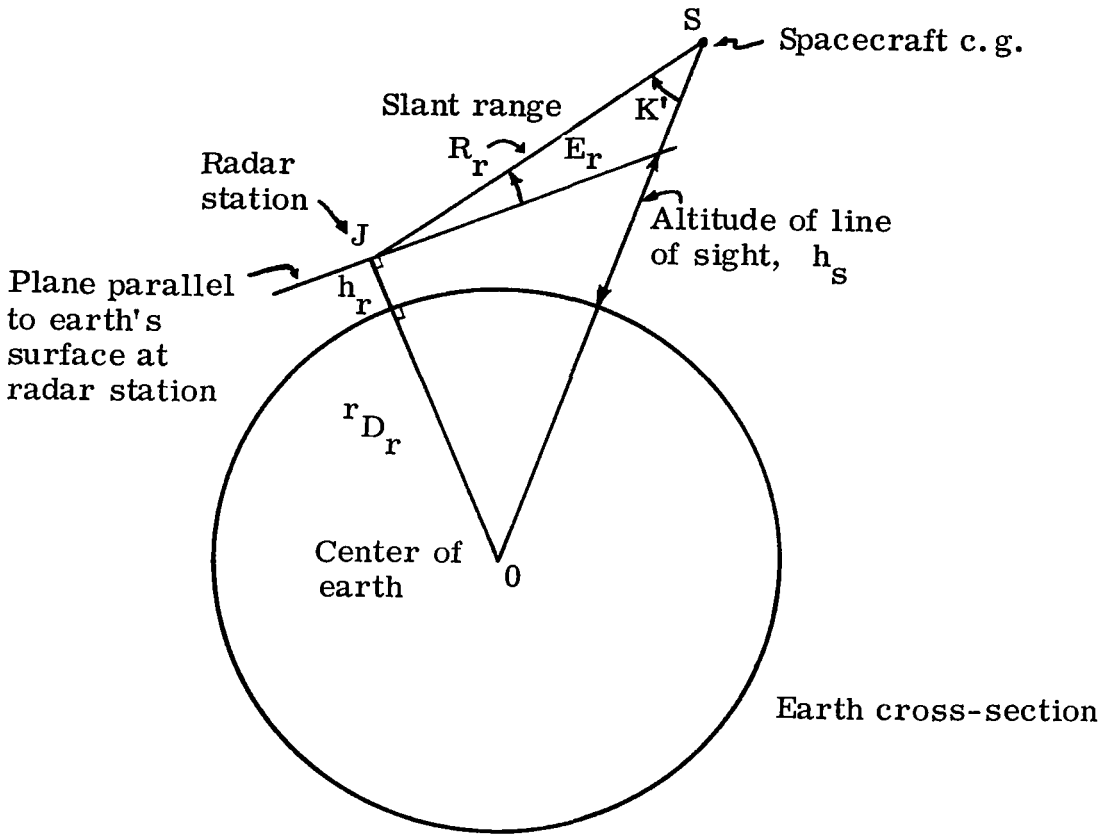

Figure 13.0-1. - Radar station output (Output 9). The plane of the page (0JS plane) is that defined by the spacecraft S, the earth center 0, and the radar station antenna J. The altitude h_s of the line of sight, slant range R_r, and the elevation angle E_r all lie in the 0JS plane.

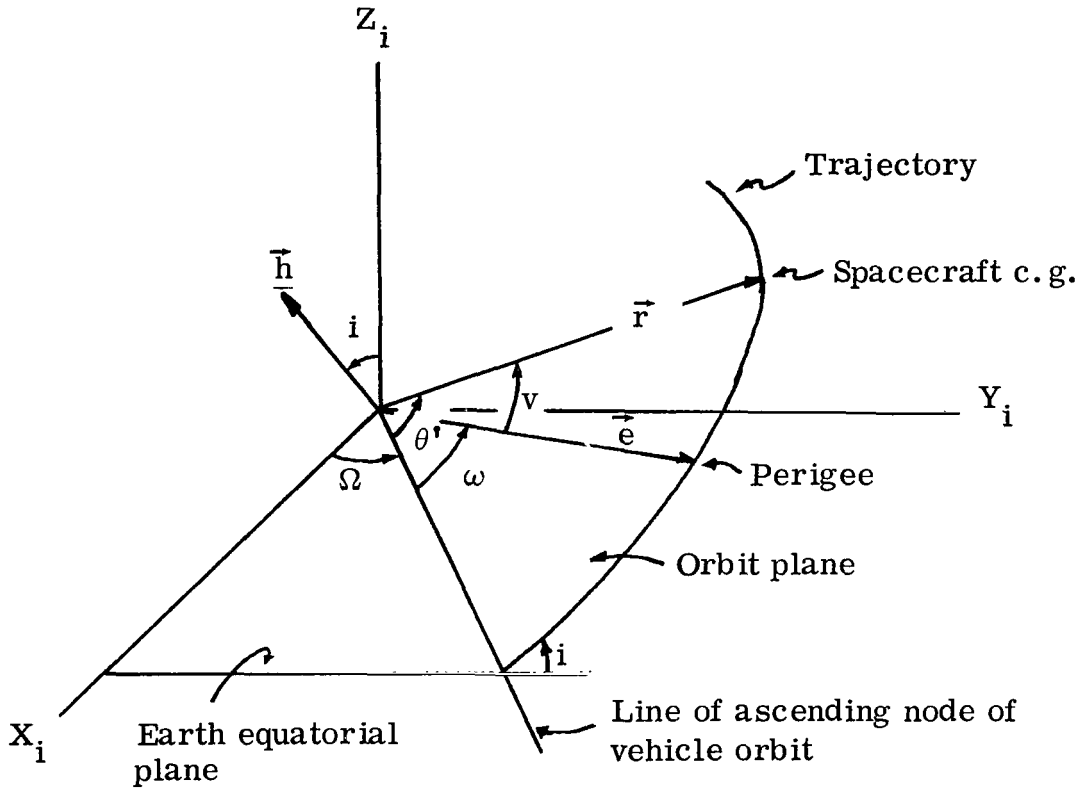

Figure 13.0-2.- Orbital parameters (Output 10) in relation to inertial X_i, Y_i, Z_i coordinates. Shown are the argument of the line of the ascending node Ω, argument of perigee ω, true anomaly v, the angle θ' between the line of the ascending node and $\vec{r}$, and the inclination i of the orbit plane with respect to the earth equatorial plane. Note that ω and v are measured in the orbit plane. The vector $\vec{e}$ is always directed toward the perigee.

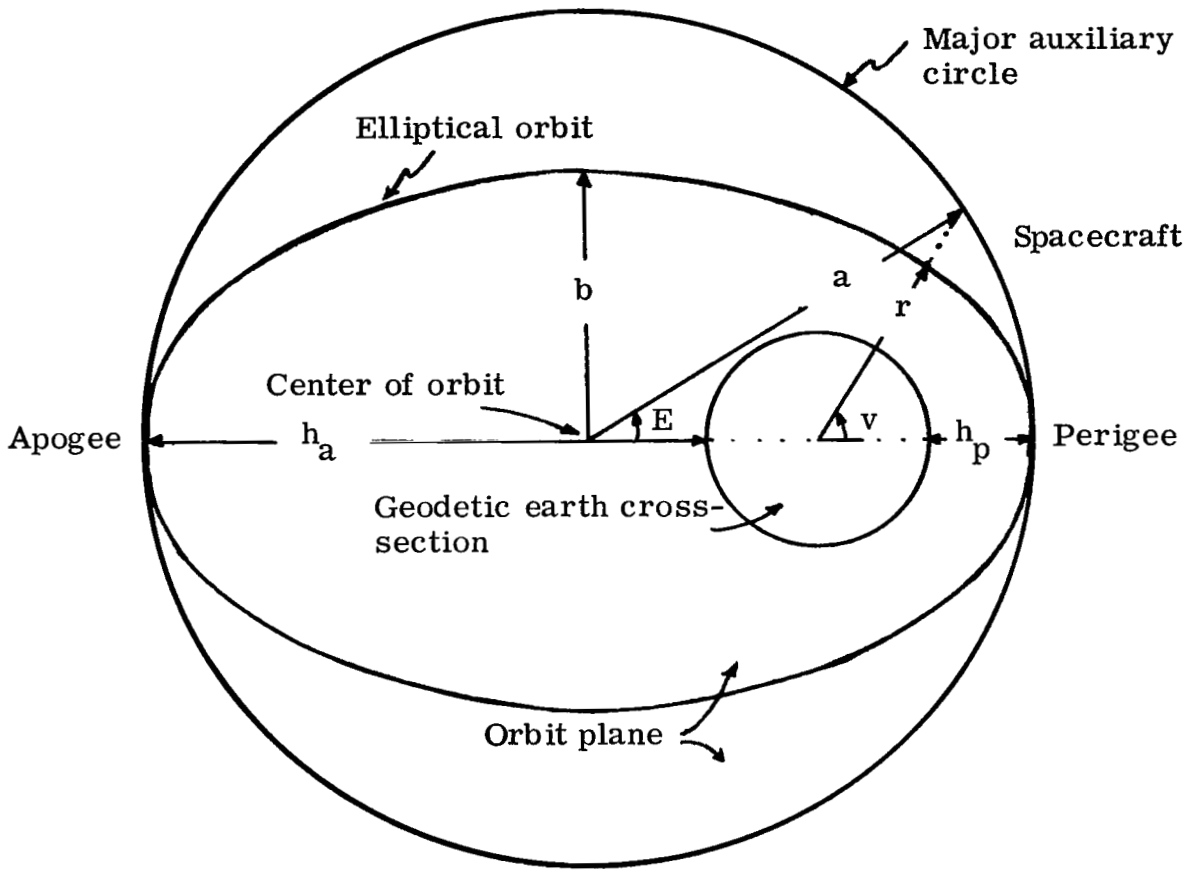

Figure 13.0-3. - Orbital parameters shown in the orbit plane (Output 10). This diagram shows the semimajor axis a, semiminor axis b, true anomaly v, eccentric anomaly E, attitude of perigee h_p, and altitude of apogee h_a.

First Line

h_p perigee altitude above the reference spheroid, n. mi.

h_a apogee altitude above the reference spheroid, n. mi.

λ_p longitude at which perigee occurs relative to Greenwich, deg

L_{D_p} geodetic latitude of perigee, deg

L_p geocentric latitude of perigee, deg

λ_a longitude at which apogee occurs relative to Greenwich, deg

L_{D_a} geodetic latitude of apogee, deg

i inclination of orbit plane with respect to earth equatorial plane, deg

Second Line

e orbit eccentricity

T_p satellite period, min

ω argument of perigee, deg

E eccentric anomaly, deg

v true anomaly, deg

λ_n longitude of line of ascending node relative to Greenwich, deg

τ_p elapsed time of next perigee passage, relative to launch or reference time, sec

a orbit semimajor axis, ft

Output 11

Not used.

Output 12

Used in conjunction with Special Option 17.

Output 13

This output is automatically activated by the program any time Special Option 7 or 23 is activated, likewise deactivation of these Special Options deactivates this output. Special Option 23 causes all the information below to be printed; Special Option 7 prints the same information with the exception of the molecular heat rate and integral. Output 13 must not be activated on the 590 card.

First Line

ρ atmospheric density, slug/ft^3

T_m molecular scale temperature, °R

$\dot{H}_c$ convective heat rate, Btu/ft^2-sec

H_c convective heat integral, Btu/ft^2

$\dot{H}_r$ radiative heat rate, Btu/ft^2-sec

H_r radiative heat integral, Btu/ft^2

$\dot{H}_t$ total heat rate $\left(\dot{H}_c + \dot{H}_r\right.$ for Special Option 7 or $\dot{H}_c + \dot{H}_r + \dot{H}_m$ for Special Option 23$\left.\right)$, Btu/ft^2-sec

H_t total heat integral $\left(H_c + H_r\right.$ for Special Option 7 or $H_c + H_r + H_m$ for Special Option 23$\left.\right)$, Btu/ft^2

Second Line

ν air viscosity, slug/ft-sec

N_{Re} Reynolds number

$\dot{H}_c R_n^{\frac{1}{2}}$ convective heat rate times square root of nose radius of curvature of body, Btu/ft$^{\frac{3}{2}}$-sec

$H_c R_n^{\frac{1}{2}}$ convective heat integral times square root of nose radius of curvature of body, Btu/ft$^{\frac{3}{2}}$

$\dot{H}_r R_n^{-\frac{1}{2}}$ radiative heat rate divided by square root of nose radius of curvature of body, Btu/ft$^{\frac{5}{2}}$-sec

$H_r R_n^{-\frac{1}{2}}$ radiative heat integral divided by square root of nose radius of curvature of body, Btu/ft$^{\frac{5}{2}}$

$\dot{H}_m$ molecular heat rate, Btu/ft^2-sec (Special Option 23 only)

H_m molecular heat integral, Btu/ft^2 (Special Option 23 only)

Output 14

h	altitude above reference spheroid, n. mi.
χ	ground track, n. mi.
r	orbit radius, n. mi.
F_r	radial force (in L, λ, r coordinate system), lb
θ_c	central angle traveled since start of this case, deg
V_i/V_{i_r}	inertial velocity divided by minimum orbital velocity (if Special Option 15 is activated)
ΔV	incremental change in velocity since start of this section, ft/sec (if Special Option 24 is activated)
φ_r	roll angle, deg (if Special Option 10 or 32 is activated)

Outputs 15 through 18

Not used

Output 19

Special Option 27 automatically activates this output to generate the X-Y plotter tape. Output 19 must not be activated on the 590 card.

14.0 RETROROCKET FIRING TIME PREDICTION

The program can be used to predict the time to fire retrograde rockets in order to land the vehicle at a particular Greenwich referenced longitude. To utilize this feature, the data input deck must be constructed in a particular fashion, which will be subsequently explained.

In using the program for this purpose, the desired landing longitude λ_i, the revolution number N in which the landing will occur, and a first approximation to the retrorocket firing time t_{rf}, or some other allowed termination

condition, must be known. If the first estimate t_{rf} is reasonably close, and if the desired landing longitude can be attained from the particular orbit in question, then normally three iterations will result in determination of the correct retrofire time.

The retrograde rockets are first fired at the termination condition specified by the input data, and a resulting impact longitude λ_n computed. If this is not the desired longitude, then a correction δt to the retrofiring time t_n is made by

$$\delta t = \frac{\lambda_n - \lambda_i}{\dot{\lambda}} \tag{123}$$

On all subsequent iterations δt is given by

$$\delta t = \frac{\left(\lambda_n - \lambda_i\right)}{\left(\lambda_{n-1} - \lambda_n\right)} \left(t_n - t_{n-1}\right) \tag{124}$$

14.1 Data Input Requirements for Retrotime Prediction

No special options, outputs, or additions to the program are required to use the retrotime prediction mode, but the data deck must be set up in a prescribed manner. An auxiliary tape is required on tape drive A4, onto which the data between the TRA 530 and the first TRA 2, 4 card are stored. These data are then repeatedly used during the iteration process to determine the desired retrofiring time.

A detailed description of the retrotime prediction data deck setup is now given. Appendix J contains a sample retrotime prediction deck. Immediately following the * CO3E card is a TRA 530 card, which is then followed by the remaining section data of the section which is to precede the retrofire step. These data must not include any termination conditions. The section data are terminated by a TRA 3, 4. Next is the section data for the retrorocket firing step, and they differ in no respect from the way this step could normally be set up. Then any other desired sections of data are added in the usual fashion. The retrofire section and all subsequent ones must each include termination conditions, and each, except the last, is ended with a TRA 3, 4 card. The

last section ends with the two cards: TRA 541, TRA 2, 4. These are the final data stored on tape A4.

Beginning at this point is the normal case data (500 BCD cards, etc.) which are then followed by any number of sections to be executed. The case data and each section, except the last one before the retrofire step, are terminated by a TRA 3, 4. This last step must contain the revolution number N, landing longitude λ_i, and the first approximation to the retrofire time t_{rf} or some other termination condition

790 DEC N, λ_i

900 DEC t_{rf}

The last card in this section is a TRA 540. The remainder of the data for this section is read from tape A4, where it was previously stored, and upon encountering a TRA 3, 4 begins execution of the section. All the sections of data stored on tape A4 are processed and then an adjustment is made to the retrofire time by equation (123) or (124). Then the sections on tape A4 are rerun and this procedure repeated until the desired landing longitude is achieved. The trajectory conditions existing at the start of retrofire are retained during the iteration process so that the δt variation is effected from that point. If for some reason λ_i cannot be reached, the program will continue running until manually stopped by the computer operator.

Upon impacting at the longitude λ_i, the program expects other data to follow the TRA 540 card. If retrofire times are to be predicted for other landing longitudes, the appropriate data cards containing λ_i, N, and t_{rf} are added along with another TRA 540. There is no restriction on the number of retrofiring time predictions. The initial computing interval is positive if the $n + 1st\ \lambda_i$ is east of the $nth\ \lambda_i$ and negative if the $n + 1st\ \lambda_i$ is west of the $nth\ \lambda_i$. It is permissible to intermix regular sections terminated by TRA 3,4 cards and retrotime predictions in a trajectory; cases may also be stacked.

Iterations cease when the spacecraft has impacted at longitude $\lambda_i \pm \delta$ where δ is normally $0.01°$. The tolerance δ can be changed by using the card 792 DEC δ.

During retrotime prediction, the program automatically assumes a very large print frequency unless Special Option 29 is activated in case data, then the 581 card controls the print frequency. Special Option 30 may also be activated to delete on-line printing, if desired.

15.0 GENERAL COMMENTS ON THE PROGRAM

The program is written in the 7094 FAP language and is assembled in absolute. Absolute refers to the machine language instructions of the program being assigned to specific core locations by the programer. In a relocatable program, the monitor loader assigns the instructions in accordance with available core locations; the programer has no direct control over where, in the memory, a relocatable program may reside.

CO3E is a completely self-contained program in that all the necessary arithmetic, library, and input-output routines are supplied as a part of the program, thus making the program independent of the 7094 FORTRAN II monitor. Though the program and all its supporting routines are in absolute, a provision has been made to allow FORTRAN II and FAP relocatable subroutines to be used. To explain this feature, a description of program operation is required. The following instructions are of use primarily to the programer and not to the user. Deck setup and program usage are explained in the sections dealing with these subjects.

The program, all supporting subroutines, and relocatable routines are stored on a magnetic tape, and then this tape is used to execute trajectories. This tape can be called by a one-card loader or by the FORTRAN II monitor, as is done at NASA-MSC in Houston where the monitor was modified to recognize * CO3E as a valid control card.

In order to make this program tape, the following deck setup is required.

$ Monitor control cards as required

FAP load program, BSS loader, date card using columns 1 to 12

CO3E absolute binary program followed by absolute library routines

FORTRAN II subroutines followed by the required relocatable supporting routines

Transfer card with 12-7-9 punches in column 1

TRA 1076

TRA 2, 4

7/8 card

This deck is then run as a regular monitor job. The load program, BSS loader, and date card are processed as a FORTRAN II monitor job. The loader reads the CO3E absolute binary cards and assigns them to the designated locations. Upon encountering the relocatable routines of the program, the first of these is loaded beginning at $21000)_8$ and continues until the transfer card is reached. A load map of the relocatable routines is written and control is then transferred by the loader to location $2074)_8$, which is the first executable instruction of the program. The program is then in core and ready to compute a trajectory, and then it reads the TRA 1076 card. The input routine will recognize this card as a transfer operation and transfers control to location $1076)_{10}$. At this location begins a section of the program which writes locations $144)_8$ - $60000)_8$ of core onto file 1, tape B5 in a binary format. Control then returns to location $2074)_8$ and the TRA 2, 4 card is read. Control is returned to the monitor for the next job. Tape B5 is then file protected and saved for future use. To use this tape, the CO3E data deck is prepared in the following manner

$ Monitor control cards as required

* Pause card

CO3E data deck

7/8 card

When the monitor reaches the pause card, the one-card loader is read into the on-line card reader by pressing the "clear" and "load cards" keys on the 7094 console. The binary program is then read from tape B5, file 1, and the trajectory is executed. Upon completion of the job, control is automatically returned to the monitor.

If it is desired to eliminate the use of the one-card loader, it is necessary to modify the monitor to recognize the * CO3E card as a valid monitor control card. This card will then replace the pause card in the foregoing sample deck setup. The monitor must then select tape B5 in order to read the CO3E program into core. Alternatively, a FAP program can be used to read tape B5 as a monitor job. The first three words on tape B5 are

IOCD $144)_8, 0, 57634)_8$

TCOB 1

TTR $2074)_8$

By replacing the TRA $1076)_{10}$ card with a TRA $100)_{10}$ card when generating tape B5, the program will be written on file 2, tape B5 instead of on file 1. This will permit CO3E to be stored on a tape that can be used for other monitor purposes without requiring the use of an additional tape.

The ability to handle relocatable FORTRAN II and FAP programs along with the absolute CO3E program is a useful feature which was accomplished by modifying the loader used in making the program tape referred to previously. The first of the relocatable programs should be a main program consisting of only a series of CALL statements for the relocatable subroutines. The transfer vector for these subroutines appears at the beginning of the compilation of this main program, and is thus loaded beginning at $21000)_8$. At the time loading occurs, the loader replaces the BCD names in the transfer vector with TTR's to the entry points of the subroutines so referenced. Thus to gain entry to the nth relocatable subroutine in the main program transfer vector from the absolute section of CO3E, it is only necessary to execute a TSX $\left[21000 + (n-1)\right]_8, 4$. The relocatable routines can utilize calling arguments or common or both as permitted by the FORTRAN language. Note that any utility or library routines required by the user-supplied FORTRAN II or FAP programs must also be included in the program deck.

The program is easily adapted for use as a real-time computing tool, and it was used extensively as such during Project Mercury and on into the Gemini Program. Basically the program, as well as all input data that can be preset in advance of a mission, are stored on several files of a tape. This tape is then called into memory by another one-card loader read by the on-line card reader. The data deck, also read through the on-line card reader, consists of the initial position and velocity, and any other data required to update that which has been previously stored on the tape. The trajectory is then

executed and pertinent information about the run printed both on- and off-line. Setting up this tape is a rather detailed task and will not be discussed here. This information can be obtained from members on the Flight Mechanics Applications Branch, Computation and Analysis Division of the Manned Spacecraft Center in Houston.

Wide use of the program over the period 1960-1966 was made at Space Task Group and at its successor, the Manned Spacecraft Center. The numerical integration technique is considered sufficiently accurate for up to 30 orbits; after this point, round-off and truncation error may be large enough to render the output questionable. It should be noted, however, that excellent results were obtained when the program was used in real-time to predict retrofiring times during the Mercury and several of the Gemini missions.

There exist certain differential equations which are difficult to integrate numerically. A particular example that cannot be evaluated by CO3E is one which has rapidly changing or highly erratic second derivatives, that is, $\ddot{L}, \ddot{\lambda}, \ddot{H}$. In this instance, the integration over a single time-step results in a longitude traversed of the order of 10^8 deg with corresponding errors in the other integrated equations of motion. Sometimes the difficulty can be circumvented by using fixed integration step size (Special Option 16) with a very small Δt, say 0.001 sec or smaller. Caution should be exercised when interpreting the output from such a case as the data may be of doubtful value.

Another problem may arise with the use of Special Option 23 in computing Gemini or Apollo reentry heating data. When the radiative heat rate is of the order of the small value or accuracy criteria, ϵ_i and δ_i, the integration step size may be halved until, for all practical purposes, it is zero. This difficulty may also be alleviated by resorting to fixed interval integration with Δt of the order of 0.1 sec for a few seconds of trajectory time. Polar orbits (those with $L = 90°$) cannot be computed by CO3E, but those differing from 90° by a few hundredths of a degree can be satisfactorily run. The differential equation for $\ddot{\lambda}$ contains the factor secant L. Synchronous orbits whose period is the same as the earth's day also cannot be handled because these derivatives vanish in spherical polar coordinates.

If an input data card cannot be interpreted when it is read by the input routine, the erroneous card is printed off-line along with an appropriate comment. The program then ceases execution of the trajectory and halts at location $167)_8$.

A common error message is "Some thing wrong, end of case". This occurs when there have been over 20 accumulator or MQ overflows, and divide

checks in a single computer run. A misplaced decimal point frequently causes certain trajectory parameters to take on unrealistic values, resulting in this message. A very small weight can also cause this error condition, particularly if thrusting is involved. Very high drag forces, for example a large overspeed on reentry, is another such condition. Use of the incorrect pseudo-operation (DEC, OCT, BCD) on the input cards can cause subsequent trajectory errors.

The message "No convergence, end of case" occurs when after 20 successive halvings of the integration interval Δt, the results of the whole and two half-step integrations cannot be brought to within the ϵ_i specified on card 520. Probably the ϵ_i are too small or one of the case description cards (512 or 515) has a blank in column 12 resulting in one or more of the ϵ_i being effectively zero.

The input-output devices required by the program depends on the sense-switch settings and the outputs and special options activated. The minimum requirements are: tape drives A2, input; A3, output; B5, binary program tape; and the A-channel on-line printer. Depressing sense-switch 1 allows data to be input through the on-line card reader attached to channel A. Several output tapes can be written, as explained in section 7.0. Appendix I gives the sense-switch controls.

Modifications can be made to the program at the time a trajectory is run in two ways. Octal corrections to the program can be included in the data deck: N OCT M, where M is the 12-digit octal equivalent of the machine language instruction that is to occupy decimal location N in the 7094 memory. Absolute FAP binary cards can be read as data and must be the first cards in the deck following the * CO3E card. The setup for reading these binary cards is:

TRA 7712

Absolute FAP binary cards

Absolute transfer card consisting of a 7 - 9 punch in column 1 and 11 - 4 - 5 - 6 - 7 punches in column 3

Manned Spacecraft Center
National Aeronautics and Space Administration
Houston, Texas, April 7, 1966

APPENDIX A

DERIVATION OF SPHERICAL POLAR EQUATIONS OF MOTION

[See ref. 1.]

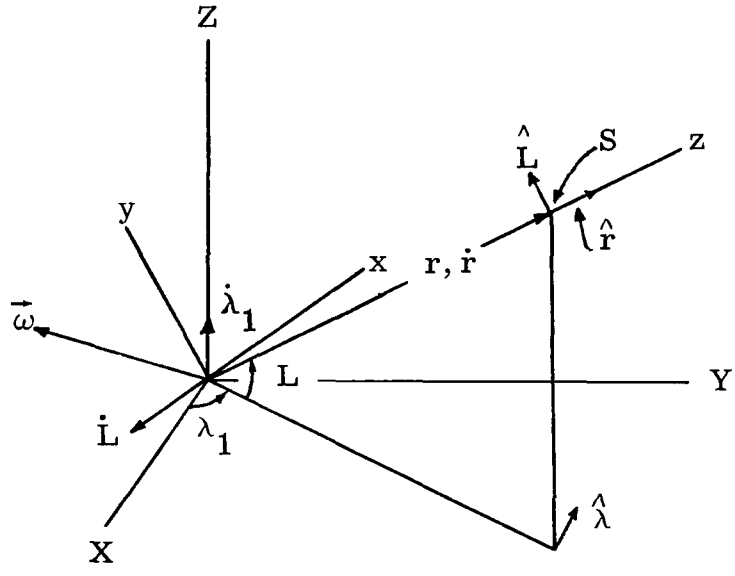

Figure A1. - Coordinates x, y, z rotating with the angular velocity $\vec{\omega}$ with respect to inertial coordinates X, Y, Z.

The following derivation of the spherical polar equations of motion of a spacecraft near rotating reference coordinates was supplied by Mr. John N. Shoosmith.

In figure A1 consider X, Y, Z to be an inertial, right-hand Cartesian set of coordinates. Let S be a particle having spherical polar coordinates of east longitude λ_1, declination or geocentric latitude L and radius vector r. Let x, y, z be another right-hand Cartesian coordinate frame, concentric with X, Y, Z, but rotating with angular velocity $\vec{\omega}$ with respect to X, Y, Z. The coordinates x, y, z are rotated from X, Y, Z into the position shown by a rotation of $\left(\frac{\pi}{2} + \lambda_1\right)$ about the Z-axis, and then a rotation of $\left(\frac{\pi}{2} - L\right)$ about the resulting x-axis. Thus the z-axis now coincides with r, the y-axis lies

in the r-Z plane, and the x-axis is perpendicular to the r-Z plane and lies in the X-Y plane. The latitude rate $\dot{L}$ is perpendicular to the y-z plane and is represented as a vector lying along the negative x-axis, while the vector representing λ_1 lies along the Z-axis.

To find the equations of motion of the particle S, its inertial acceleration $\ddot{\vec{r}}_i$ is to be found. The time rate of change of a vector $\vec{r}$ (ref. 9) expressed in terms of its derivative in the rotating coordinates x, y, z is given by

$$\dot{\vec{r}}_i = \dot{\vec{r}} + \left(\vec{\omega} \times \vec{r}\right) \tag{A1}$$

where $\dot{\vec{r}}_i$ is the time rate of change of $\vec{r}$ with respect to the inertial frame, and $\dot{\vec{r}}$ is the time rate of change of $\vec{r}$ with respect to the rotating coordinates. A second time differentiation (ref. 9) yields the acceleration or $\vec{r}$ in the inertial frame.

$$\ddot{\vec{r}}_i = \ddot{\vec{r}} + 2\left(\vec{\omega} \times \dot{\vec{r}}\right) + \left(\dot{\vec{\omega}} \times \vec{r}\right) + \left[\vec{\omega} \times \left(\vec{\omega} \times \vec{r}\right)\right] \tag{A2}$$

In order to determine the three components of $\ddot{\vec{r}}_i$, consider the components of $\vec{r}$ and $\vec{\omega}$ in the rotating x, y, z coordinates. By inspection of figure A1,

$$\vec{r} = \begin{bmatrix} 0 \\ 0 \\ r \end{bmatrix} \tag{A3}$$

$$\vec{\omega} = \begin{bmatrix} -\dot{L} \\ \dot{\lambda}_1 \cos L \\ \dot{\lambda}_1 \sin L \end{bmatrix} \tag{A4}$$

Differentiation yields

$$\dot{\vec{r}} = \begin{bmatrix} 0 \\ 0 \\ \dot{r} \end{bmatrix} \tag{A5}$$

$$\ddot{\vec{r}} = \begin{bmatrix} 0 \\ 0 \\ \ddot{r} \end{bmatrix} \tag{A6}$$

$$\dot{\vec{\omega}} = \begin{bmatrix} -\ddot{L} \\ \ddot{\lambda}_1 \cos L - \dot{\lambda}_1 \dot{L} \sin L \\ \ddot{\lambda}_1 \sin L + \dot{\lambda}_1 \dot{L} \cos L \end{bmatrix} \tag{A7}$$

Applying the indicated vector cross products, the following results are obtained

$$2\left(\vec{\omega} \times \dot{\vec{r}}\right) = \begin{bmatrix} 2\dot{r}\dot{\lambda}_1 \cos L \\ 2\dot{r}\dot{L} \\ 0 \end{bmatrix} \tag{A8}$$

$$\dot{\vec{\omega}} \times \vec{r} = \begin{bmatrix} r\ddot{\lambda}_1 \cos L - r\dot{\lambda}_1 \dot{L} \sin L \\ r\ddot{L} \\ 0 \end{bmatrix} \tag{A9}$$

$$\left[\vec{\omega} \times \left(\vec{\omega} \times \vec{r}\right)\right] = \begin{bmatrix} -r\dot{L}\dot{\lambda}_1 \sin L \\ r\dot{\lambda}_1^2 \sin L \cos L \\ -r\dot{L}^2 - r\dot{\lambda}_1^2 \cos^2 L \end{bmatrix} \tag{A10}$$

If the forces F_λ, F_L, and F_r are associated with the x-, y-, z-axes, respectively, $\ddot{\vec{r}}_i$ can be expressed by equations (A11) through (A13) in terms of its components in the rotating coordinates.

$$\ddot{\vec{r}}_i = \begin{bmatrix} \frac{F_\lambda}{m} \\ \frac{F_L}{m} \\ \frac{F_r}{m} \end{bmatrix} = \begin{bmatrix} 2\dot{r}\dot{\lambda}_1 \cos L + r\ddot{\lambda}_1 \cos L - 2r\dot{\lambda}_1\dot{L} \sin L \\ 2\dot{r}\dot{L} + r\ddot{L} + r\dot{\lambda}_1^2 \sin L \cos L \\ \ddot{r} - r\dot{L}^2 - r\dot{\lambda}_1^2 \cos^2 L \end{bmatrix} \quad \begin{matrix} \text{(A11)} \\ \text{(A12)} \\ \text{(A13)} \end{matrix}$$

The resulting equations of motion, namely $\ddot{\lambda}$, $\ddot{L}$, and $\ddot{r}$, can thus be obtained from equations (A11) through (A13).

Application To A Particle Near An Oblate, Rotating Earth

If the origin of the X, Y, Z coordinate system is taken to be the center of the earth, and the Z-axis passes through the North Pole, then λ_1 becomes the inertial longitude. Since the earth rotates about the Z-axis with angular velocity ω_e, and since it is customary to measure longitude with respect to the rotating earth, $\dot{\lambda}_1$ can be written

$$\dot{\lambda}_1 = \dot{\lambda} + \omega_e \tag{A14}$$

where $\dot{\lambda}$ is the longitude rate of a particle measured relative to the earth.

Due to the oblateness of the earth, the gravitational acceleration vector has two components, $\vec{g}_r$ along $\vec{r}$, and $\vec{g}_L$ perpendicular to $\vec{r}$ in the $r\text{-}Z_i$ plane (fig. 3.2-1). By restricting F_λ, F_L, and F_r to nongravitational

forces, equations (A11) through (A13) are solved to obtain the equations of motion for a particle S near an oblate, rotating earth.

$$\ddot{\lambda} = \frac{1}{r \cos L}\left[\frac{F_\lambda}{m} - 2\dot{r}\left(\dot{\lambda} + \omega_e\right)\cos L + 2r\dot{L}\left(\dot{\lambda} + \omega_e\right)\sin L\right] \tag{1}$$

$$\ddot{L} = \frac{1}{r}\left[\frac{F_L}{m} + g_L - 2\dot{r}\dot{L} - r\left(\dot{\lambda} + \omega_e\right)^2 \sin L \cos L\right] \tag{2}$$

$$\ddot{r} = \left[\frac{F_r}{m} + g_r + r\dot{L}^2 + r\left(\dot{\lambda} + \omega_e\right)^2 \cos^2 L\right] \tag{3}$$

It should be kept in mind that F_λ, F_L, and F_r determine the trajectory, since these include thrust and aerodynamic effects and are generally of much greater magnitude than the gravitational forces.

APPENDIX B

DERIVATION OF TRANSFORMATION FROM LOCAL GEODETIC TO BODY COORDINATE SYSTEM AND FROM LOCAL GEODETIC TO LOCAL GEOCENTRIC COORDINATE SYSTEM

Local Geodetic To Body Coordinate System Transformation

The transformation matrix, equation (B4), relates the local geodetic coordinate system X_D, Y_D, Z_D to the body system x_b, y_b, z_b in figure 3.1-7. It represents three successive rotations. The notation T_{G2B} should be read as the "geodetic to body coordinate system transformation."

A rotation about the Z_D axis through the angle $+\left(\frac{\pi}{2} - \varphi\right)$ carries the X_D, Y_D, Z_D system to an intermediate system X_1, Y_1, Z_1, and T_1 is the matrix of this rotation.

$$T_1 = \begin{bmatrix} \cos\left(\frac{\pi}{2} - \varphi\right) & \sin\left(\frac{\pi}{2} - \varphi\right) & 0 \\ -\sin\left(\frac{\pi}{2} - \varphi\right) & \cos\left(\frac{\pi}{2} - \varphi\right) & 0 \\ 0 & 0 & 1 \end{bmatrix} \tag{B1}$$

Next, a rotation about the Y_1 axis through the angle $+\theta$ carries X_1, Y_1, Z_1 into a second intermediate system X_2, Y_2, Z_2; T_2 is the corresponding rotation matrix.

$$T_2 = \begin{bmatrix} \cos\theta & 0 & \sin\theta \\ 0 & 1 & 0 \\ -\sin\theta & 0 & \cos\theta \end{bmatrix} \tag{B2}$$

A final rotation about X_2 through the angle π completes the transformation; T_3 represents this last rotation.

$$T_3 = \begin{bmatrix} 1 & 0 & 0 \\ 0 & -1 & 0 \\ 0 & 0 & -1 \end{bmatrix} \tag{B3}$$

The complete transformation is then

$$T_{G2B} = T_3 T_2 T_1 = \begin{bmatrix} \cos\theta \sin\varphi & \cos\theta \cos\varphi & \sin\theta \\ \cos\varphi & -\sin\varphi & 0 \\ \sin\theta \sin\varphi & \sin\theta \cos\varphi & -\cos\theta \end{bmatrix} \tag{B4}$$

Local Geodetic to Local Geocentric Coordinate System Transformation

Figure 3.3-1 illustrates the relation between the local geodetic and local geocentric coordinate systems. A single rotation about the X_D axis through the angle $+\left(L_D - L\right)$ results in the transformation matrix T_{G2C}

$$T_{G2C} = \begin{bmatrix} 1 & 0 & 0 \\ 0 & \cos\left(L_D - L\right) & \sin\left(L_D - L\right) \\ 0 & -\sin\left(L_D - L\right) & \cos\left(L_D - L\right) \end{bmatrix} \tag{B5}$$

Since these matrices are orthogonal, the inverse and the transpose are the same, a useful fact when one wishes to transform from body coordinates to geodetic coordinates, for example. Thus

$$T_{B2G} = T_{G2B}^{-1} = \tilde{T}_{G2B} \tag{B6}$$

$$T_{C2G} = T_{G2C}^{-1} = \tilde{T}_{G2C} \tag{B7}$$

APPENDIX C

TRANSFORMATION EQUATIONS FOR INPUT COORDINATE SYSTEMS

A thorough discussion of the derivation of the equations used in the input transformations will be given here for the eight allowed input numbers 1 through 8. It should be kept in mind that Outputs 1 through 8 used the corresponding inverse transformation. It is assumed that the reader is sufficiently familiar with the symbolism set forth in appendix K, and consequently, descriptions of the variable symbols used will be omitted at this point.

Input 1

The coordinates for this input are geodetic latitude, earth referenced longitude, altitude above the reference spheroid, and the inertial velocity, flight-path angle, and azimuth. Transformation to earth centered, rotating, spherical, polar coordinates is effected by the following equations (figs. 3.3-1 and 3.3-2).

$$L = \tan^{-1}\left[\frac{r_p^2}{r_e^2}\tan L_D\right] \tag{C1}$$

$$\lambda = \lambda \tag{C2}$$

$$H = h - \Delta h \tag{C3}$$

$$r = H + r_e \tag{C3a}$$

$$\dot{L} = \frac{V_i}{r}\cos\gamma_i \cos\psi_i \tag{C4}$$

$$\dot{\lambda} = \frac{V_i \cos \gamma_i \sin \psi_i}{r \cos L} - \omega_e \tag{C5}$$

$$\dot{H} = V_i \sin \gamma_i \tag{C6}$$

Input 2

Input 2 uses the same position inputs as does Input 1, (eqs. (C1) through (C3a)), but the velocity is relative to the rotating earth (figs. 3.3-1 and 3.3-2).

$$\dot{L} = \frac{V_e}{r} \cos \gamma_e \cos \psi_e \tag{C7}$$

$$\dot{\lambda} = \frac{V_e \cos \gamma_e \sin \psi_e}{r \cos L} \tag{C8}$$

$$\dot{H} = V_e \sin \gamma_e \tag{C9}$$

Input 3

The transformation from the inertial, geocentric, rectangular coordinates of Input 3 is straightforward (fig. 4.0-1).

$$r = \sqrt{X_i^2 + Y_i^2 + Z_i^2} \tag{C10}$$

$$\lambda_3 = \tan^{-1}\left(\frac{Y_i}{X_i}\right) \tag{C10a}$$

$$L = \tan^{-1}\left(\frac{Z_i}{\sqrt{X_i^2 + Y_i^2}}\right) \tag{C11}$$

$$\lambda = \lambda_3 + \lambda_x - \omega_e\left(t - t_x\right) \tag{C12}$$

$$H = r - r_e \tag{C13}$$

$$\dot{L} = \frac{1}{r}\left[\dot{Z}_i \cos L - \left(\dot{X}_i \cos \lambda_3 + \dot{Y}_i \sin \lambda_3\right) \sin L\right] \tag{C14}$$

$$\dot{\lambda} = \frac{1}{r \cos L}\left[-\dot{X}_i \sin \lambda_3 + \dot{Y}_i \cos \lambda_3\right] - \omega_e \tag{C15}$$

$$\dot{H} = \dot{Z}_i \sin L + \left(\dot{X}_i \cos \lambda_3 + \dot{Y}_i \sin \lambda_3\right) \cos L \tag{C16}$$

Input 4

The transformation from the quasi-inerital, geocentric, rectangular coordinates of Input 4 is very similar to that of Input 3 (figs. 4.0-1 and 4.0-2).

$$r = \sqrt{X_q^2 + Y_q^2 + Z_q^2} \tag{C17}$$

$$\lambda_4 = \tan^{-1}\left(\frac{Y_q}{X_q}\right) \tag{C17a}$$

$$L = \tan^{-1}\left(\frac{Z_q}{\sqrt{X_q^2 + Y_q^2}}\right) \tag{C18}$$

$$\lambda = \lambda_4 + \lambda_x \tag{C19}$$

$$H = r - r_e \tag{C20}$$

$$\dot{L} = \frac{1}{r}\left[\dot{Z}_q \cos L - \left(\dot{X}_q \cos \lambda_4 + \dot{Y}_q \sin \lambda_4\right) \sin L\right] \tag{C21}$$

$$\dot{\lambda} = \frac{1}{r \cos L}\left(-\dot{X}_q \sin \lambda_4 + \dot{Y}_q \cos \lambda_4\right) - \omega_e \tag{C22}$$

$$\dot{H} = \dot{Z}_q \sin L + \left(\dot{X}_q \cos \lambda_4 + \dot{Y}_q \sin \lambda_4\right) \cos L \tag{C23}$$

Input 5

The transformation from rotational, geocentric, rectangular coordinates of Input 5 follows the same pattern as that of Input 4. Position coordinates are the same in both systems (fig. 4.0-2).

$$r = \sqrt{X_e^2 + Y_e^2 + Z_e^2} \tag{C24}$$

$$\lambda_5 = \tan^{-1}\left(\frac{Y_e}{X_e}\right) \tag{C24a}$$

$$L = \tan^{-1}\left(\frac{Z_e}{\sqrt{X_e^2 + Y_e^2}}\right) \tag{C25}$$

$$\lambda = \lambda_5 + \lambda_x \tag{C26}$$

$$H = r - r_e \tag{C27}$$

$$\dot{L} = \frac{1}{r}\left[\dot{Z}_e \cos L - \left(\dot{X}_e \cos \lambda_5 + \dot{Y}_e \sin \lambda_5\right) \sin L\right] \tag{C28}$$

$$\dot{\lambda} = \frac{1}{r \cos L}\left(-\dot{X}_e \sin \lambda_5 + \dot{Y}_e \cos \lambda_5\right) \tag{C29}$$

$$\dot{H} = \dot{Z}_e \sin L + \left(\dot{X}_e \cos \lambda_5 + \dot{Y}_e \sin \lambda_5\right) \cos L \tag{C30}$$

Input 6

The transformation from the inertial, topocentric, rectangular coordinates to earth centered, rotating, spherical polar coordinates is accomplished by two major steps. First, equations (C36) and (C37) are used to transform Input 6 coordinates to a system which differs from the inertial, geocentric, rectangular coordinates of Input 3 by the rotation λ_6 (eq. (C34)), then the equations (C10) through (C16) of Input 3 are used to complete the input transformation with λ defined by equation (C38) instead of equation (C12). Figure 4.0-3 gives a graphical description.

In transforming from Input 6 coordinates to Input-3 type coordinates, three rotations and a translation occur. A rotation about the z-axis through an angle $-\left(\pi - A_q\right)$ is performed to point the x-axis south; call the resulting coordinate system x_1, y_1, z_1, and denote the matrix for this rotation by $T_1^{\,i}$

$$T_1^{\,i} = \begin{bmatrix} -\cos A_q & -\sin A_q & 0 \\ \sin A_q & -\cos A_q & 0 \\ 0 & 0 & 1 \end{bmatrix} \tag{C31}$$

A rotation about the y_1 axis through the angle $+\left(\frac{\pi}{2} - L_{D_q}\right)$ produces the x_2, y_2, z_2 system whose x_2-y_2 plane is parallel to the earth equatorial plane, and $T_2^{\,i}$ represents this rotation

$$T_2^{\,i} = \begin{bmatrix} \sin L_{D_q} & 0 & \cos L_{D_q} \\ 0 & 1 & 0 \\ -\cos L_{D_q} & 0 & \sin L_{D_q} \end{bmatrix} \tag{C32}$$

The next step is to translate the x_2, y_2, z_2 origin to the center of the earth. Equation (44) is used to convert L_{D_q} to its geocentric equivalent L_q, and the local earth radius at L_q is computed from equation (41). To this is added the altitude of the origin above sea level, and the resultant is the radius vector from the center of the earth to the origin of the topocentric coordinate system in question. Call the resulting coordinate system x_3, y_3, z_3 after the translation

$$\begin{bmatrix} x_3 \\ y_3 \\ z_3 \end{bmatrix} = T_2^{\,i}\, T_1^{\,i} \begin{bmatrix} x \\ y \\ z \end{bmatrix} + \begin{bmatrix} \left(r_{D_q} + h_q\right) \cos L_q \\ 0 \\ \left(r_{D_q} + h_q\right) \sin L_q \end{bmatrix} \tag{C33}$$

The final rotation λ_6 about the z_3 axis which produces coordinates similar to Input 3 is given by equation (C34), and the rotation matrix is equation (C35):

$$\lambda_6 = \omega_e \left(t_q - t\right) \tag{C34}$$

$$T_3^{\,i} = \begin{bmatrix} \cos \lambda_6 & -\sin \lambda_6 & 0 \\ \sin \lambda_6 & \cos \lambda_6 & 0 \\ 0 & 0 & 1 \end{bmatrix} \tag{C35}$$

The complete transformation from x, y, z coordinates of Input 6 to a system X'_i, Y'_i, Z'_i which differs from the inertial coordinates of Input 3 by the rotation λ_6 above, is summarized by

$$\begin{bmatrix} X'_i \\ Y'_i \\ Z'_i \end{bmatrix} = T_3^{\,i} \left\{ T_2^{\,i} T_1^{\,i} \begin{bmatrix} x \\ y \\ z \end{bmatrix} + \begin{bmatrix} \left(r_{D_q} + h\right) \cos L_q \\ 0 \\ \left(r_{D_q} + h\right) \sin L_q \end{bmatrix} \right\} \tag{C36}$$

In the same manner, the transformation from Input 6 velocities to a system $\dot{X}_i, \dot{Y}_i, \dot{Z}_i$ which differs from the inertial velocities $\dot{X}_i, \dot{Y}_i, \dot{Z}_i$ of Input 3 by the rotation λ_6 above is

$$\begin{bmatrix} \dot{X}'_i \\ \dot{Y}'_i \\ \dot{Z}'_i \end{bmatrix} = T_3^{\,i} T_2^{\,i} T_1^{\,i} \begin{bmatrix} \dot{x} \\ \dot{y} \\ \dot{z} \end{bmatrix} \tag{C37}$$

The second major part of the Input 6 transformation now transforms the coordinates and velocity of equations (C36) and (C37) into rotating spherical polar coordinates by using equations (C10) through (C16) of Input 3 with λ defined by equation (C38) instead of equation (C12):

$$\lambda = \lambda_3 + \lambda_x \tag{C38}$$

where

$$\lambda_3 = \tan^{-1}\left(\frac{Y'_i}{X'_i}\right) \tag{C38a}$$

Input 7

Transforming from the quasi-inertial, topocentric, rectangular coordinates of Input 7 is very similar to that of Input 6. The sequence of rotations from Input 6 is required here, with the exception of $T_3^{\,i}$. Since the coordinate origin rotates with the earth, $\lambda_6 = 0$ (eq. (C34)) and $T_3^{\,i}$ (eq. (C35)) reduces to a unit matrix. Equations (C39) and (C40) give the complete transformation from Input 7 coordinates to those of Input 4. Equations (C17) through (C23) then complete the transformation to rotating, spherical, polar coordinates. Figures 4.0-3 and 4.0-4 give a diagram of Input 7 coordinates.

$$\begin{bmatrix} X_q \\ Y_q \\ Z_q \end{bmatrix} = T_2^{\,i}\, T_1^{\,i} \begin{bmatrix} x_q \\ y_q \\ z_q \end{bmatrix} + \begin{bmatrix} \left(r_{D_q} + h_q\right) \cos L_q \\ 0 \\ \left(r_{D_q} + h_q\right) \sin L_q \end{bmatrix} \tag{C39}$$

$$\begin{bmatrix} \dot{X}_q \\ \dot{Y}_q \\ \dot{Z}_q \end{bmatrix} = T_2^{\,i}\, T_1^{\,i} \begin{bmatrix} \dot{x}_q \\ \dot{y}_q \\ \dot{z}_q \end{bmatrix} \tag{C40}$$

Input 8

The transformation from the rotational, topocentric, rectangular coordinates of this input is also very similar to that of Input 6. Since the coordinate origin rotates, the matrix $T_3^{\,i}$ (eq. (C35)) reduces to a unit matrix as a consequence of $\lambda_6 = 0$ (eq. (C34)). The other two rotations in A_q and L_{D_q} are exactly the same as for Input 6, and the transformation of the coordinates to the rotating geocentric, rectangular frame of Input 5 is given by equation (C41) (fig. 4.0-4).

$$\begin{bmatrix} X_e \\ Y_e \\ Z_e \end{bmatrix} = T_2^{\,i} T_1^{\,i} \begin{bmatrix} x_e \\ y_e \\ z_e \end{bmatrix} + \begin{bmatrix} \left(r_{D_q} + h_q\right) \cos L_q \\ 0 \\ \left(r_{D_q} + h_q\right) \sin L_q \end{bmatrix} \tag{C41}$$

Note that equations (C40) and (C41) are identical, since the coordinates in both Inputs 7 and 8 are measured relative to a rotating system. The velocities, however, differ in that those of Input 8 are given relative to rotating coordinates, and hence the component of the earth's rotation must be added to give true inertial velocity. Equation (C42) (ref. 9) gives the vector relationship between inertial velocity and that measured with respect to a body rotating with angular velocity $\vec{\omega}$, where $\vec{\omega} = \omega_e \hat{k}$

$$\dot{\vec{r}}_i = \dot{\vec{r}}_e + \vec{\omega} \times \vec{r}_e = \dot{\vec{r}}_e + \omega_e \hat{k} \times \vec{r}_e \tag{C42}$$

The velocities of Input 8 are transformed to the velocities of Input 5 by equation (C43).

$$\begin{bmatrix} \dot{X}_e \\ \dot{Y}_e \\ \dot{Z}_e \end{bmatrix} = T_2^{\,i}\, T_1^{\,i} \begin{bmatrix} \dot{x}_e \\ \dot{y}_e \\ \dot{z}_e \end{bmatrix} + \begin{bmatrix} -\omega_e Y_e \\ \omega_e X_e \\ 0 \end{bmatrix} \qquad \text{(C43)}$$

Transformation from equations (C41) and (C43) to rotating, spherical polar coordinates is again effected by equations (C24) through (C30).

APPENDIX D

TRANSFORMATION EQUATIONS FOR OUTPUT COORDINATE SYSTEMS

The purpose of this appendix is to give the derivation of the equations used in generating the various quantities which can be printed by the program. All position and velocities result essentially from coordinate transformations from earth centered, rotating spherical polar coordinates, which is the basic system for integration of the differential equations of motion, to the appropriate output coordinates.

The symbolism used here is in keeping with that in the list of symbols, and it is assumed that the reader is familiar with it. It will be noted that only those output quantities which require some type of transformation equation are covered in this discussion.

Output 0

Output 0 consists of several quantities, some of which are not coordinates, but which involve a defining equation. All these except time, revolution number, and weight are listed (figs. 3.1-2, 3.3-1, and 3.3-3).

$$L = L \tag{D1}$$

$$L_D = \tan^{-1}\left(\frac{r_e^2}{r_p^2}\tan L\right) \tag{D2}$$

$$\lambda = \lambda \tag{D3}$$

$$h = H + \Delta h \tag{D4}$$

R Appendix G gives the formulas used in computing range.

$$V_a = \sqrt{V_{a_E}^2 + V_{a_N}^2 + V_{a_U}^2} \tag{D5}$$

$$\gamma_a = \tan^{-1}\left(\frac{V_{a_U}}{\sqrt{V_{a_E}^2 + V_{a_N}^2}}\right) \tag{D6}$$

$$\psi_a = \tan^{-1}\left(\frac{V_{a_E}}{V_{a_N}}\right) \tag{D7}$$

$$g_x = \frac{F_x}{W} \tag{D8}$$

$$g_y = \frac{F_y}{W} \tag{D9}$$

$$g_z = \frac{F_z}{W} \tag{D10}$$

$$r = H + r_e \tag{D11}$$

$$T = \text{magnitude of total thrust} \tag{D12}$$

$$M = \frac{V_a}{V_s} \tag{D13}$$

$$\bar{q} = \frac{1}{2}\rho V_a^2 \tag{D14}$$

Output 1

Output 1 includes two velocity vector magnitudes and several angles related to them (figs. 3.3-2 and 3.3-3).

$$V_i = \sqrt{V_\lambda^2 + V_L^2 + V_r^2} \tag{D15}$$

$$\gamma_i = \tan^{-1}\left(\frac{V_r}{\sqrt{V_\lambda^2 + V_L^2}}\right) \tag{D16}$$

$$\psi_i = \tan^{-1}\left(\frac{V_\lambda}{V_L}\right) \tag{D17}$$

$$V_e = \sqrt{V_{e_\lambda}^2 + V_{e_L}^2 + V_{e_r}^2} \tag{D18}$$

$$\gamma_e = \tan^{-1}\left(\frac{V_{e_r}}{\sqrt{V_{e_\lambda}^2 + V_{e_L}^2}}\right) \tag{D19}$$

$$\psi_e = \tan^{-1}\left(\frac{V_{e_\lambda}}{V_{e_r}}\right) \tag{D20}$$

$$\gamma_D = \tan^{-1}\left(\frac{V_{e_U}}{\sqrt{V_{e_E}^2 + V_{e_N}^2}}\right) \tag{D21}$$

$$\psi_D = \tan^{-1}\left(\frac{V_{e_E}}{V_{e_N}}\right) \tag{D22}$$

Output 2

Output 2 gives primarily the body reference angles and aerodynamic forces. Figures 3.1-7, 3.3-4, and 3.3-5 show these quantities.

$$\eta = \cos^{-1}\left(\frac{u_a}{V_a}\right) \tag{D23}$$

$$\alpha = \tan^{-1}\left(\frac{w_a}{u_a}\right) \tag{D24}$$

$$\beta = \sin^{-1}\left(\frac{v_a}{V_a}\right) \tag{D25}$$

$$D = F_n \sin\eta - F_{a_x} \cos\eta \tag{D26}$$

$$F_{a_n} = F_n \cos\eta + F_{a_x} \sin\eta \tag{D27}$$

$$\varphi_n = \tan^{-1}\left(\frac{-u_a v_a}{w_a V_a}\right) \tag{D28}$$

θ Section 6 defines θ. (D29)

φ Section 6 defines φ. (D30)

Outputs 3 through 8 are the same coordinate systems as the corresponding Inputs. It will be seen from the equations employed here that the output transformations are the inverse of the corresponding input transformations. Note that cards 650 through 657 define both the Input and Output coordinate systems 3 through 8. Refer to section 4.0 for more information.

Output 3

The transformation from the basic polar coordinate system to the inertial, geocentric, and rectangular coordinates is the traditional one (fig. 4.0-1). The value of λ_3 is the same as in Input 3, equation (C10a).

$$\lambda_3 = \lambda - \lambda_x + \omega_e \left(t - t_x\right) \tag{D31}$$

$$X_i = r \cos L \cos \lambda_3 \tag{D32}$$

$$Y_i = r \cos L \sin \lambda_3 \tag{D33}$$

$$Z_i = r \sin L \tag{D34}$$

$$\dot{X}_i = (\dot{r} \cos L - r\dot{L} \sin L) \cos \lambda_3 - \left(\omega_e + \dot{\lambda}\right) Y_i \tag{D35}$$

$$\dot{Y}_i = (\dot{r} \cos L - r\dot{L} \sin L) \sin \lambda_3 + \left(\omega_e + \dot{\lambda}\right) X_i \tag{D36}$$

$$\dot{Z}_i = \dot{r} \sin L + r\dot{L} \cos L \tag{D37}$$

Output 4

The transformation to the quasi-inertial, geocentric rectangular coordinates of Output 4 is similar to that of Output 3 (figs. 4.0-1 and 4.0-2); λ_4 is the same as in Input 4, equation (C19).

$$\lambda_4 = \lambda - \lambda_x \tag{D38}$$

$$X_q = r \cos L \cos \lambda_4 \tag{D39}$$

$$Y_q = r \cos L \sin \lambda_4 \tag{D40}$$

$$Z_q = r \sin L \tag{D41}$$

$$\dot{X}_q = (\dot{r} \cos L - r\dot{L} \sin L) \cos \lambda_4 - \left(\omega_e + \dot{\lambda}\right) Y_q \tag{D42}$$

$$\dot{Y}_q = (\dot{r} \cos L - r\dot{L} \sin L) \sin \lambda_4 + \left(\omega_e + \dot{\lambda}\right) X_q \tag{D43}$$

$$\dot{Z}_q = \dot{r} \sin L + r\dot{L} \cos L \tag{D44}$$

Output 5

The rotational, geocentric, and rectangular coordinates of this Output follow closely those of Output 4. Note that the position coordinates of Outputs 4 and 5 are identical (fig. 4.0-2), and λ_5 is the same as in Input 5, equation (C26).

$$\lambda_5 = \lambda - \lambda_x \tag{D45}$$

$$X_e = r \cos L \cos \lambda_5 \tag{D46}$$

$$Y_e = r \cos L \sin \lambda_5 \tag{D47}$$

$$Z_e = r \sin L \tag{D48}$$

$$\dot{X}_e = (\dot{r} \cos L - r\dot{L} \sin L) \cos \lambda_5 - \dot{\lambda} Y_e \tag{D49}$$

$$\dot{Y}_e = (\dot{r} \cos L - r\dot{L} \sin L) \sin \lambda_5 + \dot{\lambda} X_e \tag{D50}$$

$$\dot{Z}_e = \dot{r} \sin L + r\dot{L} \cos L \tag{D51}$$

In Outputs 6 through 8 the transformation from earth centered, rotating, spherical, polar coordinates to the particular topocentric output system is made in two steps. First a transformation to geocentric, rectangular coordinates similar to Output 3 is made using equations (D32) through (D37) of Output 3 with λ_3 given by equation (D52) instead of equation (D31).

$$\lambda_3 = \lambda - \lambda_x \tag{D52}$$

The second step takes these position and velocity coordinates, denoted by X'_i, Y'_i, Z'_i, and $\dot{X}'_i, \dot{Y}'_i, \dot{Z}'_i$, respectively, and transforms them to the desired topocentric system. In the discussions of Outputs 6, 7, and 8 the equations listed will be only those of the second step of the total transformation, namely from $X'_i, Y'_i, Z'_i, \dot{X}'_i, \dot{Y}'_i, \dot{Z}'_i$ to the topocentric system.

Output 6

The inertial, topocentric, rectangular coordinates of Output 6 require three rotations and a translation. A rotation about the Z'_i axis through the angle λ_6 carries the beginning inertial geocentric coordinates into an

intermediate system x_1, y_1, z_1. Denote this transformation matrix by $T_3^{\,o}$. Note that λ_6 here is the same as λ_6 in Input 6.

$$\lambda_6 = \omega_e \left(t_q - t\right) \tag{D53}$$

$$T_3^{\,o} = \begin{bmatrix} \cos \lambda_6 & \sin \lambda_6 & 0 \\ -\sin \lambda_6 & \cos \lambda_6 & 0 \\ 0 & 0 & 1 \end{bmatrix} \tag{D54}$$

Next, a translation along x_1 and z_1, to the origin of the Output 6 coordinate system gives the intermediate system x_2, y_2, z_2.

$$\begin{bmatrix} x_2 \\ y_2 \\ z_2 \end{bmatrix} = T_3^{\,o} \begin{bmatrix} X_i' \\ Y_i' \\ Z_i' \end{bmatrix} - \begin{bmatrix} \left(r_{D_q} + h_q\right) \cos L_q \\ 0 \\ \left(r_{D_q} + h_q\right) \sin L_q \end{bmatrix} \tag{D55}$$

A rotation is then made about the y_2 axis through the angle $-\left(\frac{\pi}{2} - L_{D_q}\right)$ with the resulting matrix $T_2^{\,o}$ and another intermediate coordinate system x_3, y_3, z_3.

$$T_2^{\,o} = \begin{bmatrix} \sin L_{D_q} & 0 & -\cos L_{D_q} \\ 0 & 1 & 0 \\ \cos L_{D_q} & 0 & \sin L_{D_q} \end{bmatrix} \tag{D56}$$

A final rotation about the z_3 axis through the angle $(\pi - A_q)$ positions the x-axis of Output 6 at the desired azimuth from north, and $T_1^{\,o}$ is the associated rotation matrix.

$$T_1^{\,o} = \begin{bmatrix} -\cos A_q & \sin A_q & 0 \\ -\sin A_q & -\cos A_q & 0 \\ 0 & 0 & 1 \end{bmatrix} \tag{D57}$$

Equation (D58) lists the total transformation of the position coordinates while the velocities are given by equation (D59). Figure 4.0-3 shows graphically these relationships.

$$\begin{bmatrix} x \\ y \\ z \end{bmatrix} = T_1^{\,o} T_2^{\,o} \left\{ T_3^{\,o} \begin{bmatrix} X'_i \\ Y'_i \\ Z'_i \end{bmatrix} - \begin{bmatrix} \left(r_{D_q} + h_q\right) \cos L_q \\ 0 \\ \left(r_{D_q} + h_q\right) \sin L_q \end{bmatrix} \right\} \tag{D58}$$

$$\begin{bmatrix} \dot{x} \\ \dot{y} \\ \dot{z} \end{bmatrix} = T_1^{\,o} T_2^{\,o} T_3^{\,o} \begin{bmatrix} \dot{X}'_i \\ \dot{Y}'_i \\ \dot{Z}'_i \end{bmatrix} \tag{D59}$$

Comparison of Input 6 and Output 6 will show the following relation between the transformation matrices; the last equality holds because these matrices are orthogonal.

$$T_j^{\,o} = \left(T_j^{\,i}\right)^{-1} = \left(\widetilde{T_j^{\,i}}\right), \quad j = 1, 2, 3 \tag{D60}$$

This is not surprising, since the output transformations are the inverse of the corresponding input transformations.

Output 7

Only two rotations and a translation are necessary to effect the transformation from X'_i, Y'_i, Z'_i coordinates to the quasi-inertial, topocentric rectangular system of Output 7. The matrix $T_3^{\,o}$ (eq. (D54)) is a unit matrix in view of the fact that $\lambda_6 = 0$ (eq. (D53)). The same translation of the origin is made as in Output 6, followed by a rotation about the y-axis represented by $T_2^{\,o}$ (eq. (D56)) and a second rotation about the resulting intermediate z-axis, $T_1^{\,o}$ (eq. (D57)). Equations (D61) and (D62) give the complete Output 7 transformation from geocentric X'_i, Y'_i, Z'_i coordinates to quasi-inertial topocentric coordinates (figs. 4.0-3 and 4.0-4).

$$\begin{bmatrix} x_q \\ y_q \\ z_q \end{bmatrix} = T_1^{\,o} T_2^{\,o} \left\{ \begin{bmatrix} X'_i \\ Y'_i \\ Z'_i \end{bmatrix} - \begin{bmatrix} \left(r_{D_q} + h_q\right) \cos L_q \\ 0 \\ \left(r_{D_q} + h_q\right) \sin L_q \end{bmatrix} \right\} \tag{D61}$$

$$\begin{bmatrix} \dot{x}_q \\ \dot{y}_q \\ \dot{z}_q \end{bmatrix} = T_1^{\,o} T_2^{\,o} \begin{bmatrix} \dot{X}'_i \\ \dot{Y}'_i \\ \dot{Z}'_i \end{bmatrix} \tag{D62}$$

Output 8

The rotational topocentric, rectangular position coordinates of Output 8 are identical to those of Output 7. A translation is made from the geocentric X'_i, Y'_i, Z'_i origin to the origin of the rotational topocentric system and then a rotation about the y-axis symbolized by $T_2^{\,o}$ (eq. (D56)) and another

about the resulting z-axis represented by $T_1^{\,o}$ (eq. (D57)). Equation (D63) gives this total transformation (fig. 4.0-4).

The velocities require that the component of the earth's rotation be subtracted from the inertial velocities before the rotation operators are applied. Equation (C42) is rewritten to effect this.

$$\dot{\vec{r}}_e = \dot{\vec{r}}_i - \vec{\omega} \times \vec{r}_e = \dot{\vec{r}}_i - \omega_e \hat{k} \times \vec{r}_e \qquad (C42')$$

Equation (D64) then gives the velocity components of Output 8.

$$\begin{bmatrix} x_e \\ y_e \\ z_e \end{bmatrix} = T_1^{\,o} T_2^{\,o} \left\{ \begin{bmatrix} X'_i \\ Y'_i \\ Z'_i \end{bmatrix} - \begin{bmatrix} \left(r_{D_q} + h_q\right) \cos L_q \\ 0 \\ \left(r_{D_q} + h_q\right) \sin L_q \end{bmatrix} \right\} \qquad (D63)$$

$$\begin{bmatrix} \dot{x}_e \\ \dot{y}_e \\ \dot{z}_e \end{bmatrix} = T_1^{\,o} T_2^{\,o} \left\{ \begin{bmatrix} \dot{X}'_i \\ \dot{Y}'_i \\ \dot{Z}'_i \end{bmatrix} - \begin{bmatrix} -\omega_e Y'_i \\ \omega_e X'_i \\ 0 \end{bmatrix} \right\} \qquad (D64)$$

Output 9

The radar centered coordinate system of Output 9 is a rotational, topocentric, spherical polar system, situated at the radar station coordinates L_{D_r}, λ_r, h_r. The x_r axis points north, the y_r axis points west, and the z_r axis is positive up. The polar coordinates are defined in terms of the x_r, y_r, z_r coordinates. In effect this system is the same as Output 8 with two exceptions. One, the transformation of spacecraft position and velocity to

inertial, geocentric, rectangular coordinates is made using equations (D32) through (D37) with λ_3 defined by equation (D65) instead of equation (D31).

$$\lambda_3 = \lambda - \lambda_r \tag{D65}$$

The resulting geocentric, rectangular coordinates X_i', Y_i', Z_i' and $\dot{X}_i', \dot{Y}_i', \dot{Z}_i'$ are then transformed to the rotational, topocentric, rectangular radar coordinates by equations (D66) and (D67) with $A_q = 0$, which is the second difference between the radar coordinates and those of Output 8. The matrix $T_1^{\,o}$ (eq. (D57)) then represents a rotation through the angle π about the intermediate z-axis. Equations (D56') and (D57') summarize the matrices $T_1^{\,o}$ and $T_2^{\,o}$ for Output 9. Note that here also the earth's velocity components are subtracted from the inertial velocity components of the vehicle in accordance with equation (C42').

$$T_2^{\,o} = \begin{bmatrix} \sin L_{D_r} & 0 & -\cos L_{D_r} \\ 0 & 1 & 0 \\ \cos L_{D_r} & 0 & \sin L_{D_r} \end{bmatrix} \tag{D56'}$$

$$T_1^{\,o} = \begin{bmatrix} -1 & 0 & 0 \\ 0 & -1 & 0 \\ 0 & 0 & 1 \end{bmatrix} \tag{D57'}$$

$$\begin{bmatrix} x_r \\ y_r \\ z_r \end{bmatrix} = T_1^{\,o} T_2^{\,o} \left\{ \begin{bmatrix} X'_i \\ Y'_i \\ Z'_i \end{bmatrix} - \begin{bmatrix} \left(r_{D_r} + h_r\right) \cos L_r \\ 0 \\ \left(r_{D_r} + h_r\right) \sin L_r \end{bmatrix} \right\} \tag{D66}$$

$$\begin{bmatrix} \dot{x}_r \\ \dot{y}_r \\ \dot{z}_r \end{bmatrix} = T_1^{\,o} T_2^{\,o} \left\{ \begin{bmatrix} \dot{X}'_i \\ \dot{Y}'_i \\ \dot{Z}'_i \end{bmatrix} - \begin{bmatrix} -\omega_e Y'_i \\ \omega_e X'_i \\ 0 \end{bmatrix} \right\} \tag{D67}$$

The slant range R_r, elevation angle E_r, the azimuth angle A_r, their time derivatives, and the altitude of the line of sight are then given by equations (D69) through (D75). Figures 4.0-4 and 13.0-1 give more details.

$$r_o = \sqrt{X_i^2 + Y_i^2 + Z_i^2} \tag{D68}$$

$$R_r = \sqrt{x_r^2 + y_r^2 + z_r^2} \tag{D69}$$

$$E_r = \tan^{-1}\left(\frac{z_r}{\sqrt{x_r^2 + y_r^2}}\right) \tag{D70}$$

$$A_r = \tan^{-1}\left(\frac{-y_r}{x_r}\right) \tag{D71}$$

$$\dot{R}_r = \frac{x_r\dot{x}_r + y_r\dot{y}_r + z_r\dot{z}_r}{R_r} \tag{D72}$$

$$\dot{E}_r = \frac{\left(x_r^2 + y_r^2\right)\dot{z}_r - \left(x_r\dot{x}_r + y_r\dot{y}_r\right) z_r}{R_r\sqrt{x_r^2 + y_r^2}} \tag{D73}$$

$$\dot{A}_r = \frac{\dot{x}_r y_r - x_r\dot{y}_r}{x_r^2 + y_r^2} \tag{D74}$$

$$h_s = h - \frac{R_r \sin E}{\sin I'} \tag{D75}$$

The angle I' is defined by equation (D77) or (D77a).

$$K' = \cos^{-1}\left(\frac{r_o^2 + R_r^2 - r_r^2}{2r_o r}\right) \tag{D76}$$

$$I' = K' + E_r \quad \text{if } E_r < 0 \tag{D77}$$

$$I' = \pi - \left(K' + E_r\right) \quad \text{if } E_r \geq 0 \tag{D77a}$$

Output 10

As is shown by figures 13.0-2 and 13.0-3, Output 10 quantities are related to the vehicle orbit and the relation of the orbit plane to the earth. The symbols used in this discussion are consistent with those in appendix K. Consult references 6, 7, and 8.

The orbit semimajor axis is given by equation (D80), where $\vec{r}_i$ is the radius vector from the origin to the vehicle in the inertial, geocentric, rectangular coordinates of Output 3.

$$\vec{r}_i = X_i \hat{i} + Y_i \hat{j} + Z_i \hat{k} \tag{D78}$$

$$\dot{\vec{r}}_i = \dot{X}_i \hat{i} + \dot{Y}_i \hat{j} + \dot{Z}_i \hat{k} \tag{D79}$$

$$a^{-1} = \frac{2}{\left|\vec{r}_i\right|} - \frac{\left|\dot{\vec{r}}_i\right|^2}{\mu} \tag{D80}$$

The eccentricity vector $\vec{e}$ joins the inertial coordinate system origin and the perigee of the orbit. Equation (D82) gives the orbit eccentricity

$$\vec{e} = \left(\left|\vec{r}_i\right|^{-1} - a^{-1}\right) \vec{r}_i - \frac{\left(\vec{r}_i \dot{\vec{r}}_i\right)}{\mu} \dot{\vec{r}}_i = e_x \hat{i} + e_y \hat{j} + e_z \hat{k} \tag{D81}$$

$$e = \sqrt{\vec{e} \cdot \vec{e}} \tag{D82}$$

The angular momentum $\underline{\vec{h}}$ per unit mass breaks down into three components

$$\underline{\vec{h}} = \vec{r}_i \times \dot{\vec{r}}_i = \underline{h}_x \hat{i} + \underline{h}_y \hat{j} + \underline{h}_z \hat{k} \tag{D83}$$

The inclination i of the orbit plane with respect to the earth equatorial plane is

$$i = \cos^{-1}\left(\frac{h_z}{|\vec{h}|}\right) \tag{D84}$$

At any time t the radius vector $\vec{r}_i$ makes an angle θ' with respect to the line of the ascending node, while the argument of the perigee ω is the angle between the line of the ascending node and the eccentricity vector. Both θ' and ω are measured in the orbit plane.

$$\theta' = \tan^{-1}\left(\frac{\frac{Z_i}{\sin i}}{X_i \cos \Omega + Y_i \sin \Omega}\right) \tag{D85}$$

$$\omega = \tan^{-1}\left(\frac{\frac{e_z}{\sin i}}{e_x \cos \Omega + e_y \sin \Omega}\right) \tag{D86}$$

where Ω is given by equation (D89). The true anomaly v is then

$$v = \theta' - \omega \tag{D87}$$

The eccentric anomaly E is

$$E = \tan^{-1}\left(\frac{\sqrt{1 - e^2}\sin v}{e + \cos v}\right) \tag{D88}$$

The angle Ω between the inertial X_i axis and the line of the ascending node is used in determining the longitude λ_n of the ascending node relative to Greenwich

$$\Omega = \tan^{-1}\left(\frac{h_x}{-h_y}\right) \tag{D89}$$

$$\lambda_n = \Omega + \lambda_x - \omega_e\left(\tau - \frac{\omega}{2\pi} T_p - t_x\right) \tag{D90}$$

The predicted time of the next perigee τ_p and the period of the orbit T_p are

$$\tau_p = t - \sqrt{\frac{a^3}{\mu}}\,(E - e \sin E) \tag{D91}$$

$$T_p = 2\pi\sqrt{\frac{a^3}{\mu}} \tag{D92}$$

The geocentric latitude L_p of the perigee is given by

$$L_p = \tan^{-1}\left(\frac{e_z}{\sqrt{e_x^2 + e_y^2}}\right) \tag{D93}$$

Several auxiliary quantities are required in order to compute the geodetic latitude of the perigee L_{D_p}. These are the flattening f of the earth

and the distance r_p' from the center of the earth to the perigee. These equations are

$$f = \frac{r_e - r_p}{r_e} \tag{D94}$$

$$r_p' = a(1 - e) \tag{D95}$$

$$\sin\left(L_{D_p} - L_p\right) = \frac{r_e}{r_p'} f \sin 2L_p + f^2\left(\frac{r_e}{r_p'} - \frac{1}{4}\right) \sin 4L_p \tag{D96}$$

$$L_{D_p} = L_p + \tan^{-1}\left[\frac{\sin\left(L_{D_p} - L_p\right)}{\cos\left(L_{D_p} - L_p\right)}\right] \tag{D97}$$

Since the geocentric latitude of the apogee L_a is the negative of that of the perigee, equations (D96) and (D97) can be used to determine the geodetic latitude of the apogee by substituting r_a', the distance from the earth center to the apogee, for r_p', and L_a for L_p, where

$$L_a = -L_p \tag{D98}$$

$$r_a' = a(1 + e) \tag{D99}$$

The altitudes of the perigee and apogee above the reference spheroid are

$$h_p = H + r_e\left[f \sin^2 L_p + \left(\frac{f}{2}\right)^2\left(\frac{r_e}{r_p'} - \frac{1}{4}\right) \sin^2 2L_p\right] \tag{D100}$$

$$h_a = H + r_e \left[f \sin^2 L_a + \left(\frac{f}{2}\right)^2 \left(\frac{r_e}{r'_a} - \frac{1}{4}\right) \sin^2 2L_a \right] \qquad \text{(D101)}$$

The longitudes of perigee and apogee referenced to Greenwich are

$$\lambda_p = \tan^{-1}\left(\frac{e_y}{e_x}\right) + \lambda_x - \omega_e \left(\tau - t_x\right) \qquad \text{(D102)}$$

$$\lambda_a = \tan^{-1}\left(\frac{e_y}{e_x}\right) + \pi + \lambda_x - \omega_e \left(\tau - t_x + \frac{T_p}{2}\right) \qquad \text{(D103)}$$

Output 11

Not used.

Output 12

This output is controlled by Special Option 17 and should not be activated by using the 590 card. It is a general purpose output that can be modified as demands require. At present it is set to write current time t, seconds; altitude h, feet; and aerodynamic velocity V_a, feet/second, in format 3E19.8 on tape B1 whenever altitude h less than 400 000 feet and/or convective heat rate $\dot{H}_c$ is greater than 0.25 Btu/ft^2-sec. Logical tape N may be substituted for B1 by using the card 115 DEC N.

Output 13

This Output is controlled by Special Option 7 or Special Option 23 and prints the heating and atmospheric parameters generated by the activated option. Output 13 should not be activated on the 590 card.

Atmospheric Properties Computed by Both Special Options 7 and 23

Equations (D104) and (D105) are used to compute atmospheric density ρ and pressure P for the 1959 ARDC and MSC composite atmosphere models

$$\rho = \rho_b \left[\frac{T_{M_b}}{T_{M_b} + L_M \left(H' - H'_b\right)} \right]^{\left(1+GM_o\right)/L_M R^*} \tag{D104}$$

for $L_M \neq 0$

$$\rho = \rho_b \exp \left[\frac{-GM_o \left(H' - H'_b\right)}{T_{M_b} R^*} \right] \tag{D104a}$$

for $L_M = 0$

$$P = \frac{\rho T_M R^*}{M_o} \tag{D105}$$

For the 1962 U. S. Standard Atmosphere Model, equations (D106) and (D107) are used for ρ and P

$$P = P'_b \left[\frac{T_{M_b}}{T_{M_b} + L_M \left(H' - H'_b\right)} \right]^{GM_o/L_M R^*} \tag{D106}$$

for $L_M \neq 0$

$$P = P'_b \exp\left[\frac{-GM_o\left(H' - H'_b\right)}{T_{M_b} R^*}\right] \tag{D106a}$$

for $L_M = 0$

$$\rho = \frac{M_o P}{T_M R^*} \tag{D107}$$

For all three atmosphere models as well as when density is obtained as a tabular function of altitude, equations (D108) through (D113) give molecular scale temperature T_M, atmospheric temperature T_a, sound speed V_s, coefficient of viscosity ν, and Reynolds number N_{Re}.

$$T_M = T_{M_b} + L_M \left(H' - H'_b\right) \tag{D108}$$

To obtain the atmospheric temperature, equation (D109) is used. For the 1959 ARDC and MSC Composite Atmosphere Models at all altitudes and in the 1962 U. S. Standard Atmosphere Model up to an altitude of 90 km, $\frac{M'}{M_o} = 1$, and thus $T_a = T_m$. In the latter atmosphere model, M' is given by equation (D110) for altitudes above 90 km.

$$T_a = \frac{M'}{M_o} T_M \tag{D109}$$

$$M' = \sum_{i=0}^{8} \xi_i h^i \tag{D110}$$

$$V_s = \sqrt{\frac{\gamma' R^* T_M}{M_o}} \tag{D111}$$

$$\nu = \frac{\xi T_a^{\frac{3}{2}}}{S' + T_a} \tag{D112}$$

$$N_{Re} = \frac{\rho V_a d}{\nu} \tag{D113}$$

Heating Equations Used by Special Option 7

Convective heat rate is taken as the smaller of the two values computed by equations (D114) and (D115), and F'_c and F'_m are both normally unity.

$$\dot{H}_c = 17600 \frac{F'_c}{\sqrt{R_n}} \left(\frac{\rho}{\rho_o}\right)^{\frac{1}{2}} \left(\frac{V_a}{26000}\right)^{3.15} \tag{D114}$$

$$\dot{H}_m = F_m' \frac{\rho V_a^3}{1556} \tag{D115}$$

Radiative heat rate is computed by equation (D116); C_1 and C_2 are functions of aerodynamic velocity obtained from a table (see C_1, C_2 in list of constants). The quantity F'_r is usually 1.0.

$$\dot{H}_r = F'_r C_1 R_n \left(\frac{\rho}{\rho_o}\right)^{1.78} \left(\frac{V_a}{10000}\right)^{C_2} \tag{D116}$$

The heating rates are integrated numerically along with the equations of motion to obtain the heat content, equations (D117) and (D118):

$$H_c = \int_t \dot{H}_c \, dt \tag{D117}$$

$$H_r = \int_t \dot{H}_r \, dt \tag{D118}$$

The total heating rate and content are given by equations (D119) and (D120).

$$\dot{H} = \dot{H}_c + \dot{H}_r \tag{D119}$$

$$H = H_c + H_r \tag{D120}$$

The remaining items printed are the convective and radiative heating rates and integrals multiplied or divided by $\sqrt{R_n}$, hence these equations are omitted.

Heating Equations Used by Special Option 23

Convective heating rate is taken as the smaller value calculated by equations (D114) or (D115). Equation (D115) is also used to compute the molecular heating rate, and F_c' is usually some input value greater than 1.0 while F_m' normally is 1.0.

Several supporting equations are used in the calculation of the radiative heating rate, equation (D121) or (D122); these equations were derived by Messrs. D. A. Dansak and Robert C. Ried, both of NASA-MSC. These are listed below.

$$B = \log_{10} \left(\frac{\rho}{\rho_o} \right)$$

$$C = 8.41 \exp\left(-6.25 \times 10^{-5} V_a\right)$$

$$D = 0.56 \exp\left[\left(-1.58 \times 10^{-8}\right)\left(V_a - 2.6 \times 10^{4}\right)^2\right]$$

$$E = 4.15 \exp\left(-7.25 \times 10^{-5} V_a\right)$$

$$F = 8.26 \exp\left(-7.0 \times 10^{-5} V_a\right)$$

$$G = 14.25 \exp\left(-2.45 \times 10^{-4} V_a\right)$$

$$H'' = \exp\left(2.17 \times 10^{-4} V_a - 3.563\right)$$

$$I = 7.34 - 4.45 \times 10^{-6} V_a$$

$$X_s = \frac{0.55\ D'\ K}{\left[\dfrac{(1-K)^2}{1-\sqrt{1-(1-K)^2}}\right] - K}$$

$$\log_{10} A = \frac{B - C - D + 5.5}{I}$$

$$\log_{10} \delta_1 = \frac{E - B - 4.66}{0.98}$$

$$\log_{10} \delta_2 = \frac{F + G - B - 4.67}{0.98}$$

$$\delta_3 = \frac{X_s^2}{2\,\delta_1^2} \left[\frac{2\,\delta_1 A}{H'' + A\,(\delta_1 - \delta_2)} + 1 \right]$$

$$\dot{H}_r = 0.88\, F_r' \left[AX_s + (H'' - A\,\delta_2) \right] \left(1 - e^{-\delta_3}\right) \quad \text{if } \frac{H''}{A\,\delta_2} > 1 \qquad \text{(D121)}$$

$$\dot{H}_r = 0.88\, F_r' AX_s \quad \text{if } \frac{H''}{A\,\delta_2} \leq 1 \qquad \text{(D122)}$$

In the equation for X_s, the quantity $D' = 391.7$, and K is obtained from a table of K^{-1} as a function of altitude and aerodynamic velocity, and F_r' is normally unity. Locations 739 through 741 are the table control locations for the K^{-1} table.

The radiative heat content is found in the usual manner by integration of $\dot{H}_r$. The total heating rate and total heat content also contain the molecular terms, whereas in Special Option 7 these were not computed. Equations (D123) and (D125) summarize this:

$$\dot{H} = \dot{H}_c + \dot{H}_m + \dot{H}_r \qquad \text{(D123)}$$

$$H_m = \int_t \dot{H}_m \, dt \qquad \text{(D124)}$$

$$H = H_c + H_m + H_r \qquad \text{(D125)}$$

As in Special Option 7, the remaining data printed out are the convective and radiative rates and integrals multiplied or divided by $\sqrt{R_n}$.

Output 14

Some of the items of this Output do not require special formulas and for that reason will not be listed; for example, altitude in nautical miles.

Equation (D126) gives the time rate of change of track which is integrated numerically to give the ground track

$$\dot{\chi} = \frac{d\chi}{dt} = \frac{r_D}{r_e} V_e \cos \gamma_e \qquad \text{(D126)}$$

$$\chi = \int_t \dot{\chi}\, dt \qquad \text{(D127)}$$

The orbit radius, that is, the distance from the earth center to the vehicle at the current position is

$$r = H + r_e \qquad \text{(D128)}$$

Radial force F_r in pounds is given by equation (30).

Central angle θ_c is defined as the inertial longitude traveled in the orbit plane. The reference point from which θ_c is measured must be specified in locations 130 through 133.

130 DEC θ_{c_o} initial value of θ_c at start of case, deg

131 DEC t_{c_r} time at which the reference point was at longitude λ_{c_r}, sec

132 DEC $L_{D_{c_r}}$ geodetic latitude of reference point, deg

133 DEC λ_{c_r} longitude of reference point relative to Greenwich, deg

Let L_{c_r} be the geocentric equivalent of $L_{D_{c_r}}$; θ_c is then given by the law of cosines for spherical triangles

$$\theta_c = \theta_{c_o} + \cos^{-1}\left(\cos \Delta L - 2 \cos L \cos L_{c_r} \sin^2 \frac{\Delta\lambda}{2}\right) \qquad \text{(D129)}$$

where $\Delta L = L - L_{c_r}$, and $\Delta\lambda = \lambda - \lambda_{c_r} + \omega_e \left(t - t_{c_r}\right)$.

The ratio of the inertial velocity to the minimum required inertial orbital velocity is given by equation (D130). Special Option 15 must be activated in order to compute $\frac{V_i}{V_{i_r}}$

$$\frac{V_i}{V_{i_r}} = \frac{\mu}{r}\left(K_6 r + K_7\right) \qquad \text{(D130)}$$

The change in the x component of velocity in the body-centered coordinate system since the start of this section is computed by equation (D131). The index i denotes a sum over all integration intervals in the section with Δt_i being the current integration step size:

$$\Delta V = g_o \sum_i g_{x_i} \Delta t_i \qquad \text{(D131)}$$

Outputs 15 through 18

Not used.

Output 19

This output is used to write the X-Y plotter tape and is controlled by Special Option 27. It should not be activated nor deactivated on the 590 card. See Special Option 27 for instructions on setting up the required data for generating the plot tape.

APPENDIX E

BINARY TAPE WRITTEN BY SPECIAL OPTION 14

The decrement of the first word in each record contains the word count for that record and the address has a "1", thus permitting the binary tape to be read by a FORTRAN II read tape statement. The first record of each section contains the 20 BCD words of case description from locations 500 through 519 and the second record is the 4 BCD words describing the section, locations 640 through 643. Records 3 to the end of the section contain the trajectory information given below, one record for each integration step in the trajectory. Specifically, record 3 gives the 79 words of trajectory information existing at the start of the first integration step in the current section. Record 4 gives the same data for the end of the first integration step. Record 5 data are that of the end of the second integration step, and so forth. The trajectory status at the end of the last integration step in a section is recorded. The data written at the start of each subsequent section will be similar to that of the first section, beginning with record 1 repeating the case description, record 2 giving the new section description, and continuing with records 3, 4, ... as previously described.

At the end of the case, one end of file mark is written on the binary tape provided Special Option 14 is still activated at that time. Subsequent cases follow the same format as the first.

The trajectory data of records 3, 4, 5, ... are written in the following order:

1. t_s section time, sec
2. ΔL latitude traversed since start of section, rad
3. $\Delta\lambda$ longitude traversed since start of section, rad
4. H altitude above geocentric sphere, ft
5. $\dot{L}$ geocentric latitude rate, rad/sec
6. $\dot{\lambda}$ longitude rate, rad/sec
7. $\dot{H}$ altitude rate, ft/sec

8. W weight, lb

9. χ track, ft

10. H_c convective heat content, Btu/ft^2

11. H_r radiative heat content, Btu/ft^2

12. $\ddot{L}$ geocentric latitude acceleration, rad/sec^2

13. $\ddot{\lambda}$ longitude acceleration, rad/sec^2

14. $\ddot{H}$ altitude acceleration, ft/sec^2

15. $\dot{W}$ rate change of weight, lb/sec

16. $\dot{H}_c$ convective heating rate, Btu/ft^2-sec

17. $\dot{H}_r$ radiative heating rate, Btu/ft^2-sec

18. L_b geocentric latitude at beginning of case, rad

19. λ_b longitude at beginning of section, rad

20. Δh_b altitude difference between equatorial earth radius and local earth radius at beginning of case, ft

21. t_b elapsed time at beginning of case, sec

22. t_{s_o} elapsed time at beginning of section less t_b, sec

23. L_s geocentric latitude at beginning of section less L_b, rad

24. λ_s longitude at beginning of section less λ_b, rad

25. L current geocentric latitude, rad

26. λ current Greenwich referenced longitude, rad

27. r_D local earth radius, ft

28. r radius vector from geocenter to vehicle, ft

29. h altitude above oblate earth spheroid, ft

30. Δh altitude difference, ft

31. ρ atmospheric density, slug/ft^3

32. P atmospheric pressure, lb/ft^2

33. $P_o - P$ pressure difference, lb/ft^2

34. W_N north wind component, ft/sec

35. W_E east wind component, ft/sec

36. V_s speed of sound, ft/sec

37. V_{i_E} inertial east velocity, ft/sec

38. V_{e_E} relative east velocity, ft/sec

39. V_{e_N} relative north velocity, ft/sec

40. $V_{e_{hor}}$ relative horizontal velocity, ft/sec

41. $V_{a_{hor}}$ aerodynamic horizontal velocity, ft/sec

42. V_{a_E} aerodynamic east velocity, ft/sec

43. V_{a_N} aerodynamic north velocity, ft/sec

44. V_{a_U} aerodynamic upward velocity, ft/sec

45. $u_a = \dot{x}_{b_a}$ } aerodynamic velocity in body

46. $v_a = \dot{y}_{b_a}$ } coordinates, ft/sec

47. $w_a = \dot{z}_{b_a}$ }

48. V_a aerodynamic velocity, ft/sec

49. V_{a_n} vertical component of aerodynamic velocity, ft/sec

50. γ_a aerodynamic flight path angle, rad

51. ψ_a aerodynamic azimuth, rad

52. $\bar{q}$ dynamic pressure, lb/ft^2

53. $\bar{q}S$ dynamic force, lb

54. M Mach number, dimensionless

55. T total thrust, lb

56. T' corrected thrust, lb

57. m mass, slugs

58. P_b body pitch angle, rad

59. Y_b body yaw angle, rad

60. F_{a_x} aerodynamic x_b force, lb

61. F_{a_y} aerodynamic y_b force, lb

62. F_{a_z} aerodynamic z_b force, lb

63. F_{T_x} thrust, x_b component, lb

64. F_{T_y} thrust, y_b component, lb

65. F_{T_z} thrust, z_b component, lb

66. F_x total aerodynamic and thrust forces, x_b component, lb

67. F_y total aerodynamic and thrust forces, y_b component, lb

68. F_z total aerodynamic and thrust forces, z_b component, lb

69. F_{a_n} aerodynamic force normal to wind axis, lb

70. F_λ total aerodynamic and thrust forces in easterly direction, lb

71. F_N total aerodynamic and thrust forces in north direction, lb

72. F_r total aerodynamic and thrust forces in radial direction, lb

73. g_r radial gravitational acceleration, ft/sec^2

74. g_L tangential gravitational acceleration, ft/sec^2

75. α pitch angle of attack, rad

76. $|\alpha|$ absolute value of α, deg

77. C_a axial drag coefficient, dimensionless

78. C_n normal force (lift) coefficient, dimensionless

79. R range, ft or n. mi., depending on range option

APPENDIX F

SPECIAL OPTION 27, X-Y PLOTTER INFORMATION

Output quantities and their respective indexes for use in writing X-Y plotter tapes.

	Quantity	Index
	Output 0, first line	
t	elapsed time, sec	152
t	elapsed time, hr	153
	elapsed time, min	154
	elapsed time, sec	155
t_s	section time, sec	156
t_c	case time, sec	157
GMT	days	439
	hr	158
	min	159
	sec	160
L_D	geodetic latitude, deg	161
	geodetic latitude, min	162
	geodetic latitude, sec	163

	Quantity	Index
	Output 0, second line	
N	revolution number	164
λ	longitude, deg	165
	longitude, min	166
	longitude, sec	167
	Output 0, second line	
L	geocentric latitude, deg	168
L_D	geodetic latitude, deg	169
λ	longitude, deg	170
h	altitude, ft	171
R	range, ft or n. mi.	172
V_a	aerodynamic velocity, ft/sec	173
γ_a	aerodynamic flight path angle, deg	174
ψ_a	aerodynamic azimuth, deg	175
	Output 0, third line	
g_x	aerodynamic and thrust load	176
g_y	factors in body coordinates	177
g_z	g units	178
r	radius vector to vehicle, ft	179

	Quantity	Index
	Output 0, third line	
T	thrust, lb	180
W	weight, lb	181
M	Mach number	182
$\bar{q}$	dynamic pressure, lb/ft^2	183
	Output 1	
V_i	inertial velocity, ft/sec	184
γ_i	inertial flight path angle, deg	185
ψ_i	inertial azimuth, deg	186
V_e	relative velocity, ft/sec	187
γ_e	relative flight path angle, deg	188
ψ_e	relative azimuth, deg	189
γ_D	geodetic flight path angle, deg	190
ψ_D	geodetic azimuth, deg	191
	Output 2	
η	total angle of attack, deg	192
α	pitch angle of attack, deg	193
β	angle of side slip, deg	194

Quantity		Index
	Output 2	
D	drag, lb	195
F_{a_n}	aerodynamic normal force (lift), lb	196
φ_n	angle between F_{a_n} and vertical plane, deg	197
θ	body pitch, deg	198
φ	body azimuth, deg	199
	Output 3	
X_i	inertial position coordinates, ft	200
Y_i		201
Z_i		202
$\dot{X}_i$	inertial velocity coordinates, ft/sec	203
$\dot{Y}_i$		204
$\dot{Z}_i$		205
	Output 4	
X_q	quasi-inertial position coordinates, ft	208
Y_q		209
Z_q		210

Quantity		Index
	Output 4	
$\dot{X}_q$		211
$\dot{Y}_q$	quasi-inertial velocity coordinates, ft/sec	212
$\dot{Z}_q$		213
	Output 5	
X_e		216
Y_e	rotating position coordinates, ft	217
Z_e		218
$\dot{X}_e$		219
$\dot{Y}_e$	rotating velocity coordinates, ft/sec	220
$\dot{Z}_e$		221
	Output 6	
x		224
y	topocentric inertial position coordinates, ft	225
z		226
$\dot{x}$		227
$\dot{y}$	topocentric inertial velocity coordinates, ft/sec	228
$\dot{z}$		229

Quantity		Index
	Output 7	
x_q	topocentric, quasi-inertial position coordinates, ft	232
y_q		233
z_q		234
$\dot{x}_q$	topocentric, quasi-inertial velocity coordinates, ft/sec	235
$\dot{y}_q$		236
$\dot{z}_q$		237
	Output 8	
x_e	topocentric, rotating position coordinates, ft	240
y_e		241
z_e		242
$\dot{x}_e$	topocentric, rotating velocity coordinates, ft/sec	243
$\dot{y}_e$		244
$\dot{z}_e$		245

	Quantity	Index
	Output 9	
	station name	248-250
R_r	slant range, n. mi.	251
E_r	elevation angle, deg	252
A_r	azimuth angle, deg	253
$\dot{R}_r$	$\frac{dR_r}{dt}$, ft/sec	254
$\dot{E}_r$	$\frac{dE_r}{dt}$, deg/sec	255
$\dot{A}_r$	$\frac{dA_r}{dt}$, deg/sec	256
h_s	altitude of line of sight, ft	257
	Output 10, first line	
h_p	perigee altitude, n. mi.	259
h_a	apogee altitude, n. mi.	260
λ_p	perigee longitude, deg	261
L_{D_p}	geodetic latitude of perigee, deg	262
L_p	geocentric latitude of perigee, deg	263
λ_a	apogee longitude, deg	264

	Quantity	Index
	Output 10, first line	
L_{D_a}	geodetic latitude of apogee, deg	265
i	orbit plane inclination, deg	266
	Output 10, second line	
e	orbit eccentricity	267
T_p	satellite period, min	268
ω	argument of perigee, deg	269
E	eccentric anomaly, deg	270
v	true anomaly, deg	271
λ_n	Greenwich referenced longitude of line of ascending node, deg	272
τ_p	time of next perigee passage, sec	273
a	orbit semimajor axis, ft	274
	Special Option 7 or Special Option 23 Heating Output	
	First line	
ρ	atmospheric density, slug/ft^3	275
T_M	molecular scale temperature, °R	276
$\dot{H}_c$	convective heating rate, Btu/ft^2-sec	277

	First line	Index
H_c	convective heat integral, Btu/ft^2	278
$\dot{H}_r$	radiative heating rate, Btu/ft^2-sec	279
H_r	radiative heat integral, Btu/ft^2	280
$\dot{H}_t$	total heating rate, Btu/ft^2-sec	281
H_t	total heat integral, Btu/ft^2	282
	Second line	
ν	air viscosity, slug/ft-sec	283
N_{Re}	Reynolds number	284
$\dot{H}_c \sqrt{R_n}$		285
$H_c \sqrt{R_n}$		286
$\dot{H}_r / \sqrt{R_n}$		287
$H_r / \sqrt{R_n}$		288

	Second line	Index
$\dot{H}_m$	molecular heating rate, Btu/ft^2-sec (Special Option 23 only)	289
H_m	molecular heat integral, Btu/ft^2 (Special Option 23 only)	290

Output 14

h	altitude, n. mi.	291
χ	track, n. mi.	292
r	radius vector from geocenter to vehicle, n. mi.	293
F_r	radial force, lb	294
θ_c	central angle, deg	295
$\frac{V_i}{V_{i_r}}$		296
ΔV	incremental change in x_b component of body velocity, ft/sec	297
φ_r	roll angle, deg	298

SYMBOL PLOTTING CODES

Plotter symbol	Symbol code	Plotter symbol	Symbol code
1	1.	Z	31.
2	2.	,	33.
3	3.	)	34.
4	4.	-	40.
5	5.	$\overline{J}$	41.
6	6.	K	42.
7	7.	L	43.
8	10.	M	44.
9	11.	N	45.
=	13.	O	46.
⊡	14.	P	47.
0	20.	Q	50.
/	21.	R	51.
S	22.	⊙	53.
T	23.	*	54.
U	24.	+	60.
V	25.	A	61.
W	26.	B	62.
X	27.	C	63.
Y	30.	D	64.

Plotter symbol	Symbol code	Plotter symbol	Symbol code
E	65.	I	71.
F	66.	.	73.
G	67.	(	74.
H	70.	⊙	100.

APPENDIX G

FORMULAS USED IN RANGE COMPUTATION

Range Option 680 DEC 0 employs equation (G1) to give the range from the initial point of the trajectory projected onto the surface of the earth, L_o, λ_o, where L_o represents the geocentric equivalent of the initial geodetic latitude L_{D_o}.

$$R = \sqrt{\left[\left(r_D \cos L\right) \Delta\lambda - x_o\right]^2 + \left[r_D \Delta L - y_o\right]^2} \tag{G1}$$

where $\Delta\lambda = \lambda - \lambda_o$, $\Delta L = L - L_o$; and x_o, y_o are given on cards 681 and 682, respectively.

When the range given by equation (G1) exceeds 300 000 ft, the law of cosines for spherical triangles is used to give the range angle θ_r. Equations (G2) and (G3) define the changes in geocentric latitude and longitude

$$\Delta L = L - L_o - \frac{y_o}{r_D} \tag{G2}$$

$$\Delta\lambda = \lambda - \lambda_o - \frac{x_o}{r_D \cos L_o} \tag{G3}$$

$$\theta_r = \cos^{-1}\left[\cos \Delta L - 2 \cos L \cos L_o \sin^2 \frac{\Delta\lambda}{2}\right] \tag{G4}$$

The average earth radius is defined by equation (G5), and the range is then given by equation (G6).

$$R_{av} = \frac{r_{D_o} + r_D}{2} \tag{G5}$$

$$R = R_{av}\theta_r \tag{G6}$$

Range Option 680 DEC 1 uses equation (G4) to give the range angle θ_r with the geocentric latitude and longitude changes given by equations (G7) and (G8), respectively

$$\Delta L = L - L_r \tag{G7}$$

$$\Delta\lambda = \lambda - \lambda_r \tag{G8}$$

Note that L_r is the geocentric equivalent of L_{D_r}, where L_{D_r} and λ_r are specified on cards 681 and 682, respectively.

Equation (G9) gives the average earth radius, and then the range is formed from equation (G6)

$$R_{av} = \frac{r_D + r_{D_r}}{2} \tag{G9}$$

where r_{D_r} is the local earth radius at the reference point geodetic latitude L_{D_r}.

APPENDIX H

RADAR STATION INFORMATION REQUIRED BY OUTPUT 9

The radar station coordinate system has its origin at the station; its x-y plane is parallel to the geodetic earth with the z-axis positive up, the x-axis pointing north, and the y-axis pointing west. The azimuth is measured east of north and the elevation is with respect to the x-y plane. Slant range is the radius vector from the station to the vehicle expressed in the radar station coordinates. The altitude of the line of sight is defined in figure 13.0-1. Each station has a set of these right-handed, Cartesian coordinates, and the vehicle is referenced to each station within whose range it comes.

Six data words are required to describe each radar station. The first three are the BCD name or description of the station. The next three, in order, are the coordinates of the station: geodetic latitude in degrees, Greenwich referenced longitude in degrees, and altitude above the geodetic earth in feet. Thirty stations are permitted, beginning in location 5820.

5820	BCD	3 RADAR STATION 1
5823	DEC	$L_{D_{r1}}, \lambda_{r1}, h_{r1}$
.	.	.
.	.	.
.	.	.
5820 + 6 (n-1)	BCD	3 RADAR STATION n
5823 + 6 (n-1)	DEC	$L_{D_{rn}}, \lambda_{rn}, h_{rn}$

The range over which the radar station will pick up the satellite is specified by a longitude band $\Delta\lambda$ on either side of the radar station and a

maximum slant range $R_{r_{max}}$. The satellite must be within both tolerances to be picked up.

781	DEC	$\Delta\lambda$	deg
782	DEC	$R_{r_{max}}$	n. mi.

APPENDIX I

NOMINAL PROGRAM CONTENTS

In order to compute a trajectory, certain constants and controls are required in addition to the initial position and velocity. To eliminate the necessity of supplying these constants with each input deck, they have been incorporated into the program itself. If it is desired to change any values previously set in this manner, then the appropriate data cards are included in case data. For example, if the earth radius is to be 20 000 000 ft, include the card 660 DEC 20000000. with the case data for the trajectory in question.

Some locations require floating point data (numbers with a decimal point) and others must have fixed point values (integers without a decimal). On the attached list of program nominal contents, a decimal point appears where it is required, and no decimal is shown with integer data.

LIST OF INPUT LOCATIONS AND NOMINAL CONTENTS

FLOATING POINT NUMBERS CONTAIN A . FIXED POINT NUMBERS DO NOT

```
 115 BCD 187              TAPE B7 FOR SPECIAL OPTION 14 BINARY TAPE
 116 DEC 8                LOGICAL TAPE 8 (B1) FOR SPEC.OPTN. 17 OUTPUT
 117 DEC 2.302585093      LOG(E) TO LOG(10) CONVERSION FACTOR
 118 DEC 391.7            GEMINI HEAT PARAMETER, CM.

 129 DEC 0.               INITIAL ROLL ANGLE, DEG., SPEC.OPTN. 32
 130 DEC 0.               INITIAL CENTRAL ANGLE, DEG.
 131 DEC 0.               TIME (SEC.) OF CENTRAL ANGLE REFERENCE LONG.
                          COORDINATES OF CENTRAL ANGLE REFERENCE POINT
 132 DEC 0.               GEODETIC LATITUDE, DEG.    OF CENTRAL ANGLE
 133 DEC 0.               LONGITUDE, DEG.             REFERENCE POINT

 167 DEC 1.57079632       PI/2
 168 DEC 3.14159265       PI
 169 DEC 6.28318530       2PI
 170 DEC 57.2957795       RADIANS TO DEGREES CONVERSION FACTOR
 171 DEC .0174532925      DEGREES TO RADIANS CONVERSION FACTOR

 176 DEC .16457916E-3     FEET TO NAUT.MI. CONVERSION FACTOR
 177 DEC 6076.1033        NAUT. MI. TO FEET CONVERSION FACTOR
 178 DEC 32.174078        SEA LEVEL GRAVITATIONAL ACCELERATION

 181 DEC 3.2808399        METERS TO FEET CONVERSION FACTOR
 182 DEC 2116.3           SEA LEVEL ATMOSPHERIC PRESSURE,PSF

 185 DEC 20855523.        AVERAGE EARTH RADIUS,FT.

 252 DEC .785398163       PI/4          . FACTORS
 253 DEC 17.804218        C CONSTANT    . USED IN
 254 DEC 4.0236           A CONSTANT    . MERCATOR PLOTTING OF
 255 DEC .4                             . GEOD.LATITUDE AND LONGITUDE

 270 DEC 2.3769E-3        SEA LEVEL ATMOSPHERIC DENSITY,SLUGS/FT**3

     RETRO QUANTITIES FOR N RETRO FIRE MODE, SPECIAL OPTION 21

 340 DEC 0.,0.,0.,0.,0.,0.,0.,0.,0.,0.  EXIT AREA, SP.OPT. 21
 350 DEC 0.,0.,0.,0.,0.,0.,0.,0.,0.,0.  TAU, SP.OPT. 21
 360 DEC 0.,0.,0.,0.,0.,0.,0.,0.,0.,0.  SIGMA, SP.OPT. 21
 370 DEC 0.,0.,0.,0.,0.,0.,0.,0.,0.,0.  THRUSTS, SP.OPT. 21
 380 DEC 0.,0.,0.,0.,0.,0.,0.,0.,0.,0.  THRUST START TIMES, SP.OPT. 21
 390 DEC 0.,0.,0.,0.,0.,0.,0.,0.,0.,0.  THRUST STOP TIMES, SP.OPT. 21

 440 DEC 0                NUMBER OF RETROS, SPECIAL OPTION 21

 441 DEC 1.               AXIAL DRAG COEFFICIENT (CD) MULTIPLIER
 442 DEC 1.               LIFT COEFFICIENT (CN) MULTIPLIER
```

```
        TITLES

500 BCD  C03E PARTICLE TRAJECTORY NEAR AN OBLATE EARTH
510 BCD 2SECTION
512 BCD 3DATE
515 BCD 5NAME

                        INTEGRATION ACCURACY CRITERIA, EPSILONS

520 DEC 1E-5,1E-5,1E-5,1E-5,1E-5,1E-5,1E-5,1E-5,1E-5

                        INTEGRATION SMALL VALUE CRITERIA, DELTAS

550 DEC 1E-5,1E-5,1E-5,1E-5,1E-5,1E-5,1E-5,1E-5,1E-5


        PROGRAM CONTROLS

580 DEC 1.              INITIAL INTEGRATION STEP SIZE (SEC.)
581 DEC 1               PRINT FREQUENCY
582 DEC 0               CODE FOR INPUT IN METERS
583 DEC 0               GEOCENTRIC LATITUDE INPUT

586 DEC 0               CODE TO SPECIFY INPUT TAPE UNIT, SWITCH FROM
                        TAPE A2 TO TAPE A4 IN RETRO PREDICTION MODE
587 DEC 0               SKIP THIS NUMBER OF FILES BEFORE START OF
                        CASE FOR USE IN REAL TIME CALCULATIONS WITH
                        SPECIAL TAPES
588 DEC 1               INPUT CODE
589 DEC 1               TERMINATION CODE
590 DEC 0,0,0,0         OUTPUT CODES (20 LOCATIONS)

610 DEC 0,0,0,0         SPECIAL OPTION CODES(30 LOCATIONS)

640 BCD 4STEP DESCRIPTION
644 DEC 1,0,0           ATTITUDE OPTION

        CO-ORDINATE SYSTEM CONSTANTS

650 DEC 0.              LONGITUDE OF XAXIS (I-O 3,4,5) (DEG)
651 DEC 0.              ELAPSED TIME OF LONGITUDE (I-O 3) (SEC)

653 DEC 0.              GEOD LAT OF ORIGIN (I-O 6,7,8) (DEG)
654 DEC 0.              LONGITUDE OF ORIGIN (DEG) (I-O 6,7,8)
655 DEC 0.              ALTITUDE OF ORIGIN (FEET) (I-O 6,7,8)
656 DEC 0.              AZIMUTH OF X AXIS (DEG) (I-O 6,7,8)
657 DEC 0.              ELAPSED TIME OF ORIGIN (I-O 6) (SEC)

        EARTH CONSTANTS

660 DEC 20925738.       EQUATORIAL RADIUS (A) INT.FEET
661 DEC 298.29599       RECIPROCAL OF FLATTENING (1/F)
662 DEC 1.407654E16     GRAVITATIONAL CONSTANT (MU)
663 DEC 1623.46E-6      SECOND HARMONIC COEFFICIENT(J)
664 DEC 0.              THIRD HARMONIC COEFFICIENT (H)
665 DEC 8.849E-6        FOURTH HARMONIC COEFFICIENT (K)
```

```
666 DEC .729211508E-4   ROTATION RATE (OMEGA),RAD/SEC

        RANGE

680 DEC 0               RANGE OPTION
681 DEC 0.              LATITUDE OR X CO-ORD IN FEET OF RANGE REF
682 DEC 0.              LONGITUDE OR Y CO-ORD OF RANGE REF

        HEAT CONSTANTS

685 DEC 1.              RADIUS OF CURVATURE (FEET)
686 DEC 1.              CHARACTERISTIC LENGTH (FEET)
687 DEC 1.              FC (CONVECTIVE HEAT RATE MULTIPLIER)
688 DEC 1.              FM (FREE MOLECULAR HEAT RATE MULTIPLIER)
689 DEC 1.              FR (RADIATIVE HEAT RATE MULTIPLIER)

        AERODYNAMICS

690 DEC 1.              EFFECTIVE AERODYNAMIC AREA (FT**2)
691 DEC 0,0,0           AXIAL FORCE COEFF TABLE (CA)
694 DEC 0,0,0           NORMAL FORCE COEFF TABLE (CN)
697 DEC 0,0,0           WIND TABLE (NORTH AND EAST)
700 DEC 0,0,0           ROLL ANGLE TABLE (SPECIAL OPTION 10)

        WEIGHT

705 DEC 0,0,0           WEIGHT TABLE (SPECIAL OPTION 1 OR 2 ONLY)
708 DEC 0.              WEIGHT DECREMENT

        BODY ATTITUDE

710 DEC 0,0,0           BODY ATTITUDE TABLE

        THRUSTS

715 DEC 0,0,0           THRUST TABLE
718 DEC 0.              SPECIFIC IMPULSE (  SEC)
721 DEC 0.,0.,0.        EXIT AREA (FT**2)
724 DEC 0.,0.,0.        INCLINATION ANGLES (TAU) (DEG)
727 DEC 0.,0.,0.        ROTATION ANGLES (SIGMA) (DEG)
730 DEC 0.,0.,0.        THRUSTS (IF CONSTANT) (LB)
733 DEC 0.,0.,0.        CONSTANT THRUST START TIMES (SEC)
736 DEC 0.,0.,0.        CONSTANT THRUST STOP TIMES (SEC)

        ATMOSPHERE

750 DEC 1.              DENSITY MULTIPLIER
751 DEC 0,0,0           ATMOSPHERE TABLE (SPECIAL OPTION 8)

        SPECIAL OPTION 14 (WRITE BINARY OUTPUT TAPE)

780 DEC 0               SKIP THIS NO. OF FILES TO BEGIN BINARY
                        TAPE, SPECIAL OPTION 14
```

```
                        OUTPUT 9 INFO

781 DEC 20.             LONGITUDE BAND (DEGREES)
782 DEC 2000.           RADAR RANGE (NAUTICAL MILES)

        SPECIAL OPTION 15 (V/VR)

787 DEC 0.              K6
788 DEC 0.              K7

        TERMINATION CONDITIONS FOR RETRO FIRE PREDICTION ONLY

790 DEC 0               REVOLUTION NO. AND
791 DEC 0.              IMPACT LONGITUDE DESIRED (DEG) FOR
                        RETRO-PREDICTION
792 DEC .01             TOLERANCE (DEGREES)
793 DEC 0,0,0.          ELAPSED TIME OF RETRO FIRE  (HR, MIN, SEC)
796 DEC 0,0,0.          G M T OF RETRO FIRE         (HR, MIN, SEC)

        INPUT MULTIPLIERS

800 DEC 1.              TIME MULTIPLIER
801 DEC 1.              THREE POSITION MULTIPLIERS
802 DEC 1.
803 DEC 1.
804 DEC 1.              THREE VELOCITY MULTIPLIERS
805 DEC 1.
806 DEC 1.

        INITIAL CONDITIONS

823 DEC 0,0,0.          CURRENT GMT, HR,MIN,SEC.
826 DEC 0,0,0.          GMT OF REFERENCE, HR,MIN,SEC.
829 DEC 0,0,0.          ELAPSED TIME SINCE REFERENCE (826), HR,MIN,SEC.
832 DEC 0,0,0.          GEODETIC LATITUDE  DEG,MIN,SEC.
835 DEC 1               INITIAL REVOLUTION NO.
836 DEC 0,0,0.          LONGITUDE  DEG,MIN,SEC.
839 DEC -80.547403      REFERENCE LONGITUDE FOR REVOLUTION NO., DEG.
840 DEC 0.              ELAPSED TIME SEC
841 DEC 0.              THREE POSITION CO-ORDS
842 DEC 0.                DEPENDING UPON INPUT CODE
843 DEC 0.
844 DEC 0.              THREE VELOCITY CO-ORDS
845 DEC 0.                DEPENDING UPON INPUT CODE
846 DEC 0.
847 DEC 1.              WEIGHT (LB)
848 DEC 0.              RANGE, FT OR NAUT MI DEPENDING ON RANGE OPT.
849 DEC 0.              TRACK, NAUT. MI.

853 DEC 0.              CONVECTIVE HEAT CONTENT (BTU/FT**2)
854 DEC 0.              RADIATIVE HEAT CONTENT (BTU/FT**2)
```

```
        CURRENT CONDITIONS

870 DEC 0.              ELAPSED TIME (SEC)
871 DEC 0.              GEOCENTRIC LATITUDE (RADIANS)
872 DEC 0.              LONGITUDE (RADIANS)
873 DEC 0.              GEOCENTRIC ALTITUDE (FEET)
874 DEC 0.              LATITUDE RATE (RAD/SEC)
875 DEC 0.              LONGITUDE RATE (RAD/SEC)
876 DEC 0.              ALTITUDE RATE (FEET/SEC)
877 DEC 0.              WEIGHT, LB.
878 DEC 0.              RANGE, FT OR NAUT.MI. DEPENDING ON RANGE OPT.
879 DEC 0.              TRACK, NAUT. MI.

881 DEC 0.              CURRENT CASE TIME, SEC.
882 DEC 0.              CURRENT SECTION TIME, SEC.
883 DEC 0.              CURRENT CONVENCTIVE HEAT CONTENT (BTU/FT**2)
884 DEC 0.              CURRENT RADIATIVE HEAT CONTENT. (BTU/FT**2)
885 DEC 0.              CURRENT QBAR, PSF
886 DEC 0.              CURRENT TOTAL G LOAD, G INITS

888 DEC 0.              CURRENT CENTRAL ANGLE, DEG.
889 DEC 0.              CURRENT VALUE OF DELTA V FROM SP.OPT. 24
                         FT/SEC

        TERMINATION CONDITIONS

450 DEC 0,0,0.          TOTAL ELAPSED TIME, HR,MIN,SEC.
453 DEC 0,0,0.          SECTION TIME, HR,MIN,SEC.
456 DEC 0,0.            REVOLUTION NO., LONGITUDE, N,DEG.
456 DEC 0,,0,0,0.       REVOLUTION NO., LONGITUDE, N,,DEG,MIN,SEC.
461 DEC 0,0.            REVOLUTION NUMBER, TRUE ANOMALY,  N,DEG.
754 DEC 0,0,0,0.        GMT, DAYS,HR,MIN,SEC.

900 DEC 0.              ELAPSED TIME (SEC)
901 DEC 0.              THREE POSITION CO-ORDS
902 DEC 0.                DEPENDING UPON TERMINATION CODE
903 DEC 0.
904 DEC 0.              THREE VELOCITY CO-ORDS
905 DEC 0.                DEPENDING UPON TERMINATION CODE
906 DEC 0.
907 DEC 0.              WEIGHT (LB)
908 DEC 0.              RANGE, FT.OR NAUT.MI. DEPENDING ON RANGE OPT.
909 DEC 0.              TRACK, NAUT. MI.

911 DEC 0.              TIME FROM BEGINNING OF CASE (SEC)
912 DEC 0.              TIME FROM BEGINNING OF SECTION (SEC)
913 DEC 0.              CONVECTIVE HEAT CONTENT (BTU/FT**2)
914 DEC 0.              RADIATIVE HEAT CONTENT (BTU/FT**2)
915 DEC 0.              DYNAMIC PRESSURE, PSF
916 DEC 0.              TOTAL AERODYNAMIC AND THRUST LOAD IN G UNITS
918 DEC 0.              CENTRAL ANGLE, DEG.
919 DEC 0.              DELTA V STOP CONDITION IF SP. 24 ACTIVATED
                         FT/SEC
```

```
 2544 DEC 850.              SOUND SPEED ABOVE 300000 FT.,FT/SEC.

 1368 DEC 1E-5              TERMINATION TOLERANCE FOR NON-TIME QUANTITIES

 7989 DEC 1E-5              TERMINATION TOLERANCE FOR TIME

          RADAR, OUTPUT 9

          LOC = 5820+6(N-1), N LESS THAN OR EQUAL TO 30
  LOC BCD 3                 NTH RADAR STATION DESCRIPTION
LOC+3 DEC 0.                GEODETIC LATITUDE (DEG)
LOC+4 DEC 0.                LONGITUDE (DEG)
LOC+5 DEC 0.                ALTITUDE (FEET)

          CONSTANTS AND CONTROLS REQUIRED FOR X-Y PLOTTER TAPES

32031 DEC 0.,0.,0.,0.,0.,0.,0.,0.,0.,0.,0.,0.,0.,0.,0.   SYMBOL CODES

32046 DEC 0.,0.,0.,0.,0.,0.,0.,0.,0.,0.,0.,0.,0.,0.,0.   SCALE FACTORS

32061 DEC 0,0,0,0,0,0,0,0,0,0,0,0,0,0,0                  INDEXES

32076 DEC 0                NO MERCATOR PLOTTING

32077 DEC 0                NO SYMBOL PLOTTING

          TRANSFER CONTROLS

       TRA 530              MOVE SEQUENCE
       TRA 531              GO TO CARD READER
       TRA 532              GO TO TAPE
       TRA 533              SKIP AND START
       TRA 540              START RETRO FIRE PREDICTION
       TRA 541              END OF REENTRY SEQUENCE
       TRA 1172             CONTINUE WITH SECTION INPUT

          SENSE SWITCH CONTROLS

       SENSE SWITCH         PURPOSE

            1               ON-LINE CARD READER INPUT
            2               PRINT ON-LINE AT NORMAL FREQUENCY
            3               DELETE ALL OFF-LINE OUTPUT
            4               PRINT ON- AND OFF-LINE EVERY INTEGRATION
                            STEP REGARDLESS OF PRINT FREQUENCY
            5               NOT USED
            6               NOT USED
```

A large number of additional transfer controls TRA N have been defined for real-time use. These apply to specific missions and, therefore, will not be listed.

APPENDIX J

REPRESENTATIVE DATA DECKS

Three test data decks are included to illustrate how the data are set up for computing a trajectory. Comments appear on each card to explain the significance of the data contained thereon. These cases have actually been run, and a sample of the output from the first case of test deck 1 is attached.

Test deck 1 is a regular run consisting of two cases. The first case has 1 section or phase, and the second case has 17. The first case is a reentry only, while the second case runs for approximately 1 orbit, performs several functions (such as firing posigrades), and then it, too, reenters the atmosphere. This deck generates four auxiliary output tapes in addition to the normal output on A3. A9 is the binary tape written by activating Special Option 14; A7 is the BCD X-Y plotter tape from Special Option 27; B1 is the BCD tape produced by Special Option 17, in conjunction with Special Option 23; and B10 contains the microfilm output from Special Option 20.

Test deck 2 is a retrofire time-prediction case which will predict the times to fire retrorockets in order to impact at two separate points on the earth, each designated by a revolution number and a longitude. The case consists of several sections which test various program features. A pool tape is required on A4 as described in section 14.0. Note that a coast phase separates the two retrotime predictions; this demonstrates the versatility of this mode of program operation.

In both test decks, a number of data cards has been included which can normally be omitted since these cards are a part of the nominal program contents described in appendix I. These cards were included here to show how one would change the nominal program contents if it were so desired.

Test deck 3 is the ballistic trajectory executed by a three-stage sounding rocket. Note that the minimum input required is used in this case, that is, the earth model, integration accuracy criteria, etc., are not specifically included in the deck.

It will be noted that the Output data are of the form 3-14039675. The left-most digit is the power of 10 by which the mantissa is to be multiplied. A blank space is printed in place of a plus sign, and a negative characteristic or mantissa is indicated by a minus sign immediately preceding it. Thus $3\text{-}14039675 = -.14039675 \times 10^{3}$ and $-2\ 10871661 = .10871661 \times 10^{-2}$.

TEST DECK 1, NORMAL DECK SETUP

```
$JOB  213B   BOYKIN      00339 ED32  E067  1002  P   4   2
$SETUP A7      TAPE,RING,DEBLOCK,2F,200,BCD
$SETUP A9      TAPE,RING,DEBLOCK,1F,800,BIN
$SETUP B1      TAPE,RING,DEBLOCK,1F,800,BCD
$SETUP B5      (6232),BLOCK,2F,800
$SETUP B0      TAPE,RING,4020,1F,200
$EXECUTE       FORTRAN
*      C03E
   500 BCD  ON THIS PAGE IS THAT GENERATED ON TAPE A3 BY THE FIRST CASE
   510 BCD 2 THE OUTPUT
   512 BCD 30F TEST DECK 1.
   515 BCD 5FIVE(5) BCD WORDS ON THIS CARD
   520 DEC 1E-5,1E-5,1E-5,1E-5,1E-5,1E-5          INTEGRATION ACCURACY
       DEC 1E-5,1E-5,1E-5,1E-5                    CRITERIA, EPSILONS
   550 DEC 1E-5,1E-5,1E-5,1E-5,1E-5,1E-5          INTEGRATION SMALL VALUE
       DEC 1E-5,1E-5,1E-5,1E-5                    CRITERIA, DELTAS
   580 DEC 1.                    INITIAL INTEGRATION STEP SIZE
   588 DEC 1                     INPUT 1, INERTIAL QUANTITIES
   589 DEC 2                     TERMINATE ON RELATIVE QUANTITIES
   590 DEC 1,2,4,5,6,7,8,9,10    OUTPUTS
   610 DEC 20,7,27               SPECIAL OPTIONS
   644 DEC 1                     ATTITUDE CONTROL
   650 DEC -60.                  LONGITUDE OF INERTIAL X AXIS AT TIME
   651 DEC 1000.                 T SUB X
   653 DEC 20.                   GEOD. LATITUDE OF PAD FOR OUTPUTS 6,7,8
   654 DEC -60.                  LONGITUDE OF PAD FOR OUTPUTS 6,7,8
   655 DEC 50.                   ALTITUDE OF PAD FOR OUTPUTS 6,7,8
   656 DEC 40.                   AZIMUTH OF X-AXIS FOR OUTPUT 8
   660 DEC 20925000.             EARTH EQUATORIAL RADIUS
   661 DEC 298.                  RECIPROCAL OF EARTHS FLATTENING
   662 DEC 1.395E16              EARTH GRAVITATIONAL CONSTANT MU
   663 DEC 1620.E-6         2ND  GRAVITATIONAL GRADIENT COEFFICIENT
   664 DEC 0.               3RD  GRAVITATIONAL GRADIENT COEFFICIENT
   665 DEC 8.9E-6           4TH  GRAVITATIONAL GRADIENT COEFFICIENT
   666 DEC .729211508E-4         EARTH ROTATIONAL RATE
   680 DEC 1                     RANGE OPTION
   681 DEC 20.,-60.              RANGE REFERENCE POINT,GEOD.LAT.,LONGITUDE
   685 DEC 4.                    CAPSULE NOSE RADIUS
   686 DEC 1.                    CHARACTERISTIC LENGTH FOR REYNOLDS NO.
   687 DEC 1.                    CONVECTIVE HEAT MULTIPLIER
   688 DEC 1.                    RADIATIVE HEAT MULTIPLIER
   689 DEC 1.                    RADIATIVE HEAT MULTIPLIER
   690 DEC 125.                  REFERENCE AREA FOR DRAG COMPUTATIONS
   691 DEC 6000,8,0              DRAG TABLE CONTROL
  6000 DEC 0.,.45,.75,1.,1.45,4.,9.5,12.          AXIAL DRAG COEFF.
  6008 DEC 25.,28.,35.,42.,46.,48.,46.,45.        C SUB A VS. MACH NO.
   750 DEC 1.                    DENSITY MULTIPLIER
   781 DEC 20.,2000.        RADAR STA. PICKUP TOLERANCES, DEG LONG.,N.MI.
   787 DEC -.170279E-7,1.367943        K6 AND K7 FOR SPECIAL OPTION 15
   826 DEC 3,1,1.                REFERENCE GMT IN HR,MIN,SEC.
   829 DEC 20,5,6.               ELAPSED TIME SINCE REFERENCE, HR,MIN,SEC.
```

```
 835 DEC 1                  INITIAL REVOLUTION NO.
 839 DEC -80.                   REFERENCE LONGITUDE FOR REVOLUTION NO.
1368 DEC 1E-5                   TERMINATION TOLERANCE FOR NON-TIME ITEMS
7989 DEC 1E-3                   TERMINATION TOLERANCE FOR TIME
 841 DEC 13.359155              GEODETIC LATITUDE
 842 DEC -140.39675             LONGITUDE
 843 DEC 486089.15              ALTITUDE
 844 DEC 25263.831              INERTIAL VELOCITY
 845 DEC -1.0576965             INERTIAL FLIGHT PATH ANGLE
 846 DEC 51.536971              INERTIAL AZIMUTH
 847 DEC 2290.                  WEIGHT
5820 BCD 3RADAR 1A                      1ST RADAR STATION DESCRIPTION
5823 DEC 10.,160.,30.           GEOD. LAT., LONGITUDE, ALTITUDE
5826 BCD 3RADAR 2A
     DEC -10.,170.,-30.
5832 BCD 3RADAR 3A
     DEC -30.,175.,28.
5838 BCD 3RADAR 4A
5841 DEC -12.,179.,60.
5844 BCD 3RADAR 5A
5847 DEC 5.,180.,15.
5850 BCD 3RADAR 6A
     DEC 5.,-179.,50.
5856 BCD 3RADAR 7A
     DEC 20.,-175.,20.
5862 BCD 3RADAR 8A
     DEC 0.,-170.,100.
5868 BCD 3RADAR 9A
     DEC 25.,150.,34.
5874 BCD 3RADAR 10A
     DEC 40.,-90.,110.
5880 BCD 3RADAR 1
     DEC 10.,-140.,200.
5886 BCD 3RADAR 2
     DEC 30.,-110.,200.
5892 BCD 3RADAR 3
     DEC -30.,32.,50.
5898 BCD 3RADAR 4
     DEC 5.,-25.,60.
5904 BCD 3RADAR 5
     DEC -12.,20.,16.
5910 BCD 3RADAR 6
5913 DEC 40.,-10.,22.
5916 BCD 3RADAR 7
     DEC -10.,31.,85.
5922 BCD 3RADAR 8
     DEC 39.,-15.,800.
5928 BCD 3RADAR 9
     DEC 16.,18.,250.
5934 BCD 3RADAR 10
     DEC 40.,-90.,110.
5940 BCD 3RADAR 11
     DEC 25.,-75.,200.
5946 BCD 3RADAR 12
```

```
      DEC 18.,28.,40.
 5952 BCD 3RADAR 13
      DEC 37.,85.,192.
 5958 BCD 3RADAR 14
      DEC -6.,60.,501.
 5964 BCD 3RADAR 15
      DEC 33.,67.,498.
 5970 BCD 3RADAR 16
      DEC -13.,13.,50.
 5976 BCD 3RADAR 17
      DEC 30.,100.,200.
 5982 BCD 3RADAR 18
      DEC -20.,99.,668.
 5988 BCD 3RADAR 19
      DEC 32.,82.,707.
 5994 BCD 3RADAR 20                        30TH RADAR STATION DESCRIPTION
      DEC 25.,-85.,0
32046 DEC 2000.,8.8888888,8.8888888,1.,1000.,100.,1E7,1E7,1E7,1E3,1E3
      DEC 1E3,1E7,10.,10.      PLOTTING SCALE FACTORS
32061 DEC 152,169,170,182,184,195,200,209,218,227,236,245
      DEC 257,260,271          PLOTTING INDEXES
32076 DEC 1                    MERCATOR PROJECTION
32077 DEC 0                    NO SYMBOL PLOTTIMG
      TRA 3,4                  END OF CASE 1 INPUT DATA
  640 BCD 4 ALTITUDE STOP                          SECTION 1 DESCRIPTION
  581 DEC 1000                 PRINT FREQUENCY
  903 DEC 50000.               STOP ON ALTITUDE
      TRA 3,4                  END OF SECTION 1 DATA
      TRA 2,4                  END OF CASE 1
  500 BCD  TEST ON ADDITIONAL SPECIAL OPTIONS AND OUTPUTS
  510 BCD 2 18 AUG 64          DATE
  512 BCD 3CASE 2
  515 BCD 5 CONTINUE TESTING C03E
  590 DEC 14                   OUTPUT
  610 DEC 24,16,15,12          SPECIAL OPTIONS
  691 DEC 0,0,0                ELIMINATE DRAG
  694 DEC 0,0,0                NO LIFT
  750 DEC 1.05                 DENSITY MULTIPLIER
  823 DEC 22,55,8.             CURRENT GMT IN HR,MIN,SEC.
  826 DEC 12,50,6.             REFERENCE GMT IN HR,MIN,SEC.
  829 DEC 0,0,0     ELAPSED TIME SINCE REF. CURRENT GMT IS ON CARD 823
  832 DEC 30,26,28.917         GEOD. LAT. IN DEG,MIN,SEC.
  835 DEC 17                INITIAL REVOLUTION NO.
  836 DEC -72,27,18.975        LONGITUDE IN DEG,MIN,SEC.
  840 DEC 0,0,0                TIME AND POSITION ALREADY INPUT
  843 DEC 528420.92            ALTITUDE
  844 DEC 25713.332            INERTIAL VELOCITY
  845 DEC .25082192E-2         INERTIAL FLIGHT PATH ANGLE
  846 DEC 77.515542            INERTIAL AZIMUTH
  847 DEC 3036.                WEIGHT
      TRA 3,4                  END OF CASE 2 INPUT DATA
  640 BCD 4POSIS,SP.24                             SCTION 1 DESCRIPTION
  580 DEC .2                   INITIAL COMPUTING INTERVAL
  581 DEC 1                    PRINT FREQUENCY
```

```
  644 DEC 2,2,2                ATTITUDE CONTROL
  710 DEC 0,-4.0,0             PITCH P SUB B
  715 DEC 0,2000.,0            CONSTANT THRUST
  718 DEC 330.                 SPECIFIC IMPULSE
  912 DEC 1.                   STOP ON SECTION TIME
32046 DEC 1E-12,1E-7,10.       CHANGE 3 PLOTTING SCALE FACTORS FROM
32061 DEC 275,283,291          CHANGE 3 PLOTTING INDEXES     LAST CASE
      TRA 3,4                  END SECTION 1 DATA
  640 BCD 4ONE ORBIT FOR RADARS                    SECTION 2 DESCRIPTION
  580 DEC 2.                   INITIAL COMPUTING INTERVAL
  581 DEC 1000                 PRINT FREQUENCY
  590 DEC -2,-4,-5,-6,-7,-8          OUTPUTS
  610 DEC -15,-16,-20,-27,-12,-7     SPECIAL OPTIONS
  644 DEC 1                    ATTITUDE CONTROL
  710 DEC 0,0,0                ZERO OUT P SUB B
  715 DEC 0,0,0                ZERO OUT THRUST
  912 DEC 700.                 STOP ON SECTION TIME
      TRA 3,4                  END SECTION 2 DATA
  640 BCD 4 COAST STAGE                            SECTION 3 DESCRIPTION
  904 DEC 24313.               STOP ON RELATIVE VELOCITY OR
  912 DEC 5310.                SECTION TIME, WHICHEVER COMES FIRST
      TRA 3,4                  END SECTION 3 DATA
  640 BCD 4REGULAR RETROS                          SECTION 4 DESCRIPTION
  115 BCD 1A9              TAPE A9 FOR SP.OPT.14 BINARY TAPE OUTPUT
  580 DEC 1.                   INITIAL COMPUTING INTERVAL
  610 DEC 16,14            SPECIAL OPTIONS
  644 DEC 2,2,2                ATTITUDE CONTROL
  690 DEC 5.                   REFERENCE AREA FOR DRAG COMPUTATIONS
  691 DEC 6000,8,0    DRAG TABLE CONTROL, DRAG TABLE INPUT IN CASE 1
  710 DEC 0,35.,0              PITCH P SUB B
  718 DEC 225.                 SPECIFIC IMPULSE
  721 DEC 0,0,0                EXHAUST AREA, REGULAR RETROS
  724 DEC 165.,165.,165.       RETRO-ROCKET CANT ANGLES, TAU
  727 DEC 60.,170.,-60.        RETRO-ROCKET ROTATION ANGLES, SIGMA
  730 DEC 1500.,1500.,1500.    RETRO-ROCKET THRUSTS
  733 DEC 0,3.,6.              ROCKET START TIMES
  736 DEC 8.,11.,14.           ROCKET STOP TIMES
  912 DEC 14.                  STOP ON SECTION TIME
      TRA 3,4                  END SECTION 4 DATA
  640 BCD 4RETROS WITH SP.21                       SECTION 5 DESCRIPTION
  590 DEC -3,-4,-5,-6,-7,-8,-9,-10,2  OUTPUTS
  610 DEC 21,23,17         SPECIAL OPTIONS
  724 DEC 0,0,0                CLEAR OUT
  727 DEC 0,0,0                REGULAR
  730 DEC 0,0,0                RETRO-
  733 DEC 0,0,0                ROCKET
  736 DEC 0,0,0                INFORMATION
  739 DEC 0,16.553,0           CONSTANT 1/K TABLE VALUE FOR SP.OPT.23
  340 DEC 0,0,0                EXHAUST AREA, SPEC.OPT.21 RETROS
  350 DEC 160.,160.,160.       ROCKET CANT ANGLES, TAU
  360 DEC 60.,170.,-60.        ROCKET ROTATION ANGLES, SIGMA
  370 DEC 1450.,1450.,1450.    ROCKET THRUSTS
  380 DEC 0,3.,6.              ROCKET START TIMES
  390 DEC 8.,11.,14.           ROCKET STOP TIMES
```

```
 440 DEC 3                      NUMBER OF RETRO ROCKETS
 912 DEC 14.                    STOP ON SECTION TIME
     TRA 3,4                    END SECTION 5 DATA
 640 BCD 4CAP.COAST,LIFT,ROLL                    SECTION 6 DESCRIPTION
 370 DEC 0,0,0                  ZERO OUT SPEC.OPT.21 RETRO THRUSTS
 610 DEC -21,10,20              SPECIAL OPTIONS
 644 DEC 2,0,0                  ATTITUDE CONTROL
 694 DEC 6160,4,0               LIFT TABLE CONTROL
6160 DEC 0,10.,20.,30.          LIFT COEFF. C SUB N VS. MACH NO.
     DEC .35,.20,.35,.4
 700 DEC 6170,4,0               ROLL ANGLE CONTROL
6170 DEC 0,10.,20.,30.          ROLL ANGLE VS. MACH NO.
     DEC -40.,-20.,0,+10.
 912 DEC 38.                    STOP ON SECTION TIME
     TRA 3,4                    END SECTION 6 DATA
 640 BCD 4PACKAGE DROP                           SECTION 7 DESCRIPTION
 610 DEC -16,-14,-20            SPECIAL OPTIONS
 708 DEC 375.                   WEIGHT DECREMENT
 900 DEC 41160.                 STOP ON TOTAL ELAPSED TIME
     TRA 3,4                    END SECTION 7 DATA
 640 BCD 4SP.16 HALF SEC.STEP                    SECTION 8 DESCRIPTION
 580 DEC 2.                     INITIAL COMPUTING INTERVAL
 610 DEC 16                SPECIAL OPTION
 903 DEC 480000.                STOP ON ALTITUDE
     TRA 3,4                    END SECTION 8 DATA
 640 BCD 4CHECK ONE                              SECTION 9 DESCRIPTION
 900 DEC 41262.                 STOP ON TOTAL ELAPSED TIME
     TRA 3,4                    END SECTION 9 DATA
 640 BCD 4TRY HALF SEC.AGAIN                     SECTION 10 DESCRIPTION
 912 DEC 5.65                   STOP ON SECTION TIME
     TRA 3,4                    END SECTION 10 DATA
 640 BCD 4CHECK CICODE                           SECTION 11 DESCRIPTION
 912 DEC 10.                    STOP ON SECTION TIME
     TRA 3,4                    END SECTION 11 DATA
 640 BCD 4COAST TO 305000 FT                     SECTION 12 DESCRIPTION
 610 DEC -16  .            SPECIAL OPTION
 580 DEC 1.                     INITIAL COMPUTING INTERVAL
 903 DEC 305000.                STOP ON ALTITUDE
     TRA 3,4                    END SECTION 12 DATA
 640 BCD 4 COAST                                 SECTION 13 DESCRIPTION
 580 DEC 2.                     INITIAL COMPUTING INTERVAL
 610 DEC 16                SPECIAL OPTION
 912 DEC 2.                     STOP ON SECTION TIME
     TRA 3,4                    END SECTION 13 DATA
 640 BCD 4 COAST AGAIN                           SECTION 14 DESCRIPTION
 903 DEC 275000.                STOP ON ALTITUDE
     TRA 3,4                    END SECTION 14 DATA
 640 BCD 4RESUME,ALT.STOP                        SECTION 15 DESCRIPTION
 580 DEC 1.                     INITIAL COMPUTING INTERVAL
 610 DEC -16               SPECIAL OPTION
 903 DEC 60000.                 STOP ON ALTITUDE
1368 DEC 1E-4                   CHANGE NON-TIME TERMINATION TOLERANCE
     TRA 3,4                    END SECTION 15 DATA
 640 BCD 4 TO PUT EOF ON TAPE B1                 SECTION 16 DESCRIPTION
```

```
610 DEC -10,-23,-17     SPECIAL OPTIONS
903 DEC 50000.              STOP ON ALTITUDE
    TRA 3,4                 END SECTION 16 DATA
640 BCD 4 CHANGE PRINT FREQUENCY              SECTION 17 DESCRIPTION
581 DEC 1                   PRINT FREQUENCY
912 DEC 10.                 STOP ON SECTION TIME
    TRA 3,4                 END SECTION 17 DATA
    TRA 2,4                 END OF CASE 2
    TRA 2,4                 END OF COMPUTER RUN
```

THE OUTPUT ON THIS PAGE IS THAT GENERATED ON TAPE A3 BY THE FIRST CASE OF TEST DECK 1.

FIVE(5) BCD WORDS ON THIS CARD

GEOGRAPHIC INERTIAL INPUT

ALTITUDE STOP

SEC.	ELAPSED TIME HR. MIN. SEC.	SECTION TIME SEC.	CASE TIME SEC.	GMT DAY HR.MIN.SEC.	GEOD. LATITUDE DEG. MIN. SEC.	ORBIT	LONGITUDE DEG. MIN. SEC.
GEOC. LAT. DEGREES	GEOD. LAT. DEGREES	LONGITUDE DEGREES	ALTITUDE FEET	RANGE NAUT. MI.	AERO.VELOCITY FEET/SECOND	AREO GAMMA DEGREES	AERO AZIMUTH DEGREES
X LOAD FACTOR G UNITS	Y LOAD FACTOR G UNITS	Z LOAD FACTOR G UNITS	ORBIT RADIUS FEET	THRUST POUNDS	WEIGHT POUNDS	MACH NUMBER	Q BAR PSF
INERTIAL VEL. FEET/SECOND	INERT. GAMMA DEGREES	INERT. AZM. DEGREES	RELATIVE VEL. FEET/SECOND	RLL. GAMMA DEGREES	REL. AZIMUTH DEGREES	GEOD. GAMMA DEGREES	GEOD. AZM. DEGREES
ETA DEGREES	ALPHA DEGREES	BETA DEGREES	DRAG POUNDS	AERO.NORM. POUNDS	PHI NORM. DEGREES	BODY PITCH DEGREES	BODY AZIMUTH DEGREES
X FEET	Y FEET	Z FEET	X DOT FEET/SECOND	Y DOT FEET/SECOND	Z DOT FEET/SECOND		
XQ FEET	YQ FEET	ZQ FEET	XQ DOT FEET/SECOND	YQ DOT FEET/SECOND	ZQ DOT FEET/SECOND		
XE FEET	YE FEET	ZE FEET	XE DOT FEET/SECOND	YE DOT FEET/SECOND	ZE DOT FEET/SECOND		
XL FEET	YL FEET	ZL FEET	XL DOT FEET/SECOND	YL DOT FEET/SECOND	ZL DOT FEET/SECOND		
XLQ FEET	YLQ FEET	ZLQ FEET	XLQ DOT FEET/SECOND	YLQ DOT FEET/SECOND	ZLQ DOT FEET/SECOND		
XLE FEET	YLE FEET	ZLE FEET	XLE DOT FEET/SECOND	YLE DOT FEET/SECOND	ZLE DOT FEET/SECOND		
RADAR STATION	SLANT RANGE NAUT. MILES	ELEVATION DEGREES	AZIMUTH DEGREES	RANGE RATE FEET/SECOND	ELEV. RATE DEG./SEC.	AZM. RATE DEG./SEC.	ALT.OF LINE OF SIGHT,FT
PERIGEE ALT. NAUT. MILES.	APOGEE ALT. NAUT. MILES	PERIG.LONG. DEGREES	PERG.GEOD.LAT. DEGREES	PERIG.DECL. DEGREES	APOG.LONG. DEGREES	APOG.GEOD.LAT. DEGREES	INCLINATION DEGREES
ECCENTRICITY	PERIOD MINUTES	PERIG.ARG. DEGREES	ECCEN.ANOMALY DEGREES	TRUE ANOMALY DEGREES	LONG.ASC.NODE DEGREES	PERG.PASS.TIME SECONDS	SEMI-MAJ.AXIS FEET
AIR DENSITY SLUGS/FT**3	MOL.AIR TEMP. DEG. RANKIN	CONVECTIVE HEAT RATE	INTEGRAL	RADIATIVE HEAT RATE	INTEGRAL	TOTAL HEAT RATE	INTEGRAL
AIR VISCOSITY SLUGS/(FT*SEC)	REYNOLDS NO.	TIMES SQUARE ROOT RADIUS OF CURVATURE		DIVIDED BY RADIUS OF CURVATURE			

72906.000	20 5 6.000	.000	.000	23 6	7.000	13 21 32.954	1 -140 23 48.309
	2 13272825	2 13359154	3-14039675	6 48608915	4 46089423	5 24112903	1-10527581 2 49289160
	-2-26704406	00000000	00000000	8 21407370	00000000	4 22900000	2 28368121 -2 10871661
	5 25283830	1-10576965	2 51536969	5 24112903	1-11090647	2 49290393	1-10527581 2 49289158
	00000000	00000000	00000000	1 61153091	00000000	00000000	1-10527581 2 49289160
	8-10524405	8-12691079	7 49148782	5 15280103	5-13222857	5 15196926	00000000 00000000
	7 34758791	8-20543556	7 49148782	5 18838698	4 73095098	5 15196926	00000000 00000000
	7 34758791	8-20543556	7 49148782	5 17340638	4 70560448	5 15196926	00000000 00000000
	7-12616828	8 17035915	8-33853588	4-10670558	5 14866722	5 20423368	00000000 00000000
	8-10543344	8 17970791	8-15969602	5 10702125	3-56173828	5 22900240	00000000 00000000
	8-10543344	8 17970791	8-15969602	5 10931696	2-38229858	5 21492524	00000000 00000000
RADAR 1		3 21929075	2 19687194	1-66039168	5 12238039	-24487355	91253451 5 36468941
	2-77106778	3 10599640	1-19429907	2 14360778	2 14266387	3 16735584	2-14355880 2 40350866
	-1 20478710	2 85375562	3 15762869	3-13581244	3-13686009	3-15515695	5 74223464 8 21008484
	-11 37396151	4 16384610	-1 33695025	00000000	00000000	00000000	-1 33695025 00000000
	-6 87692449	10282866	55060545	00000000	00000000	00000000	00000000 00000000
73440.203	20 24 .203	1134.203	1134.203	23 25	1.203	28 44 44.892	1 -118 14 45.633
	2 28583680	2 28745801	3-11824600	5 49999777	4 32070438	2 62530849	2-89985482 2 92596331
	-98775015	00000000	00000000	8 20958864	00000000	4 22900000	-1 64570000 71157102
	4 13435405	1-26676040	2 90007586	2 62530849	2-89836576	3 17490940	2-89985482 2 92596328
	00000000	00000000	00000000	4 22619479	00000000	00000000	2-89985482 2 92596331
	7-79480645	8-16599685	8 10027596	4 12341587	3-53014047	2-30073246	00000000 00000000
	7 96857314	8-15649533	8 10027596	4 11123428	3 75292097	2-30073246	00000000 00000000
	7 96857314	8-15649533	8 10027596	2-28839111	2 46626306	2-30073246	00000000 00000000
	7-20010594	8 20688593	8-23799636	3-63632608	2 38891357	4 11826569	00000000 00000000
	7-53441536	8 15944736	7-83855979	3 17088342	3-83948029	4 10349747	00000000 00000000
	7-53441536	8 15944736	7-83855979	2 15878617	2-47542564	2-37385570	00000000 00000000
RADAR 2		3 43894096	1-25786176	2-97811860	1-51544310	-2-13387675	-7 53460081 6 17097848
	4-34264158	1 82388142	2 57976271	3-20100488	2-28583681	3-12580144	2 28745413 2 28583681
	99729384	2 30139223	2-89993322	3-17980308	3-17999275	3 15363538	5 74342404 8 10493661
	-3 36396498	3 38998800	-4 19368427	3 80508200	00000000	00000000	-4 19388427 3 80508200
	-6 29647434	5 76765629	-4 38776855	4 16101640	00000000	00000000	00000000 00000000

END OF CASE. 73 LINES OUTPUT THIS CASE.

END OF FILE HAS BEEN WRITTEN ON PLOT TAPE A7.

TEST DECK 2, RETROROCKET FIRING TIME PREDICTION DECK SETUP

```
$JOB  213B   BOYKIN      00339 ED32  E067  1002  P   5   2
$SETUP A4      TAPE,RING,BLOCK,1F,800
$SETUP B5      (6232),BLOCK,2F,800
$EXECUTE       FORTRAN
*      C03E
       TRA 530                    GO TO WRITE REENTRY SEQUENCY ON TAPE A4
   640 BCD 4 RETRO TIME PREDICTION                SECTION DESCRIPTION
   580 DEC 1.                     INITIAL COMPUTING INTERVAL
   581 DEC 1000                   PRINT FREQUENCY
   610 DEC -16,-12,8          SPECIAL OPTIONS
   644 DEC 1                      ATTITUDE CONTROL
   715 DEC 0,0,0                  NO THRUST
   750 DEC .1                     DENSITY MULTIPLIER
   751 DEC 6020,14,0              DENSITY VS. ALTITUDE TABLE CONTROL
  6020 DEC 0,1E4,5E4,1E5,1.5E5,2E5,3E5,4E5,5E5,6E5,7E5,8E5,9E5,1E6
       DEC 2.37E-3,1.75E-3,3.63E-4,3.21E-5,3.56E-6,6.11E-8,4.12E-9
       DEC 2.35E-11,3.043E-12,1.08E-12,5.24E-13,2.74E-13,1.49E-13
       DEC 8.45E-14               DENSITY VS. ALTITUDE TABLE
  1368 DEC 1E-4                   NON-TIME TERMINATION TOLERANCE
  7989 DEC .01                    TIME TERMINATION TOLERANCE
       TRA 3,4                    END OF SECTION DATA
   640 BCD 4FIRE RETROS                          SECTION DESCRIPTION
   580 DEC 1.                     INITIAL COMPUTING INTERVAL
   610 DEC 16,7,-8            SPECIAL OPTIONS
   644 DEC 2,2,2                  ATTITUDE CONTROL
   710 DEC 0,34.,0                ATTITUDE, P SUB B
   718 DEC 270.                   SPECIFIC IMPULSE
   721 DEC 0,0,0                  ROCKET EXHAUST AREA
   724 DEC 160.,160.,160.         ROCKET CANT ANGLES, TAU
   727 DEC 65.,+175.,-65.         ROCKET ROTATION ANGLES, SIGMA
   730 DEC 1600.,1600.,1600.      ROCKET THRUSTS
   733 DEC 0,5.,10.               STARTING TIMES OF EACH ROCKET
   736 DEC 12.,17.,22.            STOP TIMES OF EACH ROCKET
   912 DEC 22.                    STOP ON SECTION TIME
       TRA 3,4                    END SECTION DATA
   640 BCD 4CAP COAST,LIFT AND ROLL              SECTION DESCRIPTION
   580 DEC 1.                     INITIAL COMPUTING INTERVAL
   616 DEC 10                 SPECIAL OPTION
   644 DEC 2,0,0                  ATTITUDE CONTROL FOR ROLLING VEHICLE
   694 DEC 6100,8,0               LIFT TABLE CONTROL
  6100 DEC 0.,5.,10.,12.,15.,20.,25.,30.        LIFT COEFF. C SUB N
       DEC .35,.20,.35,.35,.35,.41,.45,.47       VS. MACH NO.
   700 DEC 6150,5,0               ROLL ANGLE TABLE CONTROL
  6150 DEC 0,5.,10.,20.,30.       ROLL ANGLE VS. MACH NO.
       DEC -40.,-20.,-10.,-5.,+20.
   730 DEC 0,0,0                  ZERO OUT THRUST
   912 DEC 38.                    STOP ON SECTION TIME
       TRA 3,4                    END SECTION DATA
   640 BCD 4PACKAGE DROP AND COAST               SECTION DESCRIPTION
   610 DEC -16                SPECIAL OPTION
```

```
 708  DEC 120.                  WEIGHT DECREMENT
 912  DEC 1.                    STOP ON SECTION TIME
      TRA 3,4                   END SECTION DATA
 640  BCD 4 .05G STOP                              SECTION DESCRIPTION
 580  DEC 1.                    INITIAL COMPUTING INTERVAL
 916  DEC .05                   STOP ON TOTAL LOAD FACTOR IN G UNITS
      TRA 3,4                   END SECTION DATA
 640  BCD 4 ALTITUDE STOP                          SECTION DESCRIPTION
 580  DEC 1.                    INITIAL COMPUTING INTERVAL
 613  DEC -7               SPECIAL OPTION
 618  DEC -10              SPECIAL OPTION
 644  DEC 1                     ATTITUDE CONTROL
 694  DEC 0,0,0                 ZERO OUT LIFT COEFF. C SUB N
 700  DEC 0,0,0                 ZERO OUT ROLL TABLE CONTROL
 903  DEC 50000.                STOP ON ALTITUDE
      TRA 541                   REQUIRED FOR REENTRY SEQUENCE
      TRA 2,4                   END OF REENTRY SEQUENCE PUT ON TAPE A4
 500  BCD  START REGULAR CASE INPUT DATA WITH THIS CARD
 510  BCD 2 18 AUG 64
 512  BCD 3TESTING C3E3
 515  BCD 5 THIS IS A TEST CASE
 520  DEC 1E-5,1E-5,1E-5,1E-5,1E-5,1E-5         INTEGRATION ACCURACY
      DEC 1E-5,1E-5,1E-5,1E-5                   CRITERIA, EPSILONS
 550  DEC 1E-5,1E-5,1E-5,1E-5,1E-5,1E-5         INTEGRATION SMALL VALUE
      DEC 1E-5,1E-5,1E-5,1E-5                   CRITERIA, DELTAS
 580  DEC 1.                    INITIAL COMPUTING INTERVAL
 581  DEC 1000                  PRINT FREQUENCY
 588  DEC 2                     INPUT 2, RELATIVE QUANTITIES
 589  DEC 1                     INERTIAL QUANTITIES TERMINATION
 590  DEC 1,2                   OUTPUTS
 660  DEC 20925000.             EARTH EQUATORIAL RADIUS
 661  DEC 298.                  RECIPROCAL OF EARTHS FLATTENING
 662  DEC 1.395E16              EARTH GRAVITATIONAL CONSTANT MU
 663  DEC 1620.E-6         2ND GRAVITATIONAL GRADIENT COEFFICIENT
 664  DEC 0.               3RD GRAVITATIONAL GRADIENT COEFFICIENT
 665  DEC 8.9E-6           4TH GRAVITATIONAL GRADIENT COEFFICIENT
 666  DEC .729211508E-4         EARTH ROTATIONAL RATE
 680  DEC 0,0,0                 RANGE
 685  DEC 1.,1.,1.,1.,1.        FOR HEATING PARAMETERS
 690  DEC 100.                  REFERENCE AREA FOR DRAG
 691  DEC 6000,7,0              DRAG TABLE CONTROL
6000  DEC 0,5.,10.,15.,20.,25.,30.    DRAG COEFF. C SUB X VS. MACH NO.
      DEC 0,.6,.9,1.,1.1,1.2,1.3
 781  DEC 20.,2000.             RADAR PICKUP TOLERANCES,DEG.,NAUT.MI.
 835  DEC 1                REVOLUTION NO.
 839  DEC -80.                  REFERENCE LONGITUDE FOR ORBIT NO.
 840  DEC 5000.                 TOTAL ELAPSED TIME SINCE LIFT-OFF
 841  DEC 30.460375             GEODETIC LATITUDE
 842  DEC -72.361749            LONGITUDE
 843  DEC 528447.06             ALTITUDE
 844  DEC 24950.                EARTH REFERENCED (RELATIVE) VELOCITY
 845  DEC -.77686794E-3         RELATIVE FLIGHT PATH ANGLE
 846  DEC 66.937988             RELATIVE AZIMUTH
 847  DEC 3000.                 WEIGHT
```

```
5820 BCD 3RADAR 1                        1ST RADAR STATION DESCRIPTION
     DEC 10.,160.,30.          GEOD. LAT., LONGITUDE, ALTITUDE
5844 BCD 3RADAR 2
     DEC 5.,180.,15.
5868 BCD 3RADAR 3
     DEC 25.,150.,34.
5910 BCD 3RADAR 4
     DEC 40.,-10.,22.
5994 BCD 3RADAR 5                        LAST RADAR STATION DESCRIPTION
     DEC 25.,-85.,0
     TRA 3,4                     END OF CASE INPUT DATA
 640 BCD 4CAPSULE COAST                          SECTION DESCRIPTION
 644 DEC 1                       ATTITUDE CONTROL
 715 DEC 0,0,0                   ZERO OUT THRUST
 900 DEC 5100.                   STOP ON TOTAL ELAPSED TIME
     TRA 3,4                     END SECTION DATA
 640 BCD 4POSIS W/SP11                           SECTION DESCRIPTION
 580 DEC .1                      INITIAL COMPUTING INTERVAL
 610 DEC 16,11               SPECIAL OPTIONS
 644 DEC 2,2,2                   ATTITUDE CONTROL
 710 DEC 0,-4.,0                 PITCH P SUB B
 715 DEC 0,2000.,0               POSIGRADE THRUST
 718 DEC 340.                    SPECIFIC IMPULSE
 912 DEC .5                      STOP ON SECTION TIME
     TRA 3,4                     END SECTION DATA
 640 BCD 4POSIS W/SP12                           SECTION DESCRIPTION
 610 DEC -11,12              SPECIAL OPTIONS
 912 DEC .5                      STOP ON SECTION TIME
     TRA 3,4                     END SECTION DATA
 640 BCD 4ONL ORBIT COAST,SP8                    SECTION DESCRIPTION
 710 DEC 0,0,0                   ZERO OUT P SUB B
 900 DEC 10501.                  FIRST GUESS ON RETRO FIRE TIME TO HIT
 790 DEC 2,-46.2             REV. 2 AT -46.2 DEGREES LONGITUDE
 792 DEC .05                     TOLERANCE FOR HITTING TARGET LONGITUDE
     TRA 540                     GO TO START REENTRY SEQUENCE
 640 BCD 4 INTERMEDIATE COAST                    SECTION DESCRIPTION
 580 DEC 1.                      INITIAL COMPUTING INTERVAL
 644 DEC 1                       ATTITUDE CONTROL
 912 DEC 1000.                   STOP ON SECTION TIME
     TRA 3,4                     END OF SECTION DATA
 900 DEC 20401.                  FIRST GUESS ON RETRO FIRE TIME TO HIT
 790 DEC 3,168.              REV. 3 AT 168.0 DEGREES LONGITUDE
     TRA 540                     GO TO START REENTRY SEQUENCE
     TRA 2,4                     END OF CASE
     TRA 2,4                     END OF COMPUTER RUN
```

TEST DECK 3, BALLISTIC TRAJECTORY

```
$JOB  2136   BOYKIN      00339 ED32  E067  1002  C   2   2
$SETUP B5      (6232),BLOCK,2F,800
$EXECUTE       FORTRAN
*      CO3E
    500 BCD  STAGE SOUNDING ROCKET TEST CASE WHICH ILLUSTRATES ANOTHER
    510 BCD 2 A THREE
    512 BCD 3TYPE OF TRAJECTORY
    515 BCD 5SUPPLIED BY MR.W.T.CALLAGHAN
    568 DEC 8                    INPUT CODE
    590 DEC 1,2,8                OUTPUTS
    610 DEC 2,5,6                SPECIAL OPTIONS
    653 DEC 38.94                GEODETIC LATITUDE OF ORIGIN, INPUT 8
    654 DEC -110.075             LONGITUDE OF ORIGIN, INPUT 8
    655 DEC 4500.                ALTITUDE OF ORIGIN, INPUT 8
    656 DEC 151.8                AZIMUTH OF X AXIS, INPUT 8
    690 DEC 1.                   AERODYNAMIC AREA
    640 DEC 1.                   ELAPSED TIME
    641 DEC 137.871,0,350.       INPUT 8 COORDINATES
    644 DEC 183.25,0,465.21      INPUT 8 VELOCITIES
   6000 DEC 0.,.5,1.,2.5,4.,4.25,4.5,5.    STAGE 1,THRUST VS.ELAPSED TIME
        DEC 87000.,92500.,84000.,81500.                              TABLE
        DEC 86000.,80000.,63000.,0
   6020 DEC 0,.5,1.,2.,2.5,3.,3.5           STAGE 2,THRUST VS.SECTION TIME
        DEC 43000.,43000.,43000.,43000.,43000.,32000.,0              TABLE
   6035 DEC 0,2.,5.2,6.2,7.                 STAGE 3 THRUST VS.SECTION TIME
        DEC 45000.,45000.,50000.,10000.,0.                           TABLE
   6050 DEC 0,5.                WEIGHT VS.SECTION TIME TABLE FOR
   6052 DEC 7529.,5347.                                  STAGE 1 BURN
   6055 DEC 0,3.5               WEIGHT VS.SECTION TIME TABLE FOR
        DEC 3355.,2615.                                  STAGE 2 BURN
   6060 DEC 0,7.,1980.,776.     WT.VS.SECTION TIME TABLE FOR STAGE 3 BURN
   6065 DEC 0,.3,.6,.8,1.1,1.5,2.,2.5,3.   AXIAL DRAG COEFF.C SUB D TIMES
   6074 DEC .609,.594,.584,.564,1.825       REFERENCE AREA S VS.MACH NO.
   6079 DEC 1.629,1.388,1.21,1.081          (CDS) FOR STAGE 1 BURN
   6085 DEC .8,1.1,1.5,2.,2.5,3.            CDS TABLE FOR
        DEC .9,1.24,1.074,.922,.762,.626    COAST AFTER STAGE 1 BURN
   6100 DEC .8,1.1,1.5,2.,2.5,3.,4.,6.      CDS TABLE FOR STAGE 2 BURN
        DEC .8,.81,.672,.57,.496,.444,.432,.324
   6120 DEC 2.,2.5,3.,4.,6.,8.,12.          CDS TABLE FOR COAST AFTER
        DEC .461,.381,.313,.302,.21,.181,.151     STAGE 2 BURN
   6135 DEC 2.,2.5,3.,4.,6.,8.,12.          CDS TABLE FOR STAGE 3 BURN
        DEC .285,.248,.222,.216,.162,.151,.137
        TRA 3,4                 END CASE DATA
    640 BCD 4 STAGE 1 BURNING               SECTION 1 DESCRIPTION
    705 DEC 6050,2,0            WEIGHT TABLE CONTROL
    715 DEC 6000,8,0            THRUST TABLE CONTROL
    721 DEC 2.52                EXHAUST NOZZLE AREA, FT.**2
```

```
691 DEC 6065,9,0            CDS TABLE CONTROL
900 DEC 5.                  STOP CONDITION, ELAPSED TIME
    TRA 3,4                 END SECTION 1 DATA
640 BCD 4 COAST B4 2 IGN                SECTION 2 DESCRIPTION
610 DEC -2,-5,1             SPECIAL OPTIONS
705 DEC 0,3355.,0           CONSTANT WEIGHT TABLE
715 DEC 0,0,0               ZERO OUT THRUST
691 DEC 6085,6,0            CDS TABLE CONTROL
912 DEC 7.                  STOP CONDITION,SECTION TIME
    TRA 3,4                 END SECTION 2 DATA
640 BCD 4 STAGE 2 BURNING               SECTION 3 DESCRIPTION
705 DEC 6055,2,0            WEIGHT TABLE CONTROL
715 DEC 6020,7,0            THRUST TABLE CONTROL
691 DEC 6100,8,0            CDS TABLE CONTROL
721 DEC 1.46                EXHAUST NOZZLE AREA
912 DEC 3.5                 STOP CONDITION,SECTION TIME
    TRA 3,4                 END SECTION 3 DATA
640 BCD 4 COAST B4 3 IGN            SECTION 4 DESCRIPTION
705 DEC 0,1980.,0           WEIGHT TABLE CONTROL
715 DEC 0,0,0               ZERO OUT THRUST
721 DEC 0.                  ZERO OUT EXHAUST AREA
691 DEC 6120,7,0            CDS TABLE CONTROL
912 DEC 15.                 STOP CONDITION, SECTION TIME
    TRA 3,4                 END SECTION 4 DATA
640 BCD 4 STAGE 3 BURNING           SECTION 5 DESCRIPTION
705 DEC 6060,2,0            WEIGHT TABLE CONTROL
715 DEC 6035,5,0            THRUST TABLE CONTROL
691 DEC 6135,7,0            CDS TABLE CONTROL
721 DEC 1.16                EXHAUST AREA
912 DEC 7.                  STOP CONDITION, SECTION TIME
    TRA 3,4                 END SECTION 5 DATA
640 BCD 4 COAST TO 300K FT      SECTION 6 DESCRIPTION
705 DEC 0,776.,0            CONSTANT WEIGHT TABLE
715 DEC 0,0,0               ZERO OUT THRUST
691 DEC 6120,7,0            CDS TABLE
903 DEC 300000.             STOP CONDITION, ALTITUDE
    TRA 3,4                 END SECTION 6 DATA
640 BCD 4COAST TO APOGEE        SECTION 7 DESCRIPTION
691 DEC 0,0,0               ZERO OUT DRAG
905 DEC 0.                  STOP CONDITION,INERTIAL FLIGHT PATH ANGLE
    TRA 3,4                 END SECTION 7 DATA
640 BCD 4 COAST TO 300K FT      SECTION 8 DESCRIPTION
903 DEC 300000.             STOP CONDITION,ALTITUDE
    TRA 3,4                 END SECTION 8 DATA
640 BCD 4COAST TO IMPACT        SECTION 9 DESCRIPTION
903 DEC 4000.               STOP CONDITION, ALTITUDE
    TRA 3,4                 END SECTION 9 DATA
    TRA 2,4                 END CASE DATA
    TRA 2,4                 END OF COMPUTER RUN
```

APPENDIX K

SYMBOLS AND CONSTANTS

The symbols listed here are presented in the following order: (a) coordinate system symbols, (b) other English symbols, and (c) Greek symbols.

(a) Coordinate System Symbols

L	geocentric latitude, deg
$\hat{L}$	unit vector in L direction (fig. A1)
λ	vehicle longitude relative to Greenwich, deg
$\hat{\lambda}$	unit vector in λ direction (fig. A1)
r	radial distance from center of earth to vehicle, ft
$\hat{r}$	unit vector in r direction (fig. A1)
$\dot{L}$	$\frac{dL}{dt}$
$\dot{\lambda}$	$\frac{d\lambda}{dt}$
$\dot{r}$	$\frac{dr}{dt}$
$\ddot{L}$	$\frac{d^2L}{dt^2}$
$\ddot{\lambda}$	$\frac{d^2\lambda}{dt^2}$
$\ddot{r}$	$\frac{d^2r}{dt^2}$

x_b, y_b, z_b	body coordinates with origin at spacecraft c.g.
X_c, Y_c, Z_c	local geocentric coordinates (fig. 3.3-1)
X_D, Y_D, Z_D	local geodetic coordinates (fig. 3.3-1)
X_i, Y_i, Z_i	Input-Output 3 coordinates, ft
$\dot{X}_i, \dot{Y}_i, \dot{Z}_i$	Input-Output 3 velocities, ft/sec
X_q, Y_q, Z_q	Input-Output 4 coordinates, ft
$\dot{X}_q, \dot{Y}_q, \dot{Z}_q$	Input-Output 4 velocities, ft/sec
X_e, Y_e, Z_e	Input-Output 5 coordinates, ft
$\dot{X}_e, \dot{Y}_e, \dot{Z}_e$	Input-Output 5 velocities, ft/sec
x, y, z	Input-Output 6 coordinates, ft
$\dot{x}, \dot{y}, \dot{z}$	Input-Output 6 velocities, ft/sec
x_q, y_q, z_q	Input-Output 7 coordinates, ft
$\dot{x}_q, \dot{y}_q, \dot{z}_q$	Input-Output 7 velocities, ft/sec
x_e, y_e, z_e	Input-Output 8 coordinates, ft
$\dot{x}_e, \dot{y}_e, \dot{z}_e$	Input-Output 8 velocities, ft/sec

(b) Other English Symbols

A	rocket motor exhaust-nozzle area, ft^2
A_r	azimuth in radar station coordinates, deg

$\dot{A}_r$	$\frac{dA_r}{dt}$
a	orbit semimajor axis, ft
C'	constant used in plotting, Special Option 27
C_a	axial drag coefficient, dimensionless
C_n	normal force (lift) coefficient, dimensionless
D	atmospheric drag along wind axis, lb
E	eccentric anomaly, deg
E_r	elevation in radar station coordinates, deg
$\dot{E}_r$	$\frac{dE_r}{dt}$
e	orbit eccentricity
F_{a_n}	aerodynamic force normal to wind axis, lb
$F_{a_x}, F_{a_y}, F_{a_z}$	aerodynamic forces expressed in body coordinates, lb
F'_c	convective heating rate multiplier, dimensionless
F_E, F_N, F_U	total aerodynamic and thrust forces expressed in geodetic east, north, and up coordinates, lb
F'_m	molecular heating rate multiplier, dimensionless
F_n	aerodynamic force normal to x_b axis, lb
F'_r	radiative heating rate multiplier, dimensionless
$F_{T_x}, F_{T_y}, F_{T_z}$	thrust forces expressed in body coordinates, lb

F_x, F_y, F_z	total aerodynamic and thrust forces expressed in body coordinates, lb
F_λ, F_L, F_r	total aerodynamic and thrust forces expressed in earth-centered, rotating, spherical polar coordinates, lb
f	earth flattening, dimensionless
G	gravitational acceleration used in atmospheric computations, ft/sec^2
GET	ground elapsed time since launch or other reference time
GMT	Greenwich mean time
$\vec{g}$	total gravitational acceleration, vector sum of $\vec{g}_r$ and $\vec{g}_L$, ft/sec^2
$\vec{g}_L$	latitude or perpendicular component of gravitational acceleration, ft/sec^2
g_o	sea level acceleration of gravity, ft/sec^2
$\vec{g}_r$	radial component of gravitational acceleration, ft/sec^2
g_x, g_y, g_z	aerodynamic and thrust load factors expressed in body coordinates, g units
H	altitude above equatorial sphere, ft
H'_b	base geopotential altitude of a region of the atmosphere, and characterized by a particular value of L_M, m
H'	geopotential altitude, m
H_c	convective heat content, Btu/ft^2

$\dot{H}_c$	$\frac{dH_c}{dt}$
H_m	molecular heat content, Btu/ft^2
$\dot{H}_m$	$\frac{dH_m}{dt}$
H_r	radiative heat content, Btu/ft^2
$\dot{H}_r$	$\frac{dH_r}{dt}$
H_t	total heat content $H_c + H_r$ (Special Option 7), $H_c + H_m + H_r$ (Special Option 23)
$\dot{H}_t$	$\frac{dH_c}{dt} + \frac{dH_r}{dt}$ (Special Option 7), $\frac{dH_c}{dt} + \frac{dH_r}{dt} + \frac{dH_m}{dt}$ (Special Option 23)
h	altitude above oblate earth spheroid, ft
Δh	difference between equatorial earth radius and local earth radius at latitude L, ft
$\underline{\vec{h}}$	angular momentum vector for unit mass, slug-ft^2/sec
h_a	apogee altitude, ft
h_p	perigee altitude, ft
h_r	altitude of radar station above sea level, ft
h_s	altitude of line of sight in radar station coordinates, ft
$\underline{h}_x, \underline{h}_y, \underline{h}_z$	components of $\underline{\vec{h}}$

I_{sp}	thrust motor specific impulse, sec
i	orbit plane inclination relative to earth equatorial plane, deg
J_1', H_1', K_1'	2nd, 3rd, and 4th gravitational gradient coefficients, respectively, dimensionless
K	radiative heating constant used in Special Option 23
K_6, K_7	constants required in computing V_i / V_{i_r}, sec^2/ft^3 and sec^2/ft^2, respectively
L_D	geodetic latitude, deg
L_{D_a}	geodetic latitude of apogee, deg
L_{D_p}	geodetic latitude of perigee, deg
L_M	$\frac{dT_M}{dH}$ gradient of T_M for a region of the atmosphere (constant for a particular layer), °K/m
L_p	geocentric latitude of perigee, deg
M	Mach number
M'	mean molecular weight of the atmosphere at geopotential altitude H', dimensionless
M_o	sea level mean molecular weight of the atmosphere, dimensionless
m	mass, $lb\text{-}sec^2/ft$ (slugs)
N	revolution number N is incremented (or decremented for westerly travel) each time the vehicle crosses the reference longitude specified on the card 839

N_{Re}	Reynolds number, dimensionless
P	atmospheric pressure, lb/ft^2
P_b	pitch of the x_b axis relative to some reference vector, deg
P_b'	base pressure of a region of the atmosphere, lb/ft^2
P_o	sea level atmospheric pressure, lb/ft^2
$\bar{q}$	dynamic pressure, lb/ft^2
R	range, ft or n. mi., depending on range option
R^*	universal gas constant, ft-lb $(lb\text{-}mol)^{-1}(°R)^{-1}$
R_{a_v}	average earth radius, ft
R_n	capsule nose radius used in heating calculations, ft
R_o	initial point from which range is measured: L_o, λ_o or x_o, y_o depending on range option
R_r	slant range or radius vector from radar station to vehicle in radar station coordinates, n. mi.
$\dot{R}_r$	$\frac{dR_r}{dt}$
r	orbit radius or radius vector from geocenter to satellite, ft
r_a', r_p'	radius vector from geocenter to apogee and perigee, respectively, ft
r_D	local earth radius at geodetic latitude L_D, ft
r_e, r_p	earth equatorial and polar radii, respectively, ft
S	effective aerodynamic area used in drag computations, ft^2

S'	Sutherland's constant used in calculation of coefficient of viscosity, °R
T, T'	thrust magnitude and thrust corrected for atmospheric density effect, respectively, lb
T_a	absolute atmospheric temperature, °R
T_M	molecular scale temperature, °R, at geopotential altitude H'
T_{M_b}	value of T_M at geopotential altitude H'_b, °K
T_p	satellite period, sec
T_x, T_y, T_z	thrust, values expressed in body coordinates, lb
t	elapsed time since launch or other reference time, GET, sec
t_c	case time, sec
t_s	section time, sec
U	earth gravitational potential function
$u_a = \dot{x}_{b_a}$ $v_a = \dot{y}_{b_a}$ $w_a = \dot{z}_{b_a}$	aerodynamic velocity vector components expressed in the body coordinates, ft/sec
ΔV	incremental change in x component of body velocity since start of current section, ft/sec
V_a	magnitude of aerodynamic velocity vector, ft/sec
$V_{a_E}, V_{a_N}, V_{a_U}$	east, north, up components of aerodynamic velocity vector expressed in local geodetic coordinates, ft/sec

$V_{a_{hor}}$	horizontal component of V_a in local geodetic coordinates, ft/sec
V_e	magnitude of relative velocity vector, ft/sec
$V_{e_E}, V_{e_N}, V_{e_U}$	components of relative velocity vector expressed local geodetic coordinate system, ft/sec
$V_{e_{hor}}$	horizontal component of V_e in local geodetic coordinate system, ft/sec
V_i	magnitude of inertial velocity vector, ft/sec
$V_{i_E}, V_{i_N}, V_{i_U}$	components of inertial velocity vector expressed in local geodetic coordinates, ft/sec
$V_{i_{hor}}$	horizontal component of V_i expressed in local geodetic coordinates, ft/sec
V_{i_r}	minimum orbital value of V_i, ft/sec
V_L	north or geocentric latitude component of velocity vector, ft/sec; inertial and relative north components are identical
V_r	radial component of velocity vector, ft/sec; inertial and relative radial components are identical
V_s	speed of sound in the atmosphere, ft/sec
V_{s_o}	speed of sound at sea level, ft/sec
v	true anomaly, deg
V_{e_λ}	east or longitude component of relative velocity vector relative to a geocentric earth, ft/sec
V_λ	east or longitude component of inertial velocity vector relative to a geocentric earth, ft/sec
W	weight, lb

$\dot{W}$	$\frac{dW}{dt}$
W_E, W_N	magnitude of wind component in easterly and northerly directions, respectively, ft/sec
Y_b	yaw of x_b axis relative to some reference vector, deg

(c) Greek Symbols

α	pitch angle of attack, deg
β	angle of side slip, deg
γ'	ratio of specific heat at constant pressure to specific heat at constant volume for air, dimensionless
γ_a	aerodynamic flight path angle, deg
γ_D	geodetic flight path angle, deg
γ_e	relative flight path angle, deg
γ_i	inertial flight path angle, deg
δ_i	small value criteria used in the numerical integration of differential equations; dimensions are those of the differential equation in question
δ_v	tolerance for velocity vector component magnitudes. If the velocity vector components in question are not greater than δ_v, the angles between the vector components are set to zero
ϵ_i	accuracy criteria used in numerical integration of differential equations. Dimensions are those of the differential equation in question
η	total angle of attack, deg

θ	pitch of x_b axis relative to local geodetic horizontal, deg (fig. 3.1-7)
θ_a	angle between normal force vector F_n and the y body axis measured in y_b-z_b plane, deg
θ_c	central angle, deg
θ_r	range angle, deg
λ_a	apogee longitude relative to Greenwich, deg
λ_n	longitude of line of ascending node relative to Greenwich, deg
λ_p	perigee longitude relative to Greenwich, deg
μ	earth gravitational constant, ft^3/sec^2
ν	coefficient of viscosity of atmosphere, slugs/ft-sec
ξ	constant used in calculation of coefficient of viscosity, $\text{slug ft}^{-1}\ \text{sec}^{-1}(^\circ\text{R})^{-\frac{1}{2}}$
ξ_i	coefficient of geopotential altitude used in computing mean molecular weight of atmosphere, ft^{-i}
ρ	atmospheric density, $slug/ft^3$
ρ_b	base density of a region of the atmosphere, $slug/ft^3$
ρ_o	sea level atmospheric density, $slug/ft^3$
σ_i	thrust vector rotation angle for retrorocket i, deg

τ_i	thrust vector cant angle for retrorocket i, deg
τ_p	time of next perigee passage relative to launch or other reference time, sec
φ	yaw of x_b axis relative to north, deg (fig. 3.1-7)
φ_n	angle between the normal force vector and the vertical plane, deg
$\varphi_r, \dot{\varphi}_r$	roll angle, deg; roll rate, deg/sec
χ	ground track, n. mi.
$\dot{\chi}$	$\frac{d\chi}{dt}$
ψ, γ	yaw, pitch, respectively, of general velocity vector V, deg
ψ_a	aerodynamic azimuth, deg
ψ_D	geodetic azimuth, deg
ψ_e	relative azimuth, deg
ψ_i	inertial azimuth, deg
Ω	angle between X_i axis and the line of the ascending node of the vehicle orbit, deg (fig. 13.0-2)
ω	argument of perigee, deg
ω_e	earth rotational velocity, rad/sec

CONSTANTS

C_1, C_2 constants used in radiative heating calculations of Special Option 7; these constants are obtained from following table as functions of V_a

V_a	25 000	30 000	35 000
C_1	6.8	0.003	20.4
C_2	12.5	19.5	12.5

ft/m 3.2808399

ft/n. mi. 6076.1033

1/f 298.29599

F'_c 1.0

F'_m 1.0

F'_r 1.0

G 32.1741 ft/sec^2

g_o 32.174048 ft/sec^2

$\frac{\log_{10} x}{\log_e x}$ 2.302585093

M_o 28.966 (1959 ARDC and MSC Composite Atmospheres), dimensionless

M_o 28.9644 (1962 U.S. Standard Atmosphere), dimensionless

n. mi./ft	$.16457916 \times 10^{-3}$
P_o	2116.3 lb/ft^2 (1959 ARDC and MSC Composite Atmospheres)
P_o	2116.22 lb/ft^2 (1962 U. S. Standard Atmosphere)
π	3.14159265
$\frac{\pi}{180}$	.0174532925
$\pi/2$	1.57079632
2π	6.28318530
$180/\pi$	57.2957795
R*	1545.31 ft-lb $(lb\text{-}mol)^{-1}$ $(°R)^{-1}$
R_n	1.0 ft
r_e	20 925 738 ft
r_p	20 855 523 ft
S'	198.72° R
V_s	850 ft/sec above 300 000 ft altitude in 1959 ARDC and MSC Composite Atmosphere Models
V_s	883.9 ft/sec above 90 km altitude in 1962 U. S. Standard Atmosphere Model
V_{s_o}	1116.45 ft/sec in all three atmosphere models
γ'	1.40 dimensionless
δ_i	10^{-5}

δ_v	.01
ϵ_i	10^{-5}
ξ	7.3025E-7 lb ft^{-1} sec^{-1} $(°R)^{-\frac{1}{2}}$
ξ_o	36.084061 dimensionless
ξ_1	$-3.5282224 \times 10^{-2}$ ft^{-1}
ξ_2	5.8818356×10^{-5} ft^{-2}
ξ_3	$-6.5935946 \times 10^{-8}$ ft^{-3}
ξ_4	$3.8922403 \times 10^{-11}$ ft^{-4}
ξ_5	$-1.1549716 \times 10^{-14}$ ft^{-5}
ξ_6	$1.5172165 \times 10^{-18}$ ft^{-6}
ξ_7	$-5.3191761 \times 10^{-23}$ ft^{-7}
ρ_o	2.3769×10^{-3} slug-ft^{-3}
ω_e	$7.29211508 \times 10^{-5}$ rad/sec

REFERENCES

1. Synge, John L. ; and Griffith, Byron A. : Principles of Mechanics. McGraw-Hill Book Co., Inc., section 11.2, 1959.

2. Herrick, Samuel; and Walters, Louis G. : The Influence of the Earth's Potential Function on a Nearly Circular Satellite. Aeronutronic Publication, no. U-326, Aeronutronic Division of Ford Motor Co., Jan. 9, 1959, p. 9.

3. Nielsen, Kaj L. : Methods in Numerical Analysis. The Macmillan Co., 1956, pp. 232-235, and 239.

4. Champion, K. S. W. ; Minzner, R. A. ; and Pond, H. L. : The ARDC Model Atmosphere, 1959. Air Force Surveys in Geophysics, no. 115, Air Force Cambridge Research Center, Aug. 1959, pp. 8, 11, 13, 14, and 23.

5. Dubin, M. (NASA); Sissenwine, N. (USAF); and Wexler, H. (USWB), Cochairmen, U. S. Committee of Extension to the Standard Atmosphere: U. S. Government Printing Office, Dec. 1962, pp. 8, 10, 11, 13, and 14.

6. Baker, R. A. : Introduction to Theoretical Mechanics. McGraw-Hill Book Co., 1954, pp. 227-229.

7. Contributions to Astrodynamics, Aeronutronic Publication, no. U-880. Aeronutronic Division of Ford Motor Co., vol. 1, appendix 2-B, June 1, 1960, pp. 17-18.

8. Gersten, Robert H.: Geodetic Sub-Latitude and Altitude of a Space Vehicle. Journal of the Astronautical Sciences, vol. VIII, no. 1, spring 1961, pp. 28-29.

9. Goldstein, Herbert: Classical Mechanics. Addison-Wesley Publishing Co., Inc., 1959, pp. 132-135.

"The aeronautical and space activities of the United States shall be conducted so as to contribute . . . to the expansion of human knowledge of phenomena in the atmosphere and space. The Administration shall provide for the widest practicable and appropriate dissemination of information concerning its activities and the results thereof."

—NATIONAL AERONAUTICS AND SPACE ACT OF 1958

NASA SCIENTIFIC AND TECHNICAL PUBLICATIONS

TECHNICAL REPORTS: Scientific and technical information considered important, complete, and a lasting contribution to existing knowledge.

TECHNICAL NOTES: Information less broad in scope but nevertheless of importance as a contribution to existing knowledge.

TECHNICAL MEMORANDUMS: Information receiving limited distribution because of preliminary data, security classification, or other reasons.

CONTRACTOR REPORTS: Technical information generated in connection with a NASA contract or grant and released under NASA auspices.

TECHNICAL TRANSLATIONS: Information published in a foreign language considered to merit NASA distribution in English.

SPECIAL PUBLICATIONS: Information derived from or of value to NASA activities. Publications include conference proceedings, monographs, data compilations, handbooks, sourcebooks, and special bibliographies.

TECHNOLOGY UTILIZATION PUBLICATIONS: Information on technology used by NASA that may be of particular interest in commercial and other nonaerospace applications. Publications include Tech Briefs; Technology Utilization Reports and Notes; and Technology Surveys.

Details on the availability of these publications may be obtained from:

SCIENTIFIC AND TECHNICAL INFORMATION DIVISION

NATIONAL AERONAUTICS AND SPACE ADMINISTRATION

Washington, D.C. 20546